3M Project
San Juan Basin, Colorado and New Mexico

Hydrologic Modeling Report

Prepared for:

Southern Ute Indian Tribe, Ignacio, Colorado
Colorado Oil and Gas Conservation Commission, Denver, Colorado
Bureau of Land Management, Durango, Colorado

Prepared by:

Applied Hydrology Associates, Inc.
1200 S. Parker Road, Suite 100
Denver, Colorado 80231
303-873-0164

November 2000

Table of contents

				Page
EXECUTIVE SUMMARY				ES-1
1.0		Introduction		1-1
2.0		Project objectives		2-1
3.0		Regional geology		3-1
4.0		Hydrogeologic issues		4-1
	4.1	Hydraulic continuity		4-1
	4.2	Flow barriers		4-4
	4.3	Shingled stratigraphy		4-5
5.0		Modeling approach		5-1
6.0		Conceptual model		6-1
	6.1	Boundaries		6-1
		6.1.1 Geologic boundaries		6-1
		6.1.2 Outcrop recharge		6-6
		6.1.3 Outcrop discharge		6-9
		6.1.4 River/outcrop intersections		6-9
	6.2	Properties		6-9
		6.2.1 Permeability		6-9
			6.2.1.1 Permeability at production wells	6-9
			6.2.1.2 Effective permeability	6-10
		6.2.2 Porosity		6-10
		6.2.3 Storativity		6-13
7.0		Model development		7-1
	7.1	Grid projection and coordinates		7-1
	7.2	Discretization		7-1
	7.3	Geologic boundaries		7-1
	7.4	Outcrop recharge		7-4
	7.5	Outcrop discharge		7-4
	7.6	River/outcrop intersections		7-4
	7.7	Properties		7-7

Table of contents (continued)

			Page
8.0		Model calibration	8-1
	8.1	Recharge optimization	8-1
	8.2	Potentiometric surface target	8-1
	8.3	Modeled pathlines	8-7
	8.4	Recharge and discharge volumes	8-7
	8.5	Hydrochemistry targets and mixing	8-10
	8.5.1	Mechanical mixing	8-10
	8.5.2	Diffusive mixing	8-10
	8.6	Chloride target	8-10
	8.7	Stable isotope targets	8-12
	8.8	Geochemical evolution of Fruitland Formation recharge	8-12
	8.9	Iodine-129 and chlorine-36 age dating targets	8-16
9.0		Model scenarios and results	9-1
	9.1	Hingeline barrier	9-1
	9.2	Internal barriers	9-4
10.0		Conclusions and future work	10-1
	10.1	Conclusions	10-1
	10.1.1	Hydraulic regime	10-1
	10.1.2	Hinge line and internal barriers	10-1
	10.1.3	Recharge and discharge	10-1
	10.2	Potential problems	10-1
	10.3	Suggested future refinements	10-3
	10.3.1	Detailed modeling	10-4
	10.3.2	Hydraulic testing of the Fruitland Formation shale	10-4
	10.3.3	Effective diffusion coefficients	10-4
	10.3.4	Structural and historic geology	10-4
11.0		References	11-1

TABLES

Table 4-1 Flow in shingled coal and shale systems.....4-7

Table of contents (continued)

Page

FIGURES

Figure 4-1 Response to hingeline sealing of San Juan Basin....4-3
Figure 4-2 Stylized “shingled” stratigraphy....4-8
Figure 4-3 Modeled pathlines....4-8
Figure 4-4 Modeled pathlines - detail....4-9
Figure 4-5 Effect of coal shingling on overall flows....4-9

Figure 6-1 Conceptual model of the San Juan Basin....6-2
Figure 6-2 Alternative conceptual model of the San Juan Basin....6-3
Figure 6-3 San Juan Basin topography....6-4
Figure 6-4 San Juan Basin simplified geology....6-5
Figure 6-5 Fruitland Formation permeability distribution - Colorado....6-11
Figure 6-6 Colorado permeability distribution....6-12
Figure 6-7 Fruitland Formation porosity distribution - Colorado....6-14

Figure 7-1 Modeled top of Fruitland Formation....7-2
Figure 7-2 Modeled base of Fruitland Formation....7-3
Figure 7-3 Outcrop recharge....7-5
Figure 7-4 Constant-head (river) nodes....7-6

Figure 8-1 Calibrated recharge values....8-2
Figure 8-2 Potentiometric surface for calibration....8-3
Figure 8-3 Modeled potentiometric surface....8-4
Figure 8-4 Calibration histogram....8-5
Figure 8-5 Calibration graph....8-6
Figure 8-6 Modeled 0.1 Ma pathlines, San Juan Basin....8-8
Figure 8-7 Modeled 0.1 Ma pathlines, Colorado....8-9
Figure 8-8 Groundwater flow paths and Fruitland Formation chloride contours....8-11
Figure 8-9 Groundwater 0.1 Ma flow paths and Fruitland Formation ^{18}O temperature (° F) contours....8-13
Figure 8-10 Groundwater 0.1 Ma flow paths and Fruitland Formation ^{2}H temperature (° F) contours....8-14
Figure 8-11 Geochemical evolution of Fruitland Formation recharge....8-15
Figure 8-12 Iodine-129 ages and modeled 0.1 Ma pathlines....8-17
Figure 8-13 Chlorine-36 ages and modeled 0.1 Ma pathlines....8-18
Figure 8-14 ^{36}Cl versus ^{129}I apparent ages....8-19

Figure 9-1 Hingeline barrier scenario....9-2
Figure 9-2 Hingeline barrier calibration graph....9-3
Figure 9-3 Internal barriers and gravity anomalies....9-5
Figure 9-4 Internal barriers and magnetic anomalies....9-6
Figure 9-5 Linear barriers scenario....9-7
Figure 9-6 Linear barriers calibration graph....9-8

Table of contents (continued)

APPENDICES

Appendix A Regional recharge review
Appendix B Chloride mass balance analysis

Executive summary

Applied Hydrology Associates (AHA) was engaged by the Southern Ute Indian Tribe (SUIT), in collaboration with the Colorado Oil and Gas Conservation Commission (COGCC) and the Bureau of Land Management (BLM) Durango Office to develop a regional groundwater model for the San Juan Basin as part of the larger 3M Project.

The model code used is Visual MODFLOW® v 2.8.2, based on the USGS-developed public domain model MODFLOW, a widely accepted standard for groundwater flow modeling.

The groundwater model is linked with a reservoir model of the Colorado portion of the San Juan Basin. The groundwater model simulates pre-production conditions, and is the main basis for determining recharge boundary conditions, internal boundaries, and starting conditions for the reservoir model. The reservoir-modeling group, in turn, provided coal thickness and permeability values for the groundwater model, in an iterative process.

AHA developed a steady-state groundwater model representing pre-coalbed methane (CBM) development conditions and water balance in the Fruitland Formation. The model covers the entire San Juan Basin (approx. 6,700 square miles) at a grid spacing of ½-mile. The study included: (1) a comprehensive evaluation of outcrop recharge based on chloride mass balance, spatial geochemical patterns, CBM production well permeabilities, and initial potentiometric head distribution; (2) analysis of chloride and natural isotopes as recharge indicators and groundwater dating tools; (3) consideration of formation stratigraphy and structure, including multiple proposed barriers and baffles; (4) integration of aquifer parameters derived from reservoir modeling; (5) calibration against historic formation pressures; and (6) assessment of surface water discharge mechanisms.

Data from over 2,200 geochemical analyses from over 600 wells; over 200 initial formation pressure measurements; and precipitation data from 23 rain stations around the San Juan Basin were considered in construction of the hydrologic model.

Based on low vertical permeabilities in the underlying Lewis Shale and Pictured Cliffs Sandstone, and in the overlying Kirtland Shale, a single-layer model of the Fruitland Formation was used, with implicit impermeable upper and lower boundaries. This includes the Pictured Cliffs Sandstone where it is more permeable and hydraulically connected.

Recharge rates were estimated based on several other regional basin studies in the Four Corners region, and on a chloride mass balance analysis using USGS rainfall chemistry data and shallow groundwater chemistry. Initial recharge rates were then adjusted to obtain the best fit in the model. Estimated recharge rates across the San Juan Basin are a low fraction (0 to 5%) of the already-low precipitation rate (~12 inches per year). However, the overall permeability of the Fruitland Formation coals is also low in regional aquifer terms. Therefore, the estimated low recharge is adequate to explain the initial potentiometric heads observed at production wells. Precipitation and recharge

to the Fruitland Formation are greatest in La Plata County, where the outcrop is elevated. Little recharge occurs in the lower and more arid New Mexico portion of the outcrop. Most recharging water travels a relatively short distance to one of several nearby, lower-elevation river gaps, where it is discharged to alluvium; some is discharged at springs on the outcrop; but some enters the San Juan Basin and migrates toward the San Juan River in New Mexico, the lowest point in the San Juan Basin. The discharges to streams cutting the outcrop are very low relative to the base flow (<1%) in those streams. The modeled total stream discharge for the entire San Juan Basin is 208 acre-feet per year.

The model was used to evaluate a number of proposed barriers or baffles, which may represent offset faulting or stratigraphic discontinuities. A number of well-documented barriers/baffles were incorporated, including the Valencia Canyon and 44 Canyon faults. Other concepts of barriers/baffles were evaluated, but they were not well supported by field data, and were not essential for good model calibration. The effect of shingled stratigraphy was analyzed using a multi-layer model. Results indicate that this level of stratigraphic discontinuity does not affect regional groundwater flows. Suggested near-outcrop “hingeline” and internal “linear” barriers did not provide a satisfactory model calibration. As a result, for most of the La Plata outcrop, it is concluded that the outcrop and down dip basin are hydrologically connected.

Because of the low fracture porosity of the Fruitland Formation (effective porosity estimated at 0.01-2.5%), groundwater velocities are relatively high. Groundwater up to ten miles from the outcrop has the oxygen^{18}/deuterium signature of meteoric water, and it is relatively low in chloride, which corresponds to a recharge signature. Groundwater up to ten miles from the outcrop has an age-since-recharge derived from model runs of only a few thousand years. Ratios of oxygen^{18}/ oxygen^{16} and deuterium/hydrogen indicate the mean annual air temperature during recharge. Variations in these ratios and in chloride concentration with distance from the outcrop correlate with Pleistocene pluvial and glacial events.

To summarize, the Fruitland Formation in the San Juan Basin contains fairly low permeability rock units. The formation behaves like a classic confined aquifer system, which is regionally interconnected despite the presence of structural and stratigraphic discontinuities. This model is simple and consistent, successfully simulates observed initial potentiometric heads, agrees with observed patterns of chloride and stable isotopes, and requires no additional complexity to account for most observations.

1.0 Introduction

Applied Hydrology Associates (AHA) was engaged by the Southern Ute Indian Tribe (SUIT), in collaboration with the Colorado Oil and Gas Conservation Commission (COGCC) and the Bureau of Land Management (BLM) Durango Office to develop a regional groundwater model for the San Juan Basin as part of the larger 3M Project. The contract was awarded on April 30, 1999.

The 3M Project established a Technical Peer Review Team (TPRT), consisting of representatives of SUIT, COGCC, BLM, Colorado Geological Survey (CGS), United States Forest Service (USFS), La Plata County, Questa Engineering, Inc., and industry. The industry group, consisting of CBM operators working in the San Juan Basin, included BP Amoco, Cedar Ridge, Enervest, Hallwood, J. M. Huber, Mark West, and Vastar. The TPRT first met on February 22, 1999, and, at regular intervals throughout the project, provided input and review of the modeling approach, conceptual model development, calibration, and model scenarios.

Substantial direct assistance was provided by SUIT, COGCC, BLM, and industry, including access to databases, previous reports, well records, hydrochemistry data, and discussion of conceptual models of the San Juan Basin. This report also benefited from review by Debbie Baldwin and Cindy Scott of COGCC and Matt Janowiak of BLM.

The regional groundwater model was developed in conjunction with a basin-wide reservoir model, which was developed by Questa Engineering, Inc., of Golden, Colorado. The groundwater model was used to simulate pre-production conditions across the entire San Juan Basin. This provided the input state for the reservoir model, which in turn was used to simulate production history, and to predict effects of various future management scenarios. Reservoir modeling results are presented in a separate report by Questa (2000).

Because of Questa's previous experience in the San Juan Basin, they provided much of the input data for the groundwater model, including formation geometry, hydraulic properties such as permeability and porosity, initial potentiometric heads at production wells, and presence of internal flow barriers. In turn, AHA provided Questa with results of model calibration for outcrop recharge and predicted basin-wide potentiometric configuration for initial runs of the reservoir model. Questa Engineering worked closely with AHA in an iterative process to develop both models in a coordinated manner. The groundwater model project benefited greatly from Questa's insights and experience.

This project would not have been possible without the support of the sponsors and the insights and input of those individuals and groups gratefully acknowledged above. However, any deficiencies in this report are solely the responsibility of the authors.

2.0 Project objectives

The primary objective of the hydrologic modeling project was to develop a regional groundwater model for the San Juan Basin, which together with reservoir modeling, will be used as a planning tool for overall basin CBM development and evaluation of mitigation strategies. The groundwater model simulates pre-production conditions, which are assumed to consist of one-phase flow, i.e., groundwater only. Subsequently, reservoir modeling, performed by Questa, is used to simulate production conditions and predict future scenarios, in which two-phase flow takes place, i.e., groundwater plus desorbed gas. The two-phase reservoir model incorporates changes in water and air permeability over time, which are caused by the presence of gas in the coal cleats and fractures, coupled with matrix expansion in response to pressure alleviation and matrix shrinkage in response to gas desorption.

A secondary objective of the hydrologic modeling project was to evaluate a number of conceptual models of the San Juan Basin. The normal process in groundwater model development is to first develop a conceptual model of groundwater flow. The conceptual model contains all known components and processes, which are then described mathematically, discretized (i.e., gridded) at a resolution that is controlled by spatial data availability, overall objectives, and available computational power, and used to perform numerical simulations. Components of a conceptual hydrologic model include aquifer unit boundaries and properties. Boundaries may include internal discontinuities, such as faults or stratigraphic breaks, which may be represented as flow barriers if complete, or as permeability modifiers if partial. In the case of the San Juan Basin, several conceptual models have been proposed, the primary differences being the number, location, and completeness of flow barriers.

Two main conceptual models specifically considered are:

1. **Hydraulically connected basin**. This is the traditional conceptual model of a confined aquifer, in which regional flow occurs from higher-elevation recharge areas to lower-elevation discharge areas. This model may contain partial internal barriers.

2. **"Hinge-line" barrier**. Based on the change from a gentle formation dip in the San Juan Basin, to relatively steep dips at the San Juan Basin margins, it can be argued that the change in dip may be a sharp tectonic division, e.g. a displacement fault. This would be modeled as a sharp, no-flow boundary paralleling and approximately 1.5 miles from the Fruitland Formation outcrop. Aquifer continuity and flow barriers are discussed in Section 4.1 and 4.2.

A third conceptual sub model considered the potential effect of the transgressive-regressive Fruitland Formation coal stratigraphy:

3. **"Shingle stratigraphy"**. The overprint of minor marine transgressions on an overall regression resulted in the Fruitland Formation coals being deposited as a series of offlapping, "shingled" layers. While an individual coal bed may appear to be laterally continuous over several miles from well logs, the interpreted unit

may actually be distinct units separated vertically by lower-permeability shale. This could be modeled either as (a) a series of internal stratigraphic discontinuity barriers (if their locations were accurately mapped), or (b) an overall reduction in permeability from that deduced from production data. Calculated effects of shingled stratigraphy are discussed in Section 4.3.

3.0 Regional geology

Only a brief outline of the San Juan Basin geology is presented here. The recently published report by the Colorado Geological Survey (Wray, 2000[1]), an integral part of the 3M project, contains an extensive bibliography relating to San Juan Basin stratigraphy, coalbed methane origins, structure, both large- and small-scale tectonism, and environmental issues of CBM development. It is assumed that the reader is already familiar with previous work on the geology of the San Juan Basin, including the main coal-bearing formation, the Fruitland Formation.

The Fruitland Formation is the major coal-bearing rock unit in the San Juan Basin of New Mexico and Colorado (Laubach and Tremain, 1994). The Fruitland Formation occupies approximately 6,700 square miles within the San Juan Basin, contains over 200 billion tons of coal within this area, and crops out around most of the margin of the San Juan Basin (Fassett et al, 1997). It is conformably overlain by the Kirtland Shale, and underlain by the Pictured Cliffs Sandstone and the Lewis Shale. The Pictured Cliffs, Fruitland Formation, and Kirtland together represent a fining-upward, nearshore marine to deltaic environment, and successively form an offlapping sequence due to the regression of the Cretaceous Western Interior seaway.

[1] This report may be obtained via the Colorado Geological Survey, reference Open-File Report 00-18.

4.0 Hydrogeologic issues

4.1 Hydraulic continuity

As introduced in Section 2.0, a primary issue regarding regional hydrogeology is the degree of hydraulic continuity within the Fruitland Formation coals. In previous work, authors have considered the Fruitland Formation to be in overall hydraulic continuity across the San Juan Basin, i.e., the traditional confined aquifer conceptual model described in Section 2.0. For example:

1. Based on trends shown in a composite potentiometric-surface map of the entire San Juan Basin, Kaiser et al (1994) concluded: "Regionally, the Fruitland Formation is a single hydrologic unit, but compartmentalization is indicated locally by large vertical and lateral pressure gradients".

2. Hill et al (2000) described the Fruitland Formation in the San Juan Basin as being characterized throughout the 1990s within the Gas Research Institute (GRI) as "… thick beds of laterally continuous, thermally mature, high gas content coal having communication with an active, regional hydrologic flow regime".

The interpretations of a regionally connected hydrologic unit are based on the observation that potentiometric heads are highest in the wettest part of the outcrop area in La Plata County, the topographically highest part of the San Juan Basin, and generally decline with distance into the basin and towards the San Juan River near Farmington, New Mexico, the topographically lowest Fruitland Formation outcrop. These observations are consistent with an active flow regime experiencing outcrop recharge and discharge connected by basin flow. This pattern of regional flow, from elevated outcrop areas to lower-elevation discharge areas is extremely common, and is often used in hydrogeology textbooks to illustrate the hydrologic cycle.

A more complex alternative explanation for the pattern of potentiometric heads is related to the "hinge-line barrier" conceptual model introduced in Section 2.0. This explanation invokes the concept of "fossil" heads that reflect active hydrodynamic conditions that existed at an earlier geologic time, but whose recharge and discharge boundaries have since been removed by hinge-line faulting effectively sealing off the San Juan Basin, and whose pressures have been "sealed" in place through low formation permeability and/or fault compartmentalization. If hingeline sealing occurred without compartmentalization, eventually potentiometric heads would equalize across the whole San Juan Basin. This explanation requires a specific series of geologic conditions:

1. The San Juan Basin must be regionally hydraulically connected at the time that the Fruitland Formation was first exposed through erosion.
2. Sufficient time must pass to allow the observed potentiometric surface to develop, before the generation of hinge-line and internal faulting.
3. Sealing barriers must be generated relatively quickly to trap pressures before they dissipate.

4. Barriers, and the overlying and underlying shale aquitards, must have sufficiently low permeability to maintain pressures relatively unchanged from the time of trapping to the present day. In this proposed scenario, the “fossil” gradient remains in place because the low formation permeability results in a very long relaxation time.
5. Basin uplift and erosion must be such that the trapped heads near the outcrop are coincidentally close to the topographic surface and trapped heads elsewhere are fortuitously close to the traditional .

Fossil hydraulic gradients have been documented elsewhere, notably in the Nubian Sandstone of Libya and the Disi and Saq Sandstones of Jordan and Saudi Arabia peninsula. However, gradients in these formations are maintained because the relevant distances are large (thousands of miles) and because the affected formations have a relatively high storage coefficient of 10-20%. In the San Juan Basin, the Fruitland Formation unconfined storage coefficient (fracture porosity) is only about 0.01-2.5% and the confined storage coefficient (porosity-compressibility-thickness product) is several orders of magnitude less.

AHA examined the feasibility of the fossil gradient scenario by running the San Juan Basin model in transient mode, starting with the existing potentiometric surface, and then applying the hingeline-sealing scenario. The simulation was run for 65 million years. The initial heads equilibrated to an average value, decreasing in the high head area and increasing in the low head area. Modeled equilibration was relatively rapid and was about 80% complete within about 2 million years (Ma) (see Figure 4-1). The suggested “trapping” event therefore must have occurred more recently than 2 Ma, in order to preserve “fossil” pressures to the present day without significant re-equilibration. This poses the question as to whether there was a major orogeny or other hingeline-forming event during this time period.

To set these time periods in perspective, deposition of the Fruitland-Kirtland sequence was complete by approximately 68 Ma (Molenaar, 1983). Laramide tectonism began in the late Cretaceous (85 Ma), peaked in the Paleocene (62.5 Ma) and waned in the Eocene (45 Ma). During this period, the San Juan structural basin was formed. Subsequent extensional tectonics in the Oligocene (30 Ma) resulted in the eruption of the San Juan volcanics, which are related to the thermal enhancement of coal maturity in the northern San Juan Basin. Large volumes of volcanic rocks buried the underlying sedimentary sequence. Regional uplift and erosion of the Colorado Plateau began in the Miocene (5-23 Ma). This allowed erosion of Oligocene volcanics and volcanoclastics from the northern flank of the San Juan Basin, exposed the Fruitland Formation, and allowed meteoric and stream recharge to commence. Therefore, the freshwater component of the Fruitland Formation‘s hydrogeologic history may have started at about 20 Ma at the earliest.

Figure 4-1

Response to hingeline sealing of San Juan Basin

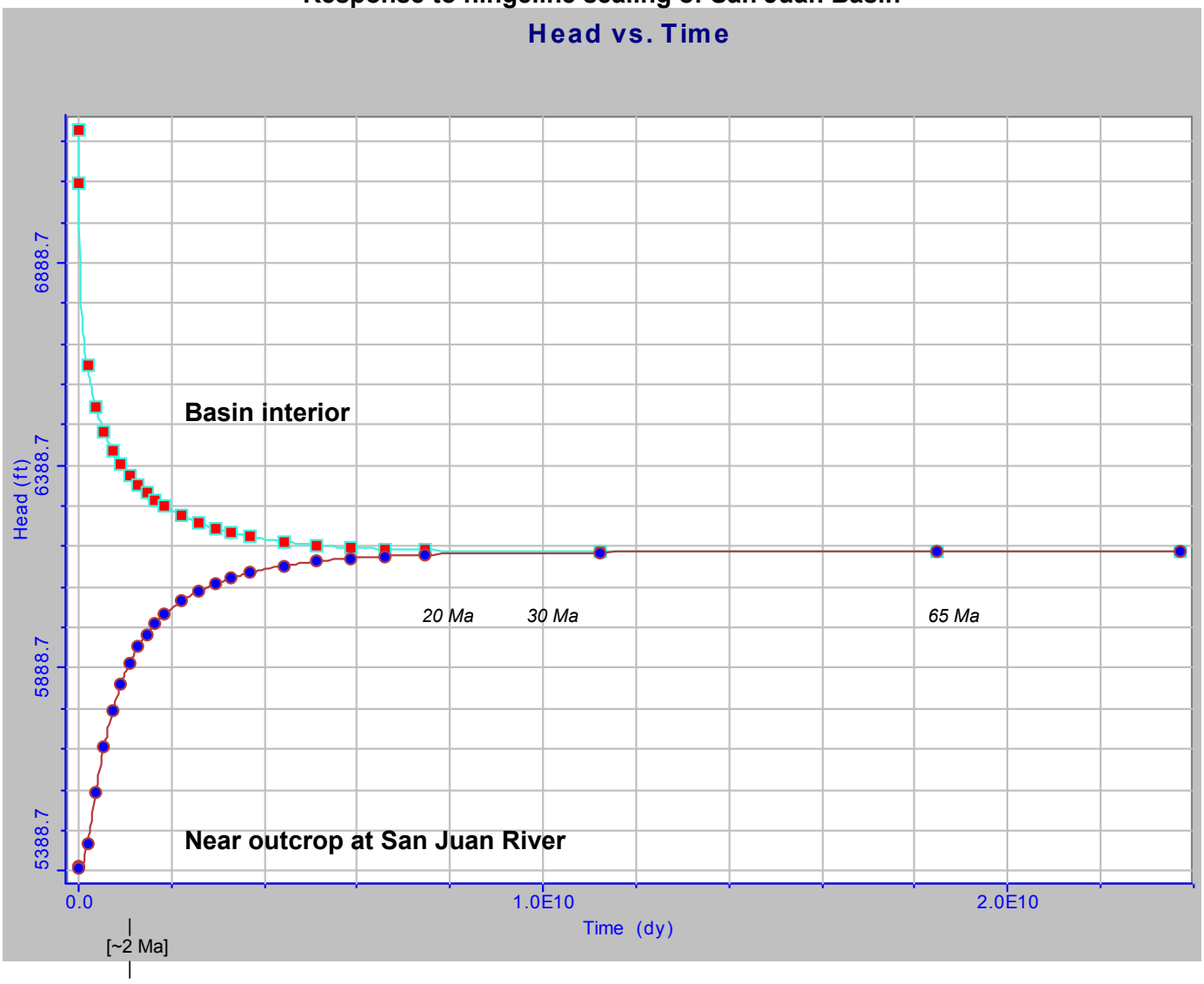

The simple confined-basin recharge-discharge pattern is also consistent with the area where the Fruitland Formation is "overpressured". Overpressured formations, by definition, occur in confined areas with potentiometric heads that are artesian, i.e., above the ground surface. This commonly occurs where recharge areas are at a high elevation and the adjacent land is topographically lower, and is easily achieved because horizontal hydraulic gradients are much flatter than possible topographic grades. Water pressure (including artesian pressure) is not, as is sometimes suggested, generated by adsorbed gas. The relationship is the opposite: it is the pressure exerted by the head of water that keeps the gas sorbed in the coal. In the fossil gradient/hingeline barrier/sealing compartment theory, the occurrence of overpressuring is probably caused by greater uplift of the San Juan Basin in the overpressured area after sealing took place.

4.2 Flow barriers

The available data makes definite identification of flow barriers difficult. In a few areas, flow barriers are convincingly present, based on a combination of data, including mapped surface faults with displacements greater than coal bed thickness, and marked changes in both potentiometric head and distinct differences in Fruitland Formation water chemistry on either side of the feature. Examples of convincing barriers are the Valencia Canyon and 44 Canyon faults. Additional internal barriers, based on Questa Engineering's detailed knowledge and understanding of the San Juan Basin, are discussed in the reservoir modeling report. These barriers were included in all model calibration runs.

Where such a compelling amount of data is not available, the presence of flow barriers is best demonstrated through pumping tests, in which potentiometric heads are monitored over time on both sides of the proposed barrier, with pumping on only one side of the barrier. In the San Juan Basin, information about potentiometric heads is mainly limited to pre-production measurements at CBM wells. Long-term monitoring of pumping tests such as those described above has not been performed in the San Juan Basin, for a number of reasons:

1. The depth of the Fruitland Formation over most of the San Juan Basin is such that installing a well (or converting an existing production well) dedicated to monitoring Fruitland Formation pressures would be extremely expensive. At least three monitoring wells would be required for each test.
2. Even if long-term monitoring wells were available in the San Juan Basin, the current well spacing and formation permeability would limit the value of an interference test. During the period of model development, production well spacing in the San Juan Basin was 320 acres, i.e., two wells per one-square-mile section, or approximately ½ mile between wells. The Fruitland Formation permeability is very low over most of the San Juan Basin (in aquifer terms it is an unproductive formation), so the area of influence of most production wells is not large enough to observe effects at this distance.

3. Because of the large number of production wells operating at differing pumping schedules, the effect of an individual production well would be difficult to observe in isolation.
4. The reduction in effective permeability due to gas desorption at production wells further limits their hydraulic area of influence.
5. If a multi-well test were performed, it would only indicate conditions in one relatively small area, which may not be representative; numerous tests would be required to quantify conditions across the San Juan Basin.
6. The results of such tests would have significant production implications, which would make the data proprietary.

In the absence of positive evidence of flow barriers, the presence or absence of barriers can be invoked based on many lines of reasoning, including tectonic analyses, variations in Fruitland Formation water chemistry, changes in potentiometric head, and interpretations of gravity and magnetic anomalies, or other geophysical trends. While these data may support various theories of hydraulic barriers, they do not prove them conclusively. For this study, it was concluded that the best way to evaluate the various barrier theories is to treat them as alternative conceptual models, and to run the San Juan Basin model to determine how well these models appear to represent actual conditions. This evaluation is described in Section 9.0.

4.3 Shingled stratigraphy

The effects of shingled stratigraphy were evaluated with a 2-dimensional MODFLOW model representing idealized shingled conditions. The model is shown in Figure 4-2. It consists of a 20-foot wide, 400-foot deep, 10-mile long section containing 13 coal seams, each 5 feet thick and one mile long, and separated from each other by 20 feet of shale over a ¼-mile overlap. Constant heads were applied to the two end coal seams with a Δh of 1,000 ft, and the model was run to determine the resulting flow rate. The modeled flow rates under various permeability conditions were compared with that predicted by Darcy's Law for a single continuous 5-ft coal seam and a single continuous 395-ft shale unit.

Results are shown in Figures 4-3 through 4-5 and summarized in Table 4-1. Figure 4-3 shows the groundwater flow pattern resulting from a base case with a Kh_{coal}/Kh_{shale} ratio of 100:1 and a K_h/K_v ratio of 10:1. Groundwater flows from high potential to low potential and is preferentially focused along the coal seams. Figure 4-4 shows how groundwater flow is strongly refracted where the coal seams terminate, changing from horizontal flow through the coal to vertical flow through the shale. This behavior was described by Hubbert (1940)[1] and is considered normal flow in multi-layer systems. Although one might expect that this would cause significant reduction in flow, due to the lower permeability of the shale, it should be noted that the vertical area through which flow can take place increases significantly (from 100 sq. ft. horizontally to at least 26,400 sq. ft. vertically).

[1] Hubbert, M. K. 1940. *The theory of groundwater motion*. Journal of Geology, 48, pp. 785-944.

Calculated and predicted flows are summarized in Table 4-1 and Figure 4-5. For the base case shown in Figure 4-3 (Kh_{coal}/Kh_{shale} ratio of 100:1), the dimensionless flows calculated from Darcy's Law are 2 for the coal and 1.6 for shale (case number 1). For a Kh_{coal}/Kh_{shale} ratio of 1,000:1, the flows are 2 and 0.16 (case number 2). The relative flows via the shale may be considered surprising, as shale is often considered to be virtually impermeable. However, as previously noted, Fruitland Formation coal is also a low-permeability unit, and the shale thickness through which groundwater can flow is substantially greater than the coal thickness. This analysis shows that groundwater flow through shale beds could be a significant factor in overall Fruitland Formation hydrogeology. Therefore, obtaining core and field permeability values for Fruitland Formation shale would be extremely useful for future work.

The calculated flows for cases 1 and 2 were used to define "flow factors" for the coal (Q_{coal}) and shale (Q_{shale}). The flow factor is the modeled flow through a rock unit compared with the Darcy's Law flow for that unit. Darcy calculated flows for coal and shale for cases 1 and 2 were each given an arbitrary relative value of 100% for comparison with the modeled cases.

The four modeled cases cover Kh_{coal}/Kh_{shale} ratios of 100:1 and 1000:1, and horizontal to vertical permeability ratios (K_h/K_v) of 1 and 10. As described below, the Kh_{coal}/Kh_{shale} ratio is the most significant factor.

In the modeled cases with a Kh_{coal}/Kh_{shale} ratio of 100:1 (case numbers 3 and 5), the coal flow factor increases to over 100% and the shale flow factor decreases. Apparently, the interspersing of shingled coals within the shale encourages groundwater to flow from the shale to the coal. In addition, the availability of a large surface area for vertical flow actually increases the flow that can be preferentially conveyed through the coal. For the cases modeled with Kh_{coal}/Kh_{shale} ratio of 1,000:1 (case numbers 4 and 6), the coal flow factor decreases to between 80% and 100%, because the vertical permeability of the shale is now an order of magnitude lower. The shale flow factor also decreases

In summary, the effect of shingling is not as severe as might be thought, and can actually enhance groundwater flow in coal seams, due to the increased surface area exposed to groundwater contributions from over- and underlying shale beds, while reducing horizontal flow in the shale. In the range of likely Kh_{coal}/Kh_{shale} ratios, the shingling effect changes flow in the coal by only $\pm$15%. Therefore, the effect of shingling was not used to modify permeabilities in the hydrologic model. The analysis leads to the conclusion that a single-layer model accurately represents flow in higher permeability coal layers, and that the simplification of complex stratigraphy does not reduce the San Juan Basin model's applicability.

This analysis of coal/shale interaction also lends support to the concept of coal "packages", i.e., groups of coal beds sufficiently close to each other to be considered in hydraulic communication. With better knowledge of coal and shale relative permeabilities, quantitative guidelines could be developed to replace the current rules of thumb regarding how thick coal beds should be, and how close to each other, to be regarded as a "package".

Table 4-1

Flow in shingled coal and shale systems

Case	Type	Kh_{coal}	Kh_{shale}	Kh_{coal}/Kh_{shale}	K_h/K_v	Q_{coal} factor	Q_{shale} factor
1	1	1	0.01	100	NA	100%	100%
2	1	1	0.001	1000	NA	100%	100%
3	2	1	0.01	100	10	113%	61%
4	2	1	0.001	1000	10	86%	50%
5	2	1	0.01	100	1	115%	61%
6	2	1	0.001	1000	1	98%	56%

Notes

Cases 1 and 2: Flow calculated by Darcy's Law, assumes one coal seam.
Cases 3-6: Modeled shingled scenarios, various k ratios.
Units are [L] ft; [T] days.

Figure 4-2

Stylized "shingled" stratigraphy

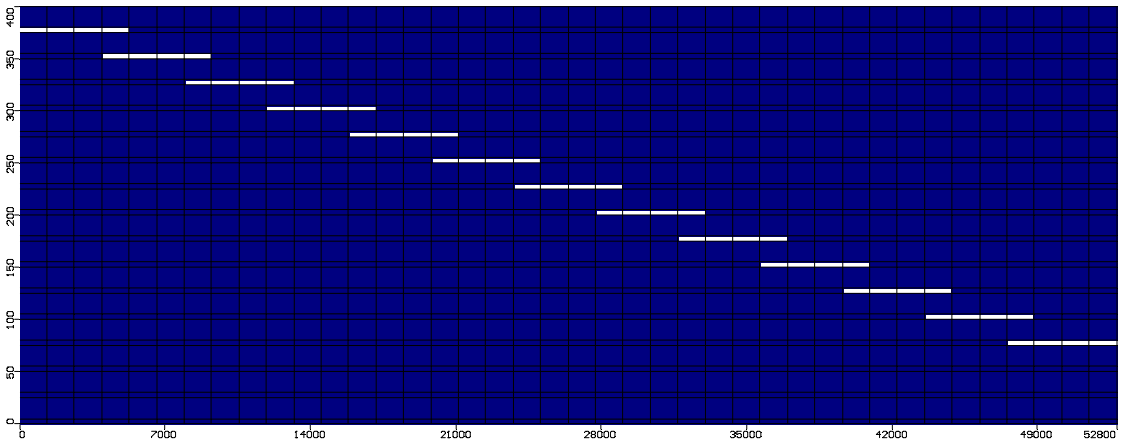

Note: this figure is not intended as an accurate representation of Fruitland Formation stratigraphy at any location. It portrays an idealized "shingled" stratigraphy of alternating permeabilities for the purposes of numerical analysis.

Figure 4-3

Modeled pathlines

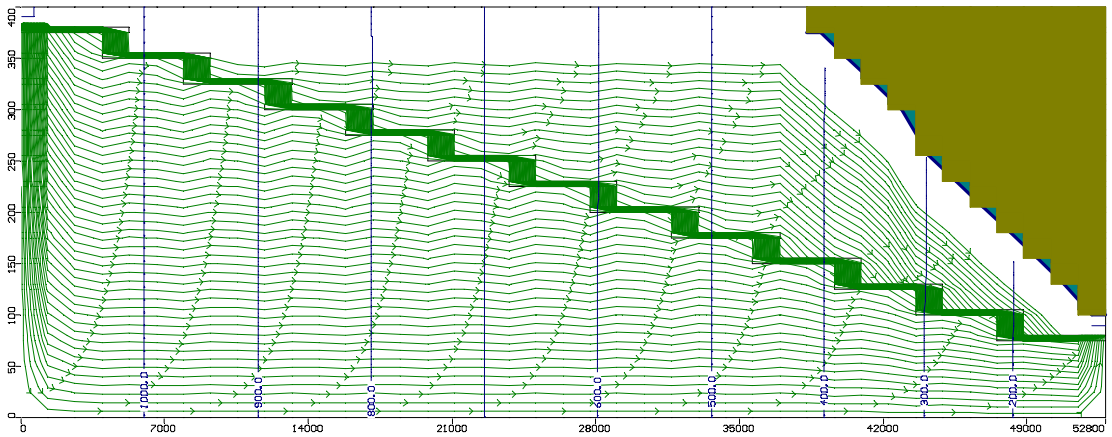

Figure 4-4

Modeled pathlines – detail

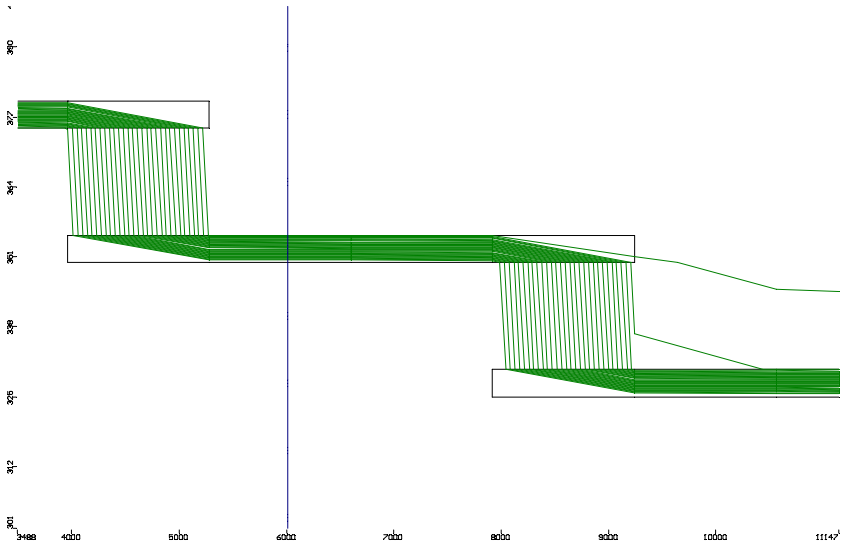

Figure 4-5

Effect of coal shingling on overall flows

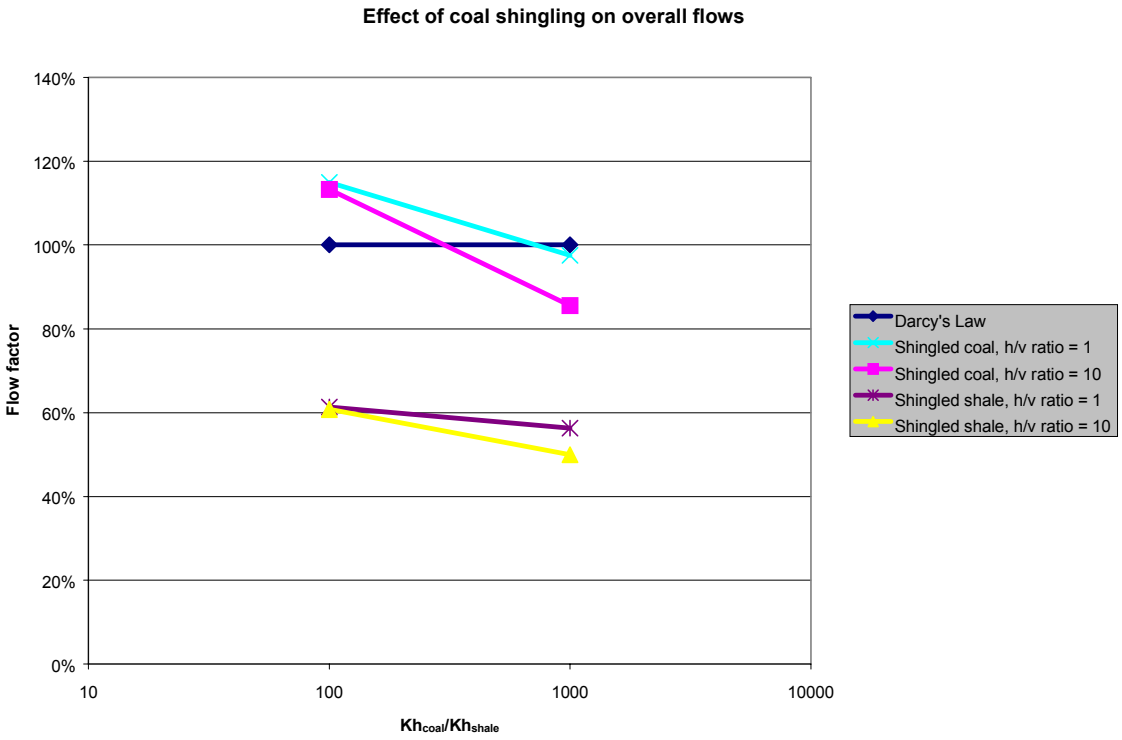

5.0 Modeling approach

MODFLOW (McDonald and Harbaugh, 1978), which was developed by the United States Geological Survey (USGS) and is available in the public domain[1], was the model code[2] used to develop and run the groundwater model. Therefore, all data generated by the modeling effort is useable by any party that has access to MODFLOW.

The MODFLOW model was built and run using version 2.8.2 (the latest available version) of Visual MODFLOW®[3] (VMODFLOW) by Waterloo Hydrologic Software, Inc. VMODFLOW is a widely used interactive pre- and post-processor program for the public domain model MODFLOW. It contains front- and back-end routines that greatly facilitate data input, output, and parameter modifications to MODFLOW, with a graphical user interface. The model files generated by VMODFLOW are completely compatible with MODFLOW and can be used without the shell program.

AHA developed a steady-state groundwater model representing pre-coalbed methane (CBM) development conditions and water balance in the Fruitland Formation. The model covers the entire San Juan Basin (approx. 6,700 square miles) on a ½-mile grid spacing. The study included:

1. A comprehensive evaluation of outcrop recharge based on chloride mass balance, spatial geochemical patterns, production well permeabilities, and initial potentiometric head distribution.
2. Analysis of chloride and natural isotopes as recharge indicators and groundwater dating tools.
3. Consideration of formation stratigraphy and structure, including multiple proposed barriers and baffles.
4. Integration of aquifer parameters derived from reservoir modeling.
5. Calibration against historic formation pressures and geochemical patterns.
6. Assessment of surface water discharge volumes.

[1] Free downloads are available via the USGS website http://water.usgs.gov/software/modflow.html.
[2] In this report, the term *model* refers to a mathematical model that represents the field situation, while the term *model code* refers to the program or set of commands that is used to solve the model. A *model* is site- and objective-specific, whereas a *code* is generic and can be applied to many sites and problems.
[3] Go to http://www.flowpath.com/Software/VisualMF/VisualMF.html for information about Visual MODFLOW®.

6.0 Conceptual model

Development of a conceptual model is a prerequisite to development of a numerical model. The conceptual model should describe the main components and processes involved in the hydrologic system. Figure 6-1 shows a simplified cross-section through the San Juan Basin, showing the principal hydrologic components and processes. The alternative conceptual model is shown in Figure 6-2. The following text discusses these items in more detail.

6.1 Boundaries

6.1.1 Geologic boundaries

The uppermost boundary of a groundwater model is the ground surface. A 3-D representation of the San Juan Basin is shown in Figure 6-3.

The Fruitland Formation is a large-scale fining-upward sequence, consisting of alternating coals and shales, with some sandstone units. The basal coals are typically thicker than stratigraphically higher coal beds, which are thinner and more discontinuous both vertically and laterally. Hydraulic permeability is conventionally considered to be orders of magnitude higher in the coal units than in the shale units, so that the overall transmissivity of the Fruitland Formation is mainly due to the coal beds. This is particularly the case when data from CBM production wells are used to test Fruitland Formation transmissivity, as these wells are typically only perforated adjacent to the main coal units.

During the period of model development, there was no publicly available, generally accepted grouping of Fruitland Formation coals into hydraulically related packages. Because of this limitation, all Fruitland Formation coals were treated as one unit, with a thickness equal to their combined thickness (net coal thickness).

The Fruitland Formation outcrop was digitized from USGS 1:500,000 base maps (combined at 1:380,160 in Fassett and Hinds, 1971). Based on low vertical permeabilities in the underlying Pictured Cliffs Sandstone and Lewis Shale, and in the overlying Kirtland Shale, a single-layer model of the Fruitland Formation was used, with implicit impermeable upper and lower boundaries. The “Fruitland” layer actually includes the Pictured Cliffs Sandstone in areas where it is more permeable and hydraulically connected.

A simplified 3-D representation of the Fruitland Formation and its over- and underlying formations is shown in Figure 6-4.

Figure 6-1

Conceptual model of the San Juan Basin

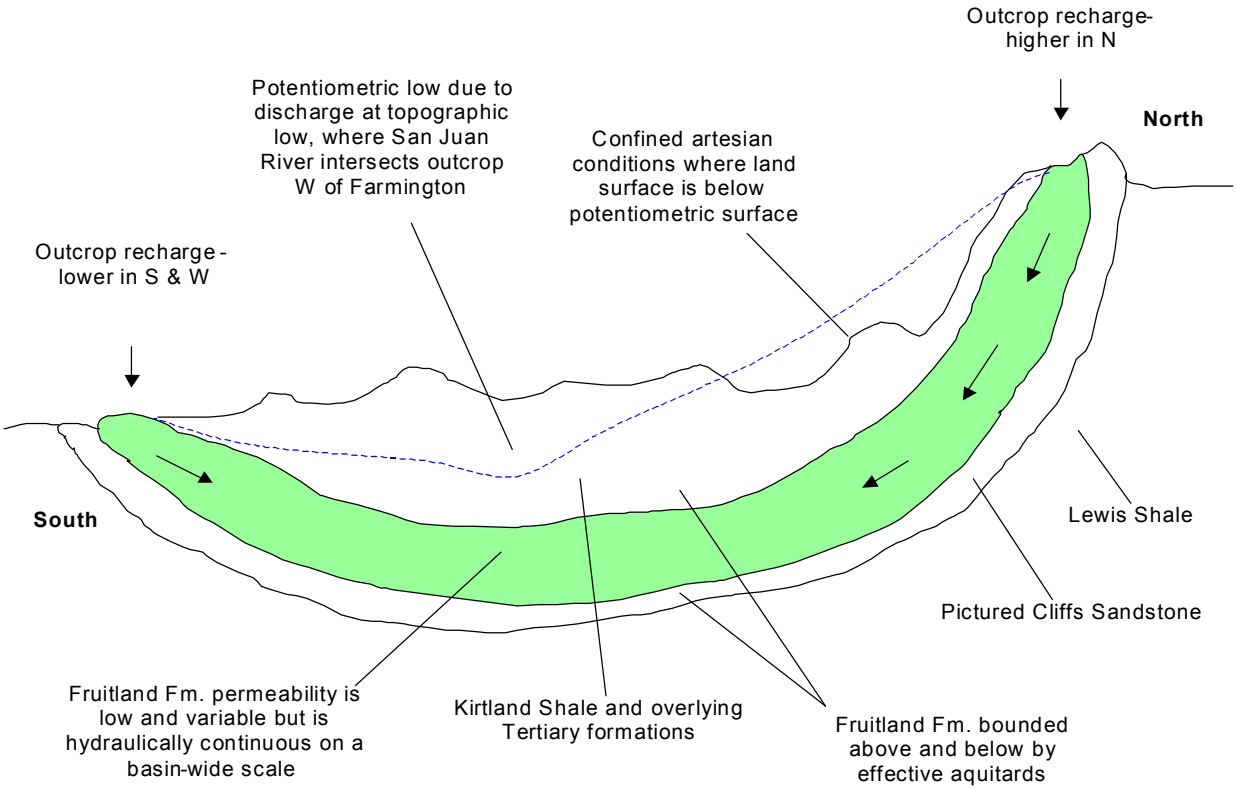

Figure 6-2

Alternative conceptual model of the San Juan Basin

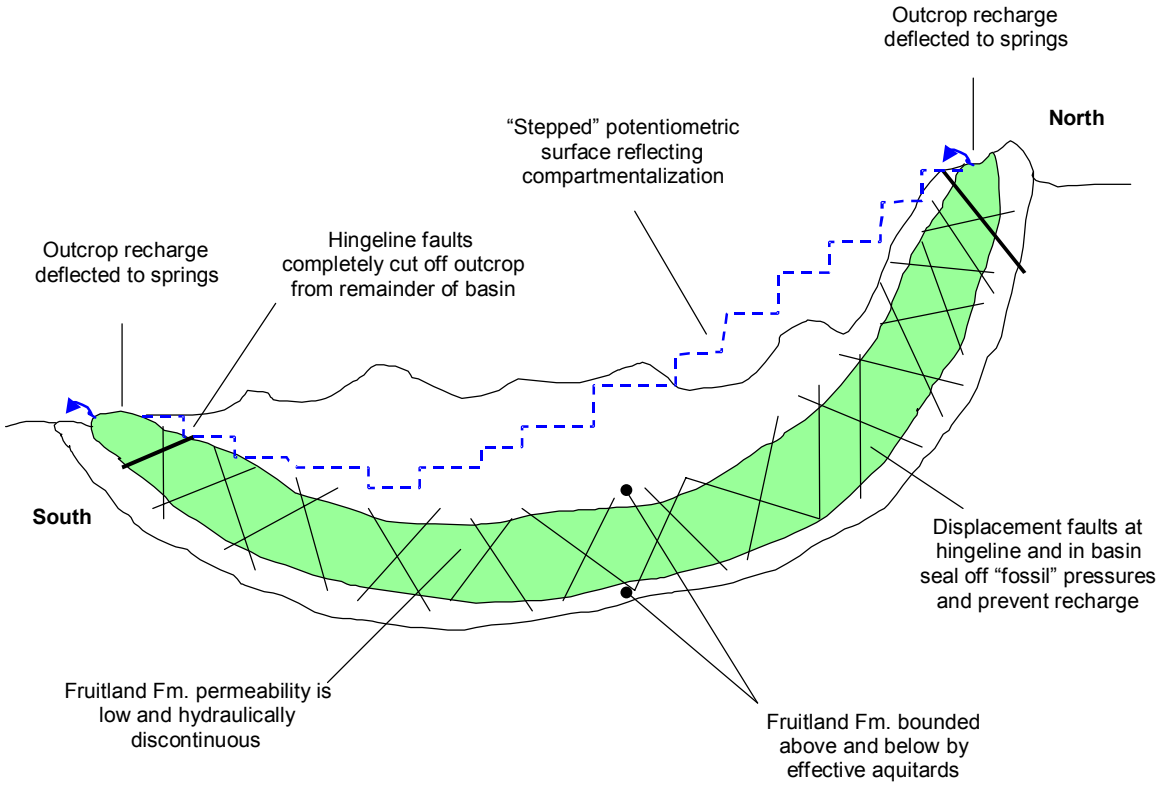

Figure 6-3

San Juan Basin topography

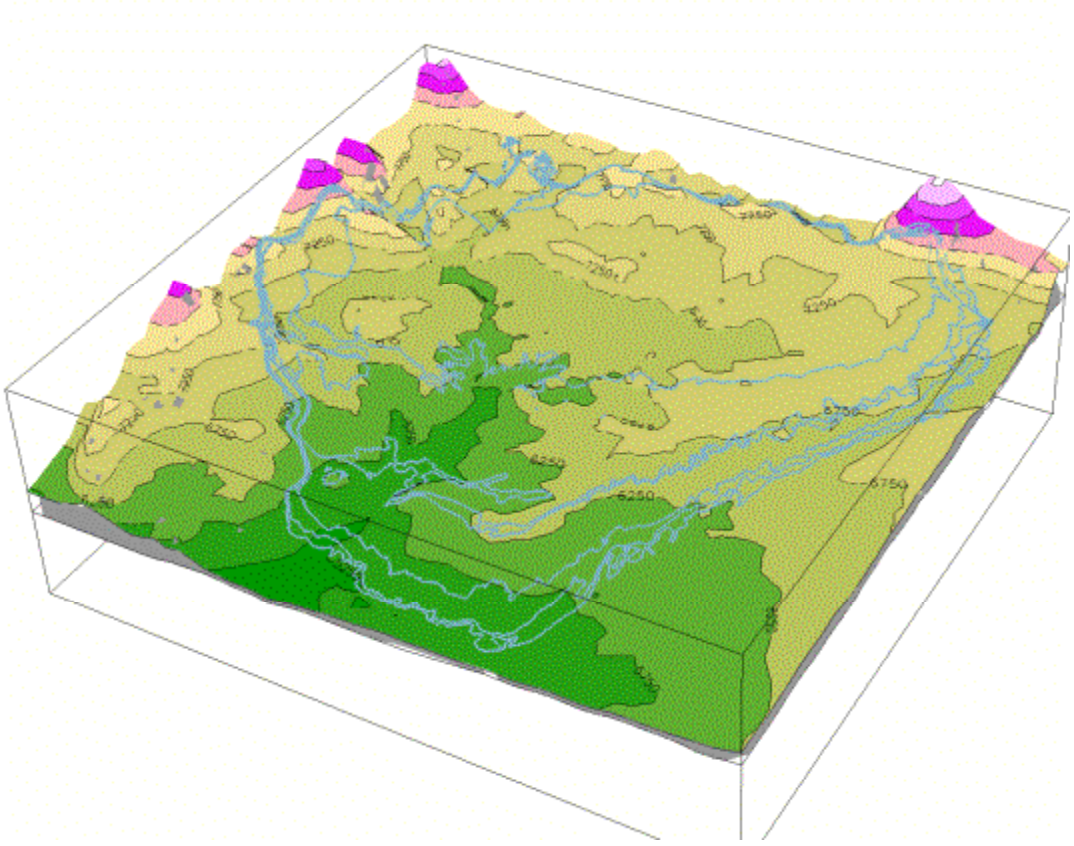

Fig. 6-3: San Juan Basin outcrop (to bottom of the Pictured Cliffs Sandstone), superimposed on vertically exaggerated 3-D surface topographic contours.

Figure 6-4

San Juan Basin simplified geology

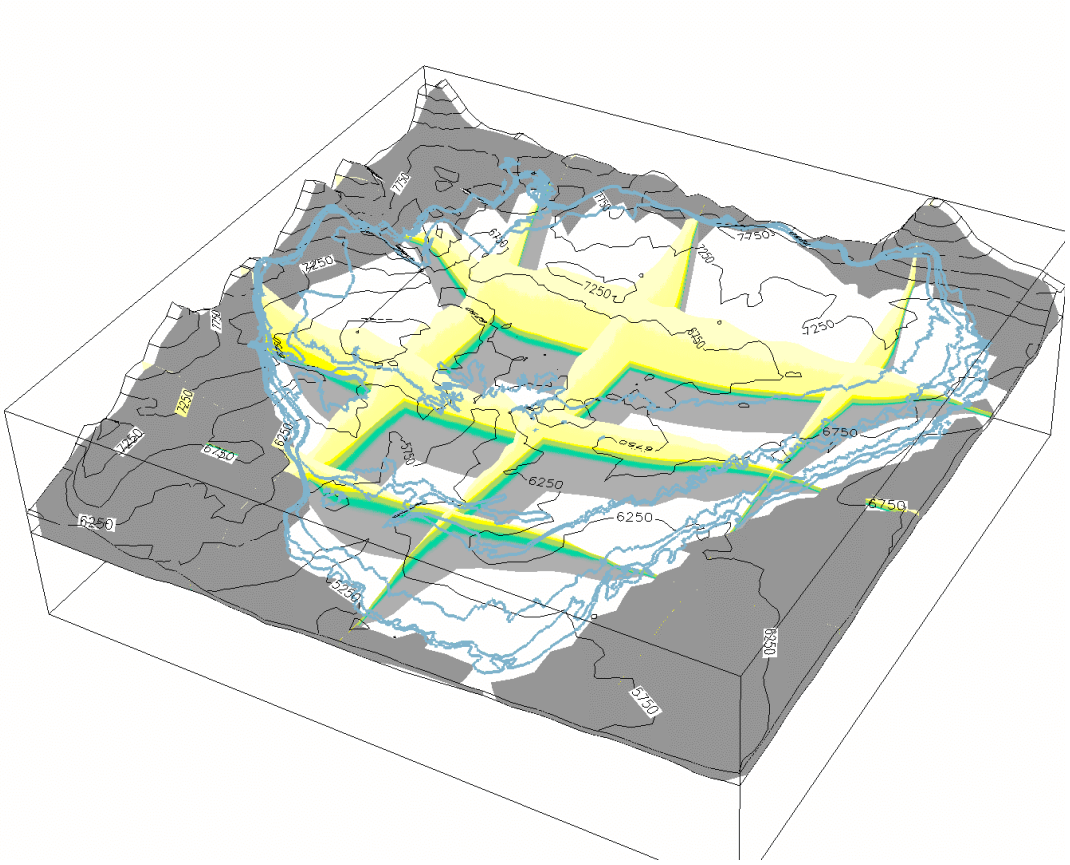

Fig. 6-4: Surface contour colors removed to show the following stratigraphic elements in fence diagram style:

- San Jose Formation
- Nacimiento Formation - Animas Formation
- Ojo Alamo Sandstone
- Kirtland Shale
- Fruitland Formation
- Pictured Cliffs Sandstone
- Lewis Shale

Dark gray is outside the modeled area (“inactive”).

Interflow between the underlying Pictured Cliffs Sandstone and the Fruitland Formation occurs in the northern part of the San Juan basin. In areas where Pictured Cliffs Sandstone is more permeable and is hydraulically connected to the Fruitland Formation, the modeled layer includes both formations.

6.1.2 Outcrop recharge

Where the Fruitland Formation outcrops, it can receive recharge from diffuse precipitation. Recharge is defined as the entry of water into the saturated zone of an aquifer. It varies with time, and for long-term groundwater modeling, a long-term average value is required, varying spatially across the model.

Recharge can be measured directly using a lysimeter, which is effectively a sub-root zone “rain gauge”. This technique is generally only useful for detailed studies of small areas: lysimeters are expensive to construct; the measured values only apply at one point; and in arid climates, recharge events may be infrequent, requiring a long measurement period to get meaningful average. Therefore, for most basin studies, recharge is usually estimated. There are several recharge estimation techniques, including:

1. Climatic data analysis
2. Groundwater hydrograph recession analysis
3. Natural tracers
4. Age-dating isotopic tracers
5. Event-marking isotopic tracers

Further details, and the applicability of these techniques to the 3M project, are discussed below.

1. Recharge can be calculated indirectly from climatic data, from which evapotranspiration is estimated and subtracted from precipitation.

   Problems: (1) evapotranspiration varies with vegetation type, root depth, leaf area index, slope, and aspect, all of which vary spatially, requiring a significant computational effort; (2) the technique does not account for surface water runoff, which has to be measured separately, and may take several years to develop an average; (3) this kind of water balance estimates recharge as the difference between two large numbers - errors in these numbers have a very large effect on the difference; (4) in arid climates, recharge is often concentrated at stream channels rather than spread out evenly.

2. Recharge can be deduced from groundwater hydrograph recession analysis by calculating the change of water in storage due to precipitation events, and correlating the result with measured rainfall.

Problems: (1) this technique requires long-term groundwater level monitoring data; (2) it requires an estimate of specific yield (effective porosity), which is normally unknown.

3. Recharge can be estimated from natural tracers. The chloride mass balance method is simple, inexpensive, and especially useful for arid climates. It requires chloride analyses of a representative set of groundwater samples and a time series of rainwater and/or surface water samples. For short-term use, chloride flux in the unsaturated zone must also be estimated. For long-term use, this can be assumed to be constant. Problem: recharge rates and chloride (Cl) concentrations likely varied over geologic time. This can be corrected for by using isotopic tracers. Also, dry chloride precipitation (i.e., deposition of dry salt dust) must be taken into account.

4. Recharge can be inferred from age-dating isotopic tracers. Isotopic ages, combined with distance from the outcrop and aquifer hydraulic parameters, can indicate the long-term rate of inflow. A well-know tracer is carbon-14 (^{14}C), which with a half-life (T½) of 5,730 years can be useful for dating historic artifacts and groundwaters from a few centuries to about 50,000 years old (the oldest detectable age depends on the lowest level of activity measurable by the laboratory equipment). Difficulties occur if the element being used is non-conservative, i.e., takes part in reactions in the aquifer (Freeze and Cherry, 1979). To back these effects out may require a complex combination of groundwater flow and hydrochemistry modeling. Isotopes that are usually more conservative are the halide isotopes iodine-129 (^{129}I) and chlorine-36 (^{36}Cl). With a T½ of 15.7 MY, ^{129}I can be useful in dating water in the 5 to 100 MY age range, while with a T½ of 0.3 MY, ^{36}Cl can be useful in the 0.1 to 5 MY age range. One problem is that, in a dynamic groundwater system, apparent isotopic ages may represent a mixture of older and younger waters.

5. Recharge can be inferred from event-marking tracers. Specifically, thermonuclear ("bomb") tritium (^{3}H) and ^{36}Cl indicate water that recharged during the main atmospheric nuclear-testing period, between 1952 and 1963. These are good tracers due to their worldwide distribution. Freons (chlorofluorocarbons, or CFCs) also indicate post-1945 recharge, but are usually only present at useful concentrations in industrial areas. Tritium (^{3}H) has been widely used but, due to its short half-life (T½) of 12.3 years, the ^{3}H bomb signal is now weak, especially in mixed waters. ^{36}Cl analysis is more expensive than ^{3}H, but it is longer lasting, has a more compact signal, and is easier to sample. Therefore, ^{36}Cl does "double duty" as an age-dating isotope and an event marker. Hence, it can be used both to identify recent recharge and to date water. Note that ^{129}I also shows a bomb event peak.

As a contribution to the 3M project, Vastar collected numerous produced water samples from the Fruitland Formation at approximately one sample per township in Colorado and the upper tier of New Mexico, and performed detailed geochemical analysis, including ^{129}I and ^{36}Cl dating (Riese, 2000). This project is continuing, and additional data will likely be presented after the date of this report.

Stable isotopes of oxygen and hydrogen can also be used as event-tracing markers. The specific ^{18}O:^{16}O and ^{2}H:H ratios can be used to infer the mean annual air temperature when the recharge took place. Therefore, a low-temperature signature can

be used to infer recharge during a glacial period. The last glacial period in North America ended at the start of the Holocene, about 11,000 y BP. Phillips et al (1986) have reconstructed the mean annual temperature for the San Juan Basin using radiocarbon dating of groundwater in the Tertiary age Ojo Alamo Sandstone overlying the Fruitland Formation, combined with noble gas (xenon-krypton) paleothermometry. Groundwater in the Ojo Alamo Sandstone formation is suitable for radiocarbon dating because the formation has a low carbonate content (Phillips et al, 1989). This work indicated a mean annual air temperature of only 2-4° C during the period 7,000 to 35,000 y BP. Therefore, a low-temperature stable isotope signature in the Fruitland Formation would infer similar age water.

For the 3M project, a multiple-technique approach to estimating recharge was made, as follows:

1. Review other regional or basin studies of aquifer recharge to obtain the likely range of recharge values.

2. Interpret the large amount of available Cl data using the chloride mass balance method, and estimate recharge rates.

3. Use these data to initialize the calibration of the steady-state groundwater model, using given permeabilities, and optimizing on recharge rates.

4. Compare the calibrated recharge values and resulting groundwater age dates with age dates based on ^{129}I ages from the Vastar study.

5. Obtain ^{36}Cl data when possible, to extend the lower age range from the Vastar study.

6. Compare groundwater path lines and age dates with stable isotope results.

A review by Prucha (2000) of several other regional basin studies in the Four Corners region is presented in Appendix A. The chloride mass balance analysis using USGS rainfall chemistry data and shallow groundwater chemistry is described in Appendix B. The calibration process and comparison with isotope age dates is presented in Section 8.0.

The summary of regional studies (Appendix A) shows that recharge varies widely over the southwestern US. However, it normally averages as a low percentage of annual precipitation. Where calculated on this basis, for the Colorado Plateau, recharge varies from 0.3% to 20% of precipitation, and for many studies is around 1%. This reflects the extremely high evapotranspiration potential in the arid to semi-arid Southwest.

The chloride mass balance study (Appendix B) produces a calculated recharge value of 0.05 inches per year over the Colorado Fruitland Formation outcrop, which is about 0.4% of average annual precipitation. This is lower than, but in the same order of

magnitude as, the value of 1% of average annual precipitation calculated for the San Juan Basin by Kernodle (1996).

These initial values for recharge rates were subsequently adjusted to get the best fit in the model, as described in Section 8.0.

6.1.3 Outcrop discharge

Where the Fruitland Formation outcrops, if the potentiometric head is above the ground surface, groundwater will discharge to springs or surface water. This is best modeled by applying a maximum head (drain boundary) to the relevant model cells, equal to the ground surface elevation at the lowest point on the outcrop.

6.1.4 River/outcrop intersections

Several perennial streams and rivers traverse the Fruitland Formation outcrop, particularly in the Colorado portion of the San Juan Basin. Where the Fruitland Formation is in direct contact with permeable alluvial deposits, the potentiometric head in the formation at that location is largely controlled by the head in the alluvium. Alluvium heads do not vary greatly from year to year. For example, in the Pine River Ranches area, the two alluvium monitoring wells with the longest continuous monitoring records, the Pick Bar and James #2 wells, show average potentiometric heads of approximately 7,146 and 7,147 ft MSL over a five-year period with a maximum annual fluctuation of only 4 feet (Oldaker, 1999). Therefore, river boundary heads may be considered to be steady over the long term.

Surface water can either recharge the formation, or can receive discharge from the formation, depending on the relative vertical hydraulic gradient. These characteristics are best modeled by applying a constant head to the relevant model cells, equal to the stream or alluvial groundwater elevation at the outcrop. However, because constant head cells imply an unlimited availability of water for recharge, modeled recharge amounts (if any) should be compared with gauged stream flows to confirm that recharge volumes are reasonable.

6.2 Properties

6.2.1 Permeability

6.2.1.1 Permeability at production wells

Permeabilities were determined by Questa, based on maximum gas and/or water production rates. The distribution of permeability values across the San Juan Basin is shown in Figure 6-5. The detailed distribution of permeability values for the Colorado portion of the San Juan Basin is shown in Figure 6-6.

Because the hydrologic model simulates the entire Fruitland Formation as one layer, coal permeabilities were corrected by multiplying by (net coal thickness)/(Fruitland Formation thickness) to obtain the same equivalent transmissivity. This ratio is generally around 20%.

6.2.1.2 Effective permeability

The effective regional permeability could be higher or lower than that determined through the Questa analysis of data from individual wells. These permeabilities apply to a specific well and its surrounding area of influence, and the data are interpolated into the San Juan Basin as a whole. As discussed above, the effect of “shingling” does not necessarily reduce overall permeability, and may actually increase it. The separation of coal packages from each other, and the stratigraphic termination of packages, may reduce overall continuity; this scenario should be tested with a multi-layer model using defensible shale permeability values.

Various authors have invoked the presence of widespread faults as either a sealing mechanism or a permeability enhancer. The spatial frequency of displacement faulting is not known for most of the San Juan Basin. However, if faults are widespread, and are always flow barriers, they should affect some production wells, presumably by reducing water and gas flows. In this case, the effect of faulting should already be incorporated into the production well analysis.

The effect of significantly reduced permeability was explored through a sensitivity analysis, which is described in Section 9.0. This showed that if permeabilities were much reduced, the net recharge to the San Juan Basin to balance heads would be virtually zero.

6.2.2 Porosity

Porosity is not an important part of a steady-state hydrologic model, as the release of water from storage does not occur. However, it is a significant factor in calculating groundwater migration rates; for a given groundwater flow, the groundwater velocity is inversely proportional to the formation effective porosity, as follows:

Figure 6-5

Fruitland Formation permeability distribution - San Juan Basin

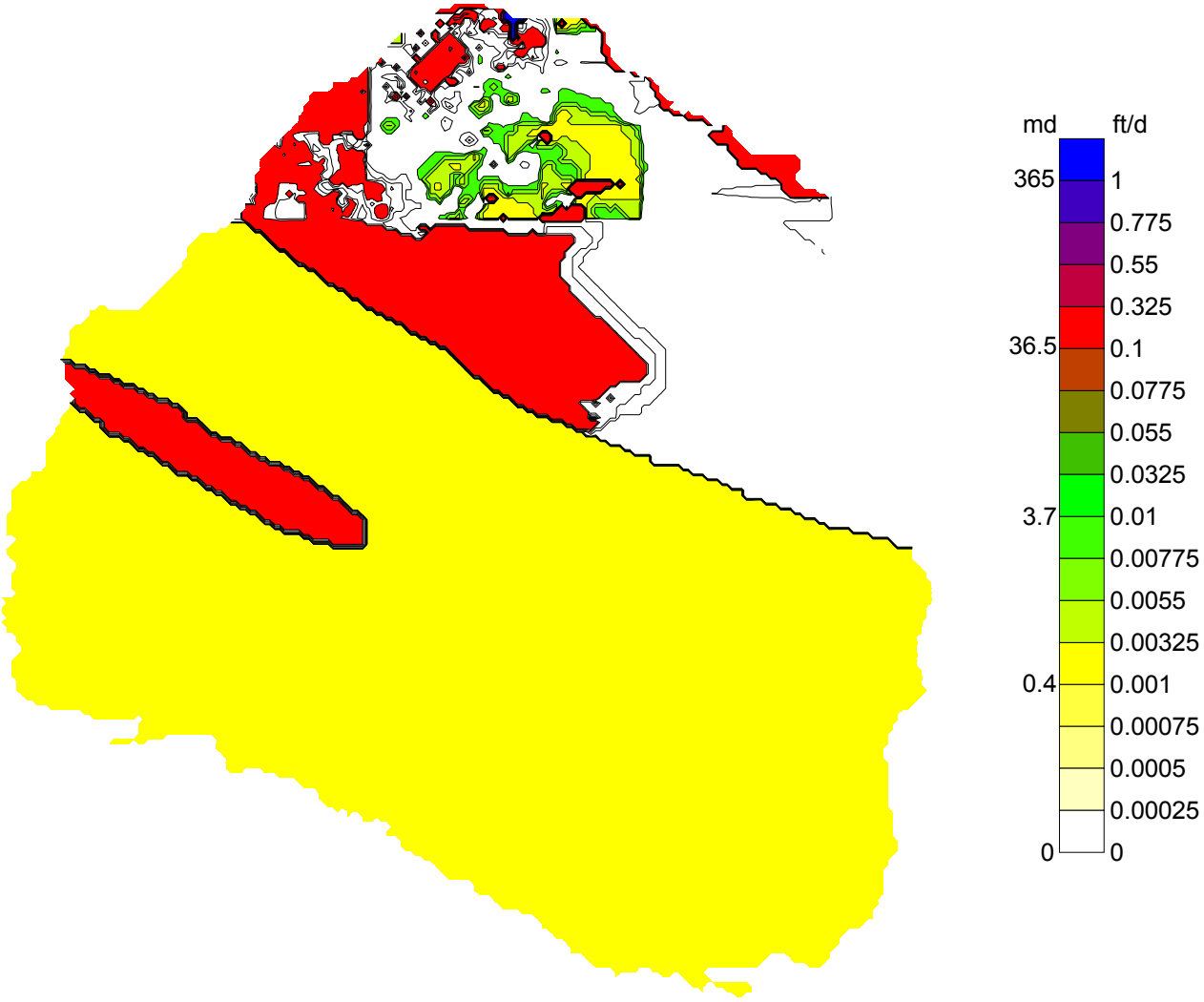

Figure 6-6

Fruitland Formation permeability distribution - Colorado

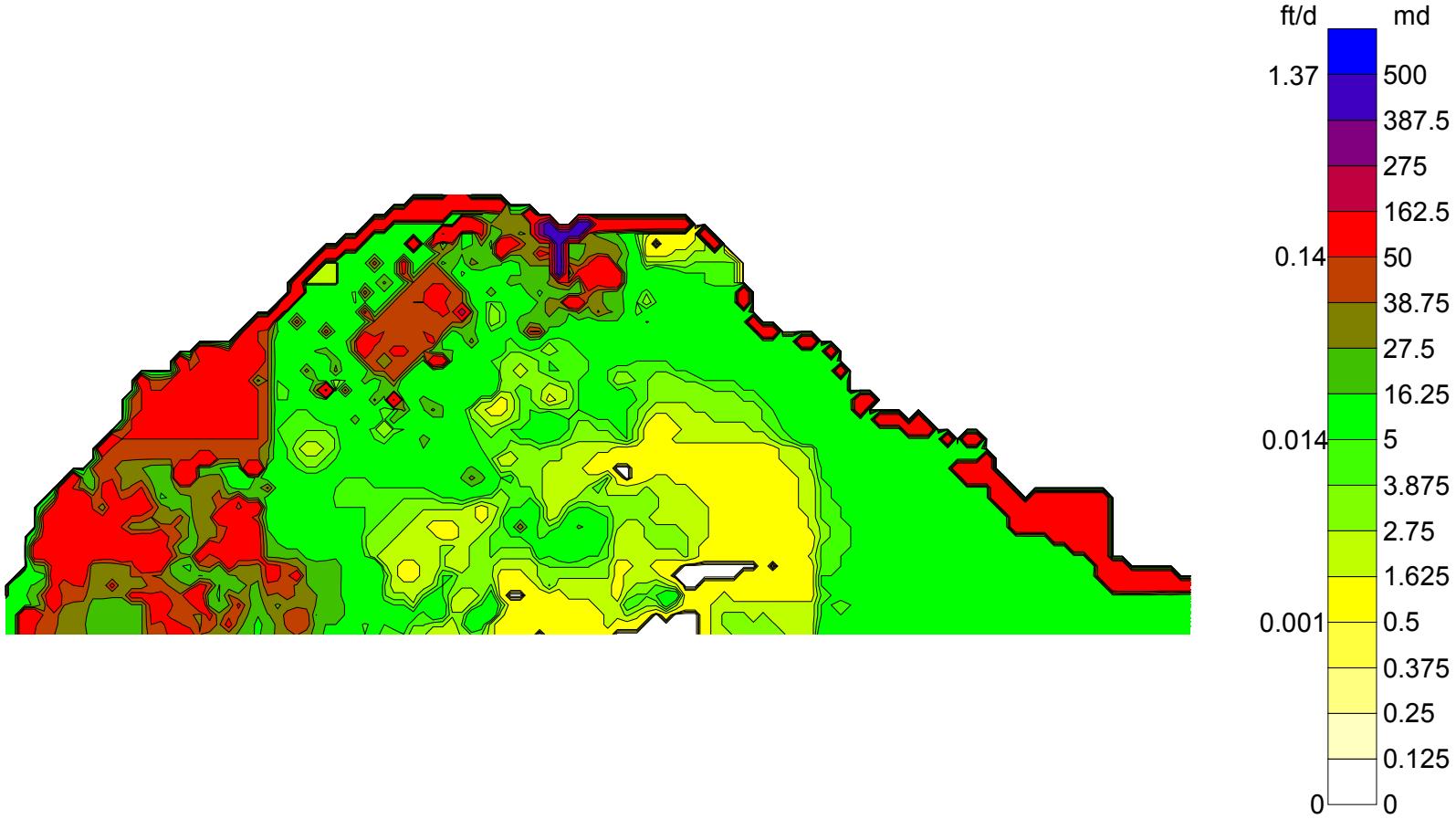

$$V_{gw} = ki/ n_e$$

Where:

V_{gw} = groundwater flow velocity
k = hydraulic conductivity
i = hydraulic gradient
n_e = effective porosity

Porosities were determined by Questa, based on historic water production rates and related pressure declines. The detailed distribution of porosity values for the Colorado portion of the San Juan Basin is shown in Figure 6-7.

6.2.3 Storativity

Similarly, storativity, which is the elastic storage due to the compressibility of the formation matrix and (to a much lesser extent) groundwater, is unimportant for steady-state hydrologic modeling and, as the above equation shows, is not a factor affecting groundwater velocity. Therefore, this parameter was not considered for the main hydrologic model. Ancillary transient models, such as the relaxation model discussed in Section 4.1, used storativities based on compressibility-porosity-thickness (ϕch) values determined by Questa.

Figure 6-7

Fruitland Formation porosity distribution – Colorado

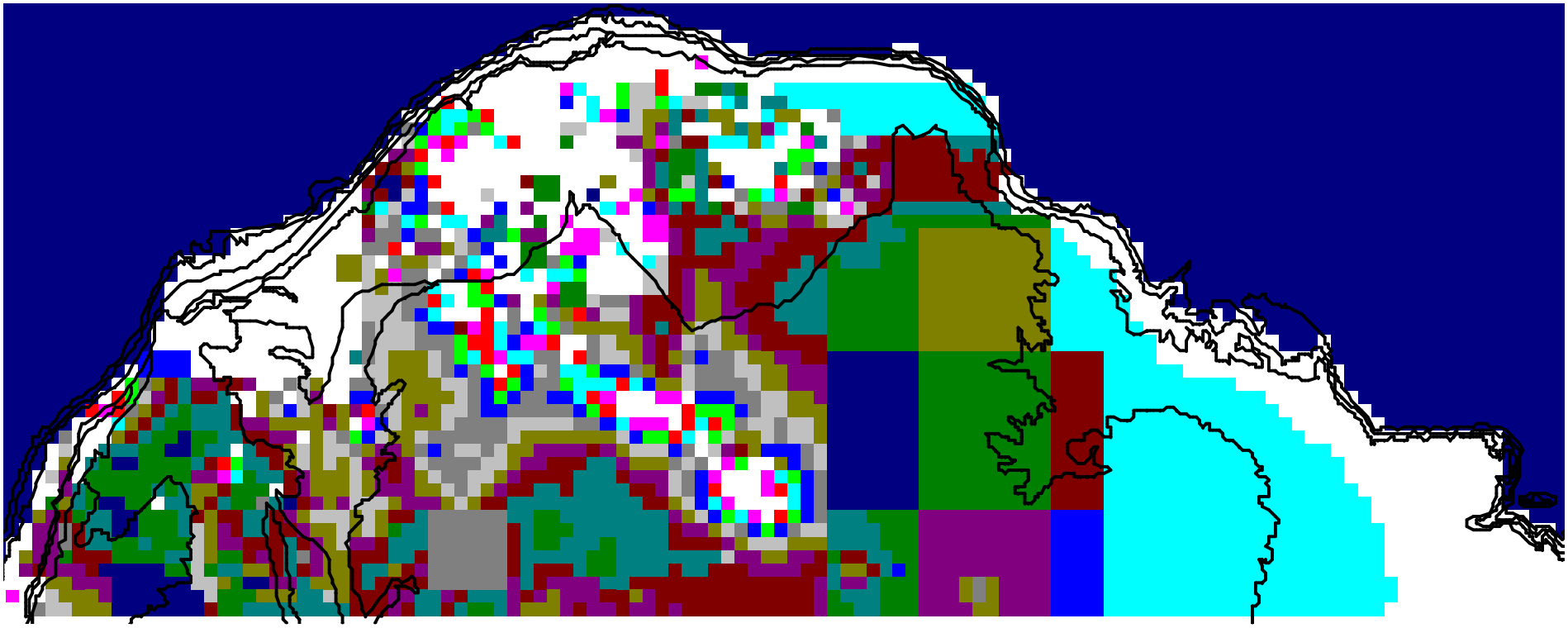

Fig. 6-7: A total of 252 porosity values were applied to fields in the San Juan Basin as shown in this figure. For full details, see model files. The uncolored areas have a “standard” porosity of 0.005%.

7.0 Model development

7.1 Grid projection and coordinates

The model grid discretization was based on a Universal Transverse Mercator (UTM) projection referenced to the North American Datum of 1927 (NAD27) with a central meridian of 107° 39' W. This projection was chosen so that the center of the reservoir model would be aligned north. Data used to construct the groundwater model was converted to model grid coordinates using the coordinate conversion program Tralaine® from Mentor Software, Inc.

7.2 Discretization

The modeling effort was conducted at two scales. For the groundwater model, the entire San Juan Basin, as defined by the contact between the base of the Fruitland Formation and the top of the Pictured Cliffs Sandstone (PCS), was discretized on a ½-mile grid with 211 columns (N-S) and 221 rows (E-W). For the reservoir model, the Colorado part of the San Juan Basin was modeled on a 1/6-mile grid spacing, to allow the effects of individual operating CBM wells or groups of wells to be simulated.

7.3 Geologic boundaries

The contact between the Fruitland Formation and the Pictured Cliffs Sandstone (PCS) was digitized from the *Geologic Map of the San Juan Basin* (USGS, 1977). The elevation of the top of the PCS was digitized from Kernodle et al (1990), and the thickness of the Fruitland Formation and Pictured Cliff Tongue were digitized from Kaiser and Ayers (1994) (Figures 2.11 and 2.9, respectively). The digitized geologic contact and upper and lower Fruitland Formation surfaces were converted to model coordinates using the program Multric® from Mentor Software, Inc.

The digitized elevation and thickness contours were then kriged onto the model grid using the mapping program Surfer® from Golden Software, Inc. The gridded Pictured Cliffs Tongue thickness was subtracted from the thickness of the Fruitland Formation. This result was in turn added to the elevation of the Fruitland Formation/PCS contact to get the elevation of the top of the model domain.

The gridded top and bottom of the Fruitland Formation were then imported into Visual MODFLOW, which was used to generate Figures 7-1 and 7-2, respectively.

Figure 7-1

Modeled top of Fruitland Formation

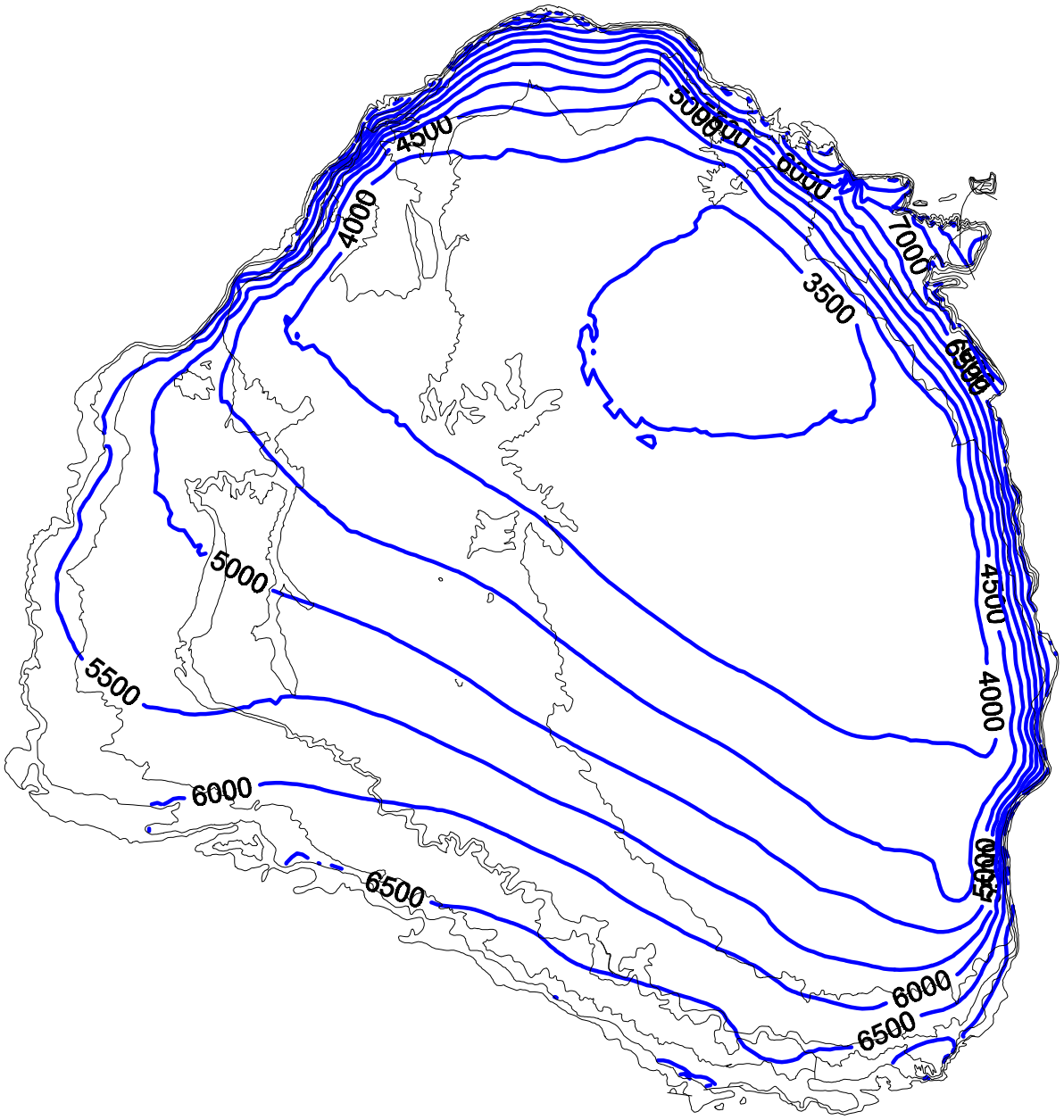

Fig. 7-1: Elevation of the top of the Fruitland Formation in ft-MSL.

Figure 7-2

Modeled base of Fruitland Formation

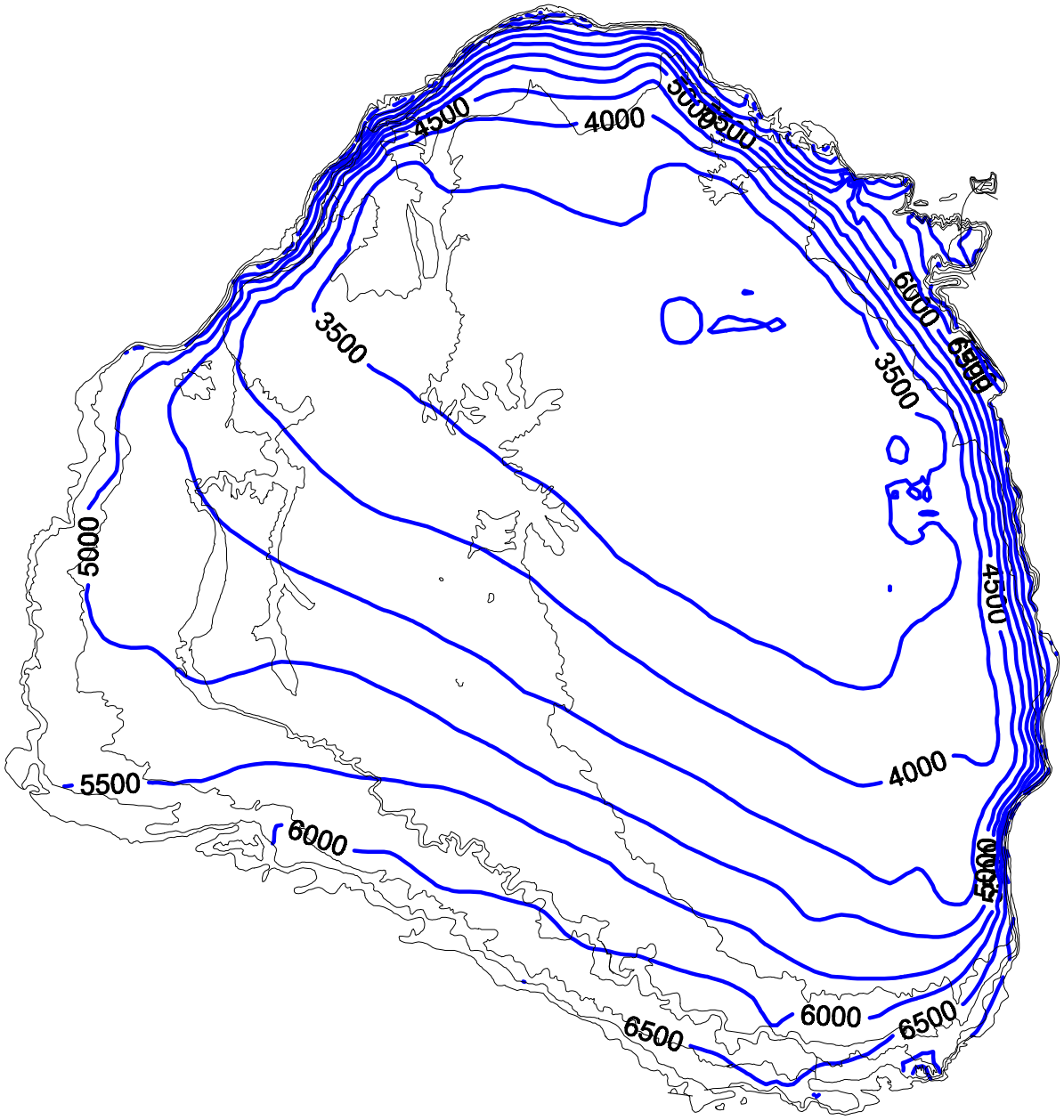

Fig. 7-2: Elevation of the base of the Fruitland Formation in ft-MSL.

7.4 Outcrop recharge

Outcrop recharge was applied at outcrop nodes, defined as those model cells occupied by at least 50% outcrop area. Recharge values applied after calibration (see Section 8.0 for details) are shown in Figure 7-3.

7.5 Outcrop discharge

Outcrop discharge was modeled by drain nodes, applied at outcrop locations occupied by springs. Only three springs were identified during the CGS field-mapping program, as follows:

Easting	Northing	Elevation
1,605,120	13,543,000	7,390
1,609,380	13,547,200	8,360
1,610,900	13,546,100	7,800

7.6 River/outcrop intersections

Locations where perennial rivers or streams intersect the Fruitland Formation outcrop were modeled as constant head boundaries in MODFLOW. Use of constant head boundaries allows for either discharge from the Fruitland Formation to the river or recharge from the river to the Fruitland Formation. The following table lists these rivers and the elevations of the Fruitland Formation outcrop at the intersections with the rivers. Outcrop elevations were taken from USGS 1:100,000 Digital Line Graph data, using the nearest (metric) elevation contour.

River	Elevation (m)	Elevation (ft)
La Plata		5,971
Animas		6,562
Florida		7,054
Los Pinos		7,218
Piedra		6,562
San Juan East		6,562
Navajo		6,562
Rio Puerco		6,726
San Juan West		6,562

Locations of constant-head nodes are shown in Figure 7-4

Figure 7-3

Outcrop recharge

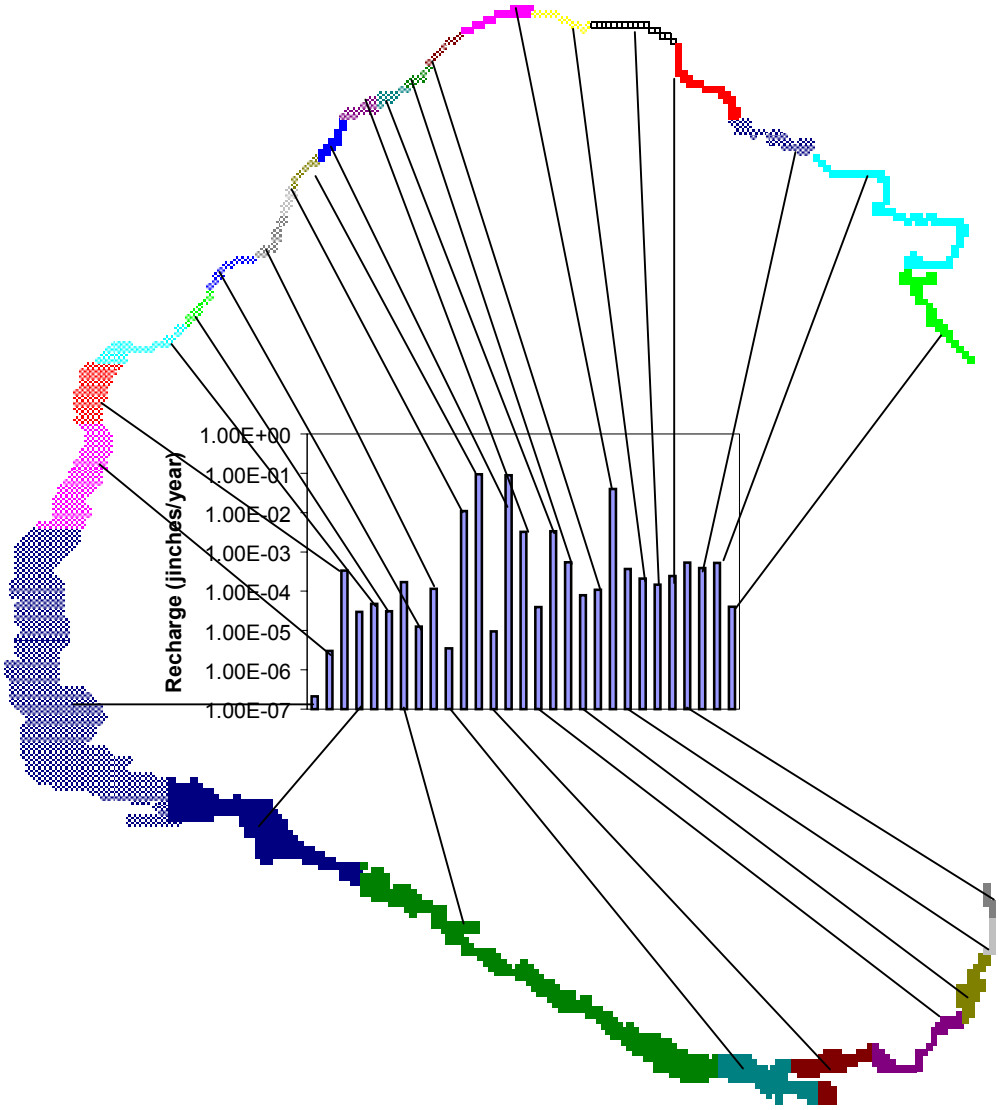

Figure 7-4

Constant-head (river) nodes

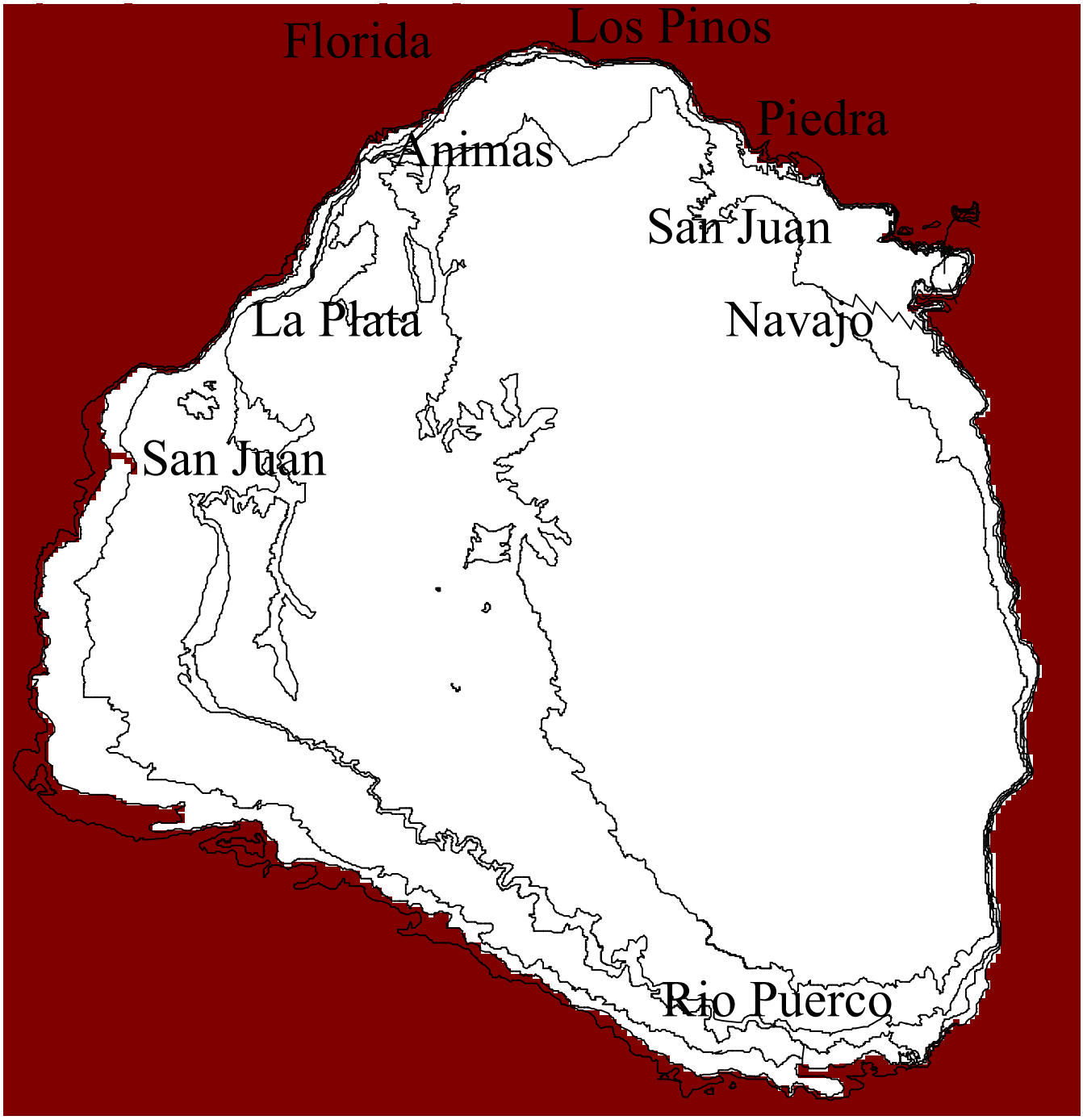

Note that the river boundary near Farmington is referred to in the text as *San Juan West*, while that on the northern outcrop is referred to as *San Juan East*.

7.7 Properties

Aquifer properties of permeability, porosity, and storativity were applied as described in Section 6.2.

8.0 Model calibration

8.1 Recharge optimization

The model was calibrated primarily to refine the initial values of recharge. This was accomplished using the inverse modeling system developed for MODFLOW by the USGS, named PEST, for Parameter ESTimation. PEST can be used to optimize any hydrologic parameter, given a match target, with all other parameters staying constant. For this project, PEST was used to optimize the initial recharge values to obtain the best match against all the target potentiometric head data, using the assigned permeability values. This is essentially a trial-and-error process, in which the model is run numerous times to determine trends and then "home in" on the best fit. The optimization process for a single steady-state time step required a computer run of several hours. This process was repeated many times in the course of the modeling project, as permeabilities and conceptual models were revised and modified.

The final calibration run resulted in varying values of recharge for segments of the outcrop. As expected, these recharge values generally decrease, from high elevation to low elevation, from north to south, and from east to west, as shown in Figure 8-1. Note that the vertical scale on the graphical insert in this figure is logarithmic, reflecting the wide range in precipitation and recharge values across the San Juan Basin.

Figure 8-1 shows that the PEST-optimized values of recharge for most of the outcrop are lower than the value of 0.047 in/yr predicted for Colorado from the chloride mass balance analysis (Appendix B). This is because (1) recharge as a percentage of precipitation varies greatly across the San Juan Basin and is generally lower in New Mexico, which is more arid, than Colorado. The optimized recharge values were used for subsequent model runs, and (2) the modeled outcrop width of ½ mile is greater than the actual Fruitland coal outcrop width.

8.2 Potentiometric head target

The target potentiometric head surface is shown in Figure 8-2. The most reliable potentiometric head data are considered to be spring elevations, water table elevations in unused (or little-used) water supply wells and observation wells, and initial bottom-hole pressures, corrected for fluid density and elevation, at newly-installed CBM wells before the start of production. The individual production wells on which this figure is based are not shown in Figure 8-2, as this data is proprietary to the individual operators. Modeled potentiometric heads are shown in Figure 8-3. Visual comparison of these figures shows that the agreement is generally good. Quantitative evaluation of the calibration graph is presented in Figures 8-4 and 8-5. These show a good match, with a very low error relative to the total variation in hydraulic elevation across the San Juan Basin. The variances show normal scatter, and calculated versus observed heads lie close to the 1:1 line.

Figure 8-1

Calibrated recharge values

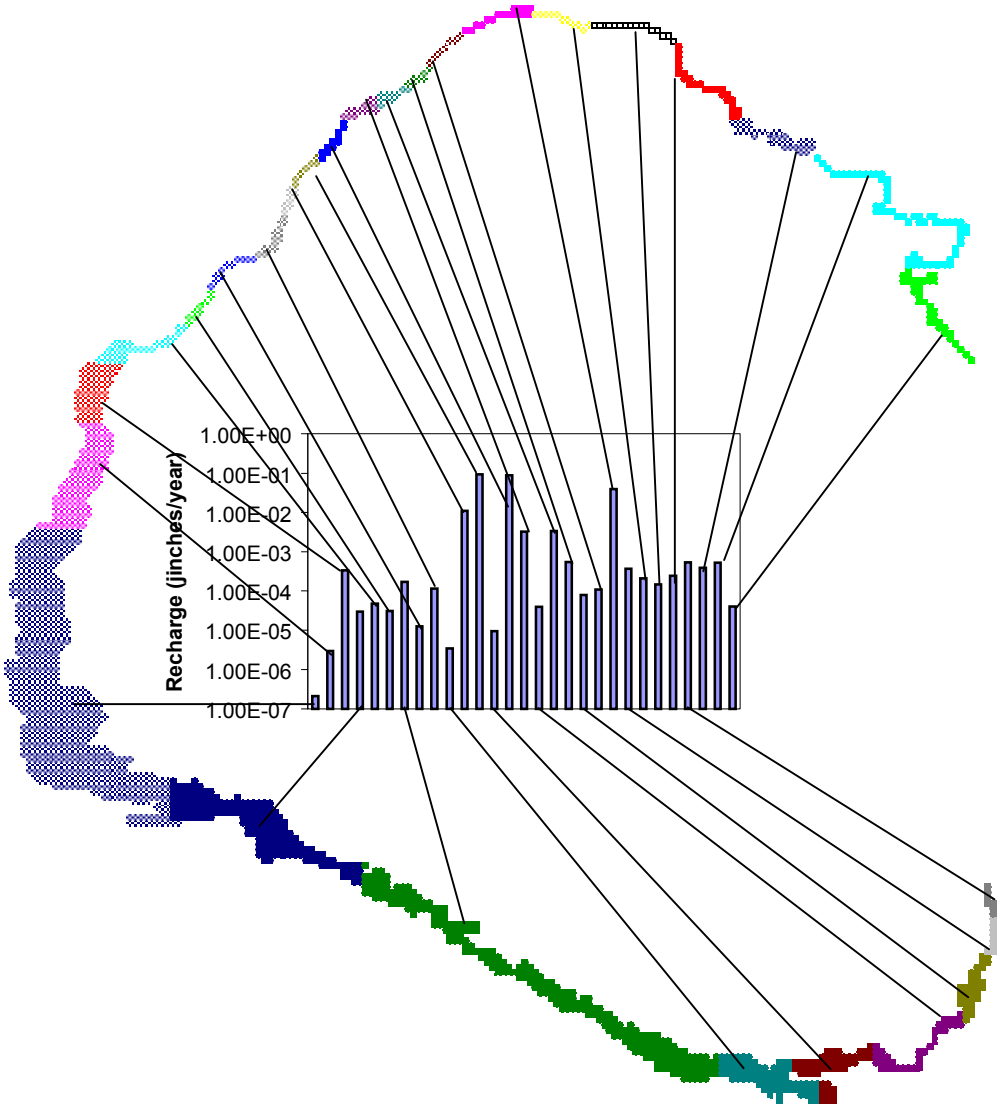

Figure 8-2

Potentiometric surface for calibration

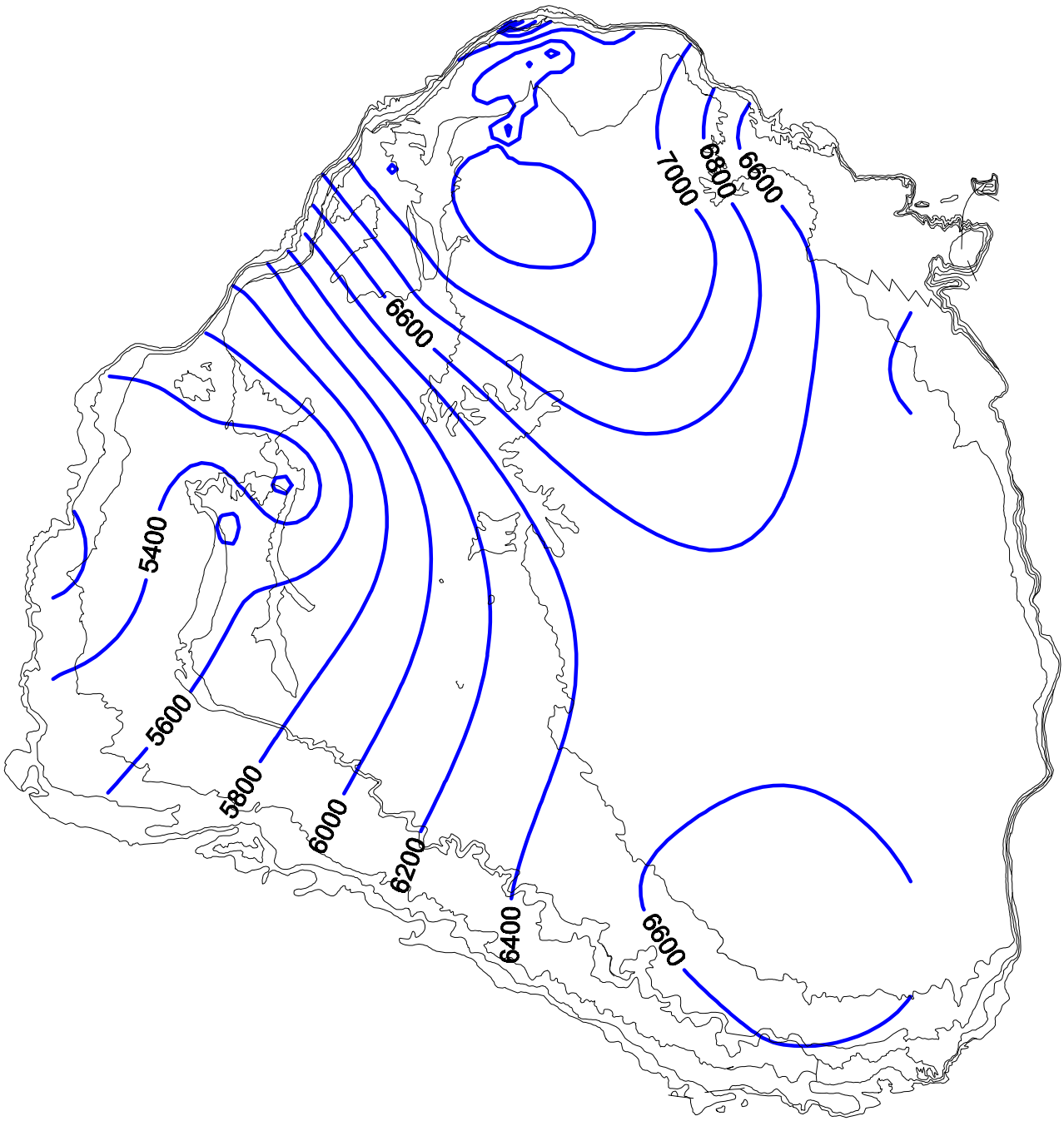

Fig. 8-2: Potentiometric surface (ft-MSL) used for calibration. 200-ft contours are interpolated between data points. Data points are not shown.

Figure 8-3

Modeled potentiometric surface

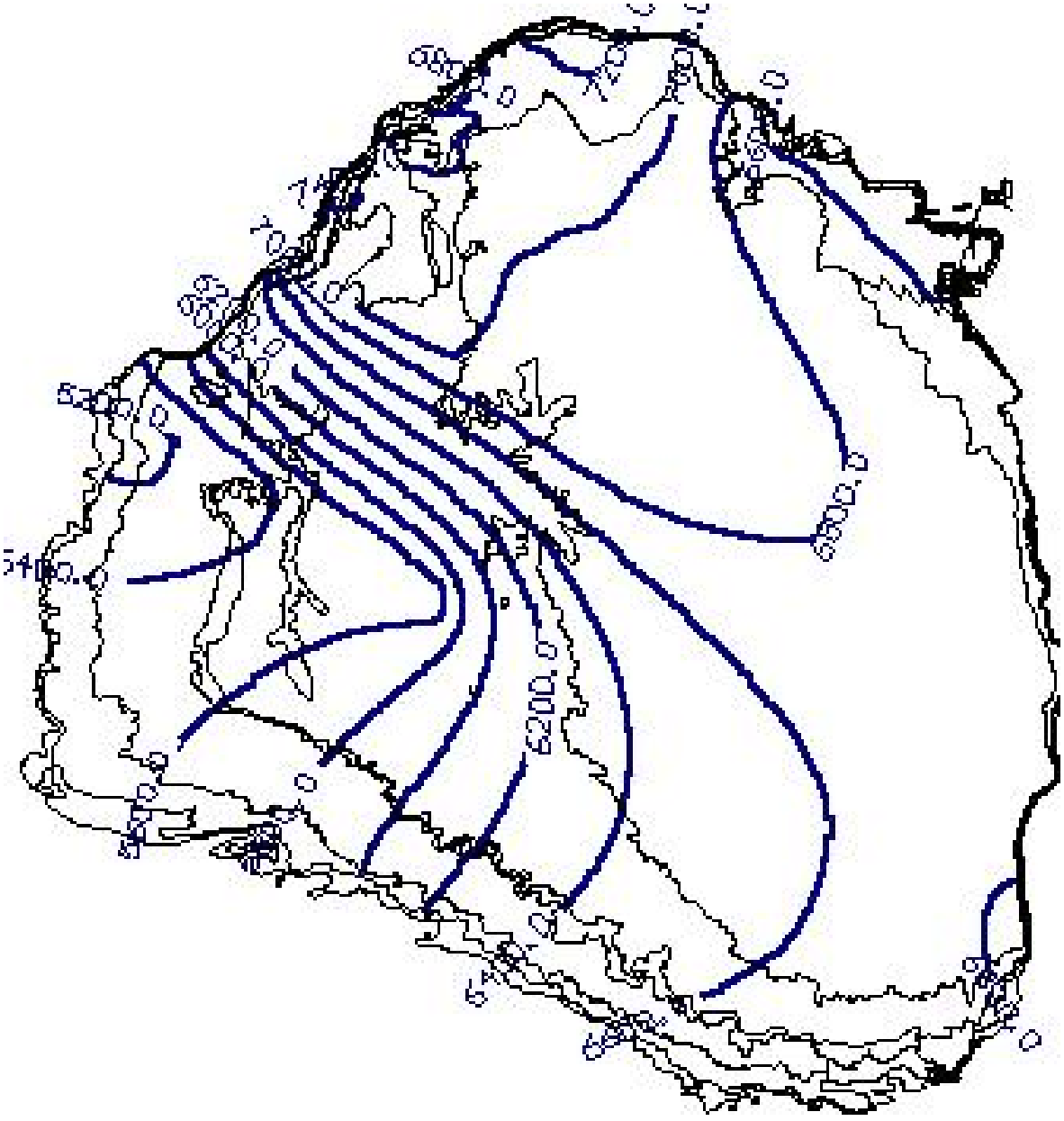

Fig. 8-3: Modeled potentiometric surface (ft-MSL). CI = 200 ft.

Figure 8-4

Calibration histogram

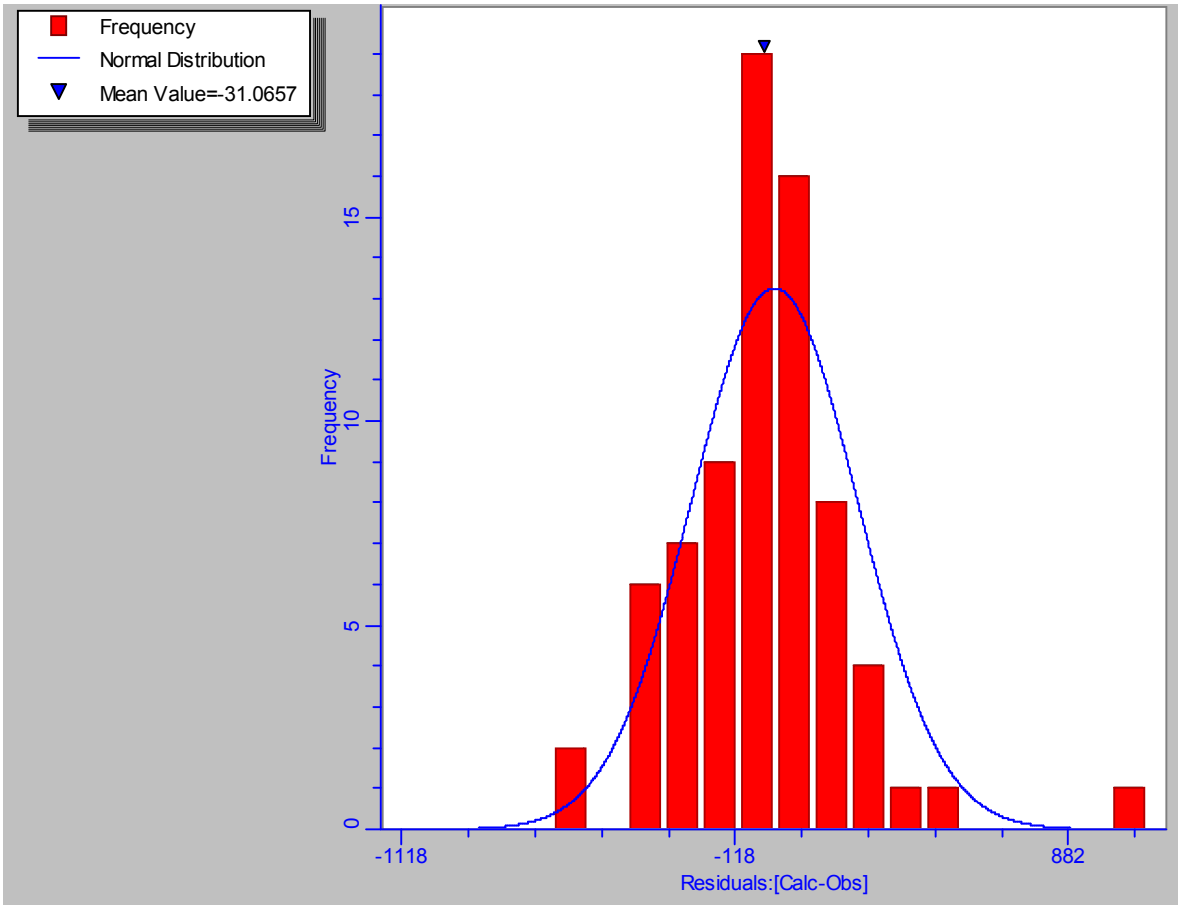

Fig 8-4: The scatter around the mean follows a typical normal distribution, indicating that variability is essentially random.

Figure 8-5

Calibration graph

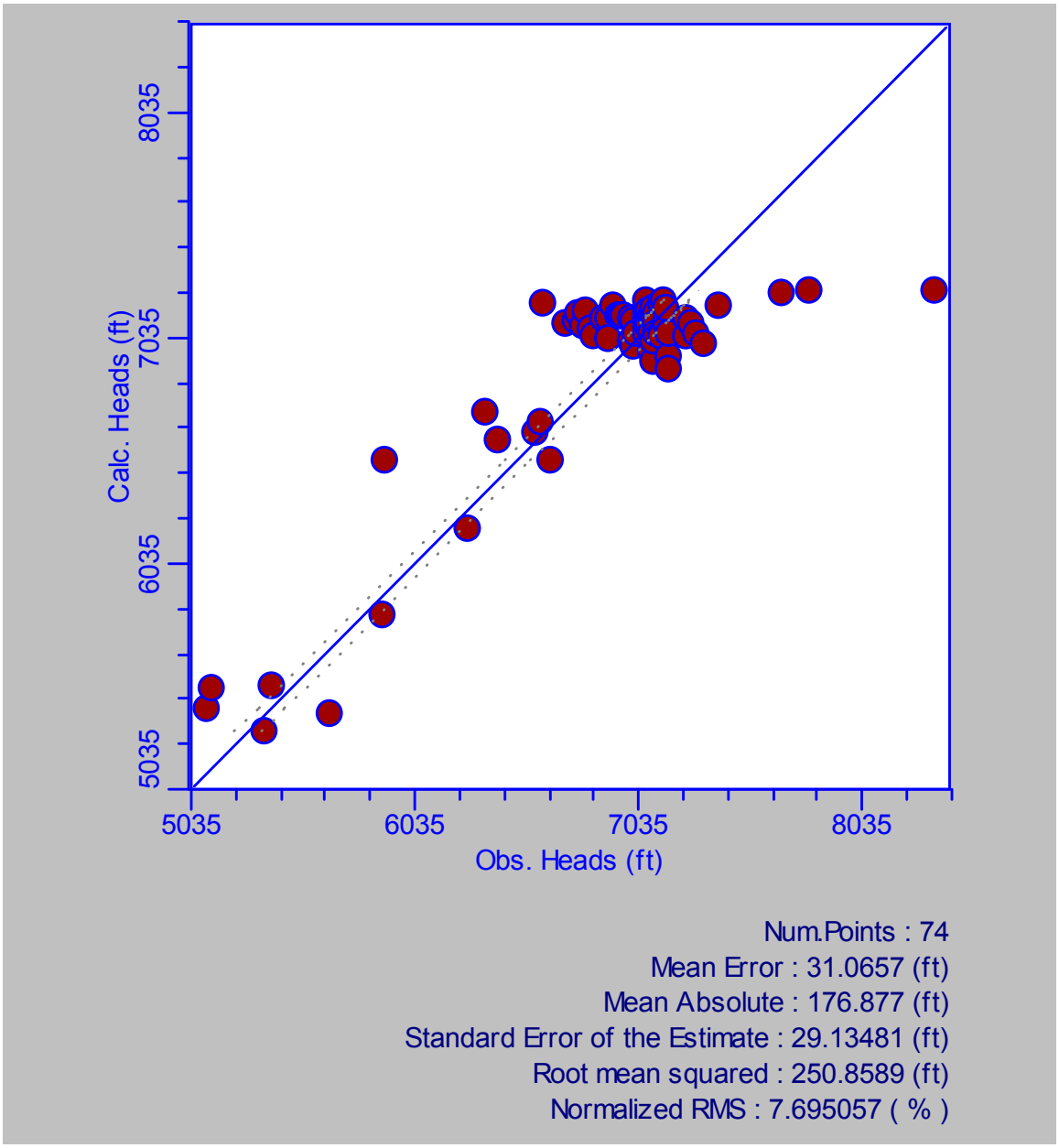

Fig. 8-5: Calculated heads versus observed heads lie close to the 1:1 line. The points show a cluster around 7,100 ft because most observations are from Colorado, where heads are around this value, whereas relatively few data points were available from New Mexico, where heads are lower.

8.3 Modeled pathlines

The calibrated model was used to predict the movement of groundwater from recharge to discharge areas. This was performed using the USGS particle-tracking code MODPATH, which is included with Visual MODFLOW®. Particle origins were applied at a regular spacing along all outcrop cells. Predicted 0.1 Ma groundwater flow paths from these origins are shown for the entire San Juan Basin in Figure 8-6 and for Colorado in Figure 8-7. Figure 8-6 shows that most flow is limited to the outcrop area, and runs from recharge areas to the nearest stream gap at a lower elevation than the recharge area. Figure 8-7 shows in better detail how a component of recharge is not captured at stream locations, and migrates into the San Juan Basin. At the stream gaps, water recharging along the outcrop flows into the San Juan Basin for a distance of up to a few miles, and then returns to the stream discharge point at the end of an arcuate pathway.

8.4 Recharge and discharge volumes

Using Visual MODFLOW's® Zone Budget system, total volumes of recharge to the Fruitland Formation and discharge to streams from the Fruitland Formation were calculated. Note that because the model is run at steady state, recharge and discharge flows are equal. Flows are summarized in the following table:

River	Fruitland discharge (ft3/d)	Fruitland discharge (ac-ft/yr)
La Plata	250	2.1
Animas & Basin Cr.	133	1.1
Florida	3,650	30.6
Los Pinos	7,239	60.6
Piedra & Stonesteimer Cr.	3,544	29.7
San Juan East	3,263	27.3
Navajo	1,890	15.8
Rio Puerco	248	2.1
San Juan West	4,587	38.4
Total recharge/discharge	**24,803**	**207.7**

Figure 8-6

Modeled 0.1 Ma pathlines, San Juan Basin

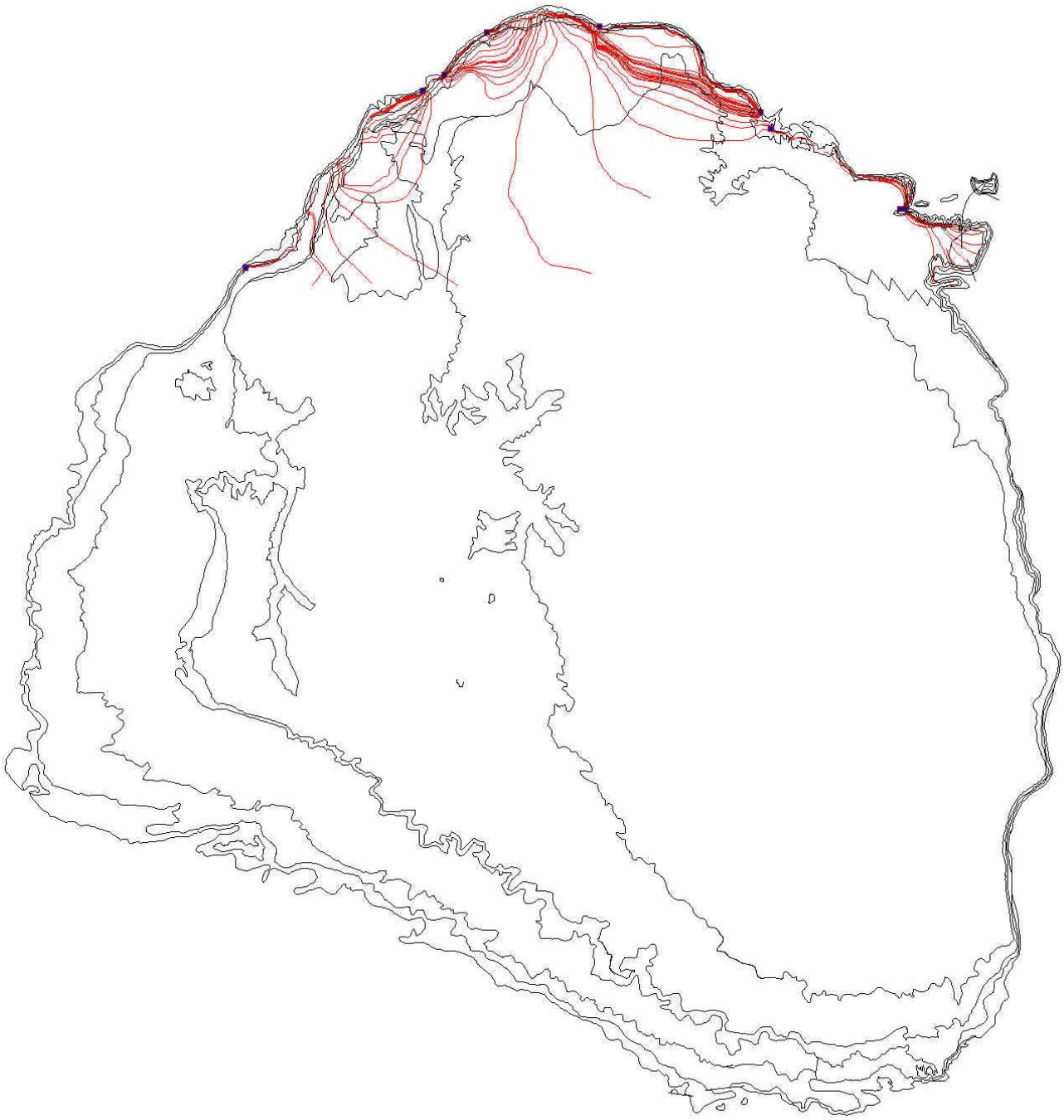

Figure 8-7

Modeled 0.1 Ma pathlines, Colorado

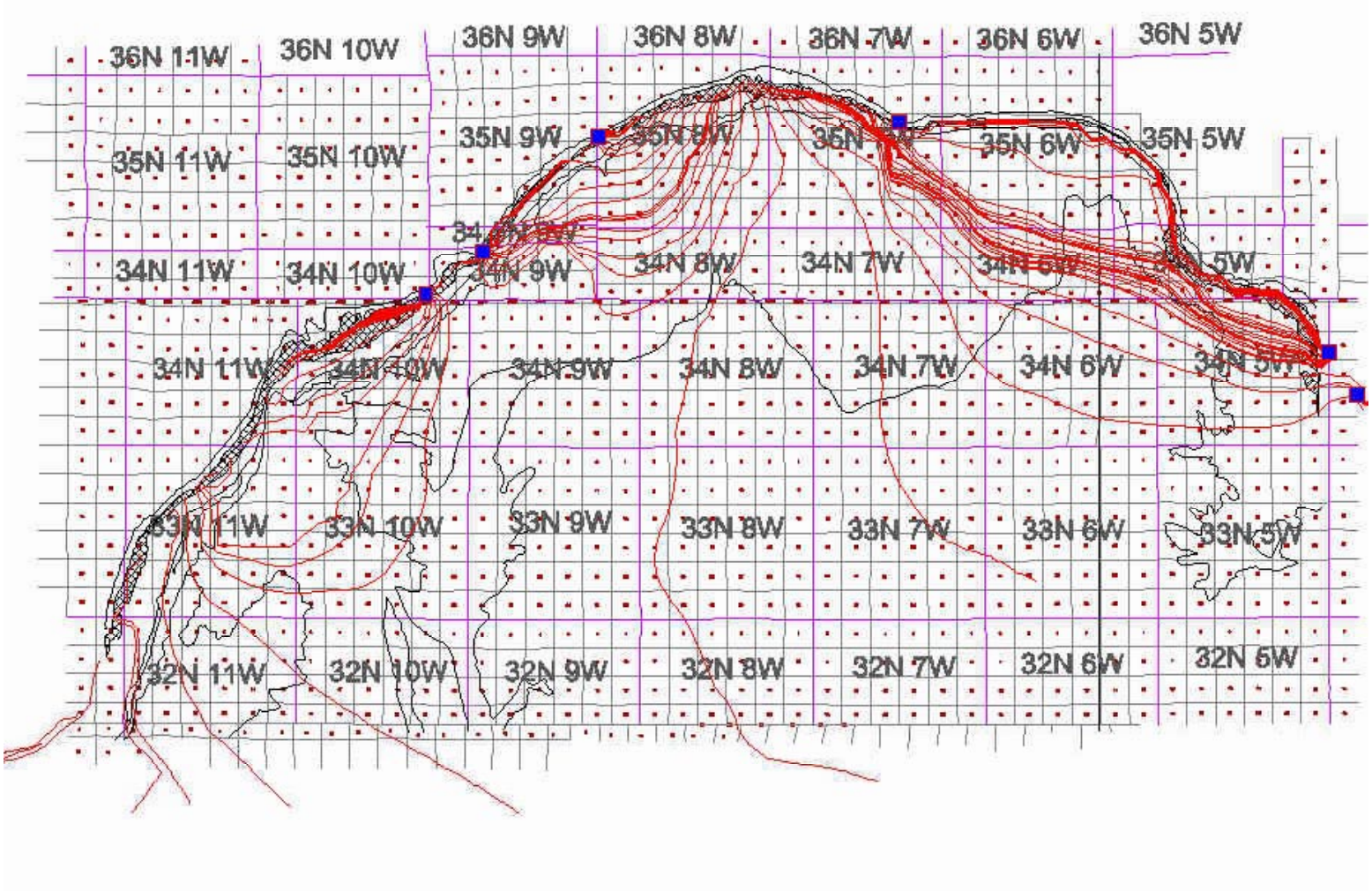

8.5 Hydrochemistry targets and mixing

The modeled flow pathlines were compared with existing hydrochemistry data. In the following discussions, the potential effect of mixing between recharge water and connate water should be taken into account. As a result of mixing, recharge water "labels" normally attenuate with distance into a confined aquifer, and the recharging water gradually takes on the chemical characteristics of connate water. Mixing of groundwaters occurs through mechanical mixing and diffusion, which are described in more detail below.

8.5.1 Mechanical mixing

Mechanical mixing occurs due to the movement of groundwater through a heterogeneous medium. At the micro scale, groundwater velocity is not constant; it reduces in larger flow passages (e.g., larger cleats) and accelerates in smaller flow passages (e.g., narrower cleats). As a result, a "front" of recharging water becomes dispersed across a wide area, whose width is proportional to the groundwater velocity, the heterogeneity of the aquifer, and the distance from the outcrop (time since recharge).

8.5.2 Diffusion

Diffusion follows Fick's Law, that is, chemicals diffuse from high to low chemical concentration at a mass transfer rate proportional to the concentration gradient. Diffusion takes place in all media, being slowest in solids and fastest in gases. It is normally considered to take place at too low a rate in groundwater to influence most aquifer systems. However, in the Fruitland Formation, groundwater migration rates are slow, and both the coal matrix and adjacent shale units may contain a relatively large volume of connate water compared with the amount of recharge water migrating through the coal cleats. Therefore, diffusion probably also alters the character of groundwater migrating through the Fruitland Formation.

8.6 Chloride target

Recharging precipitation is typically low in chloride, as indicated by the NADP data presented in Appendix B. Typical values for recharge water chloride concentration across the San Juan Basin are 0.09 mg/L. Modeled 0.1 Ma groundwater flow paths largely correspond to low-chloride areas, as shown in Figure 8-8.

Figure 8-8

Groundwater flow paths and Fruitland Formation chloride contours

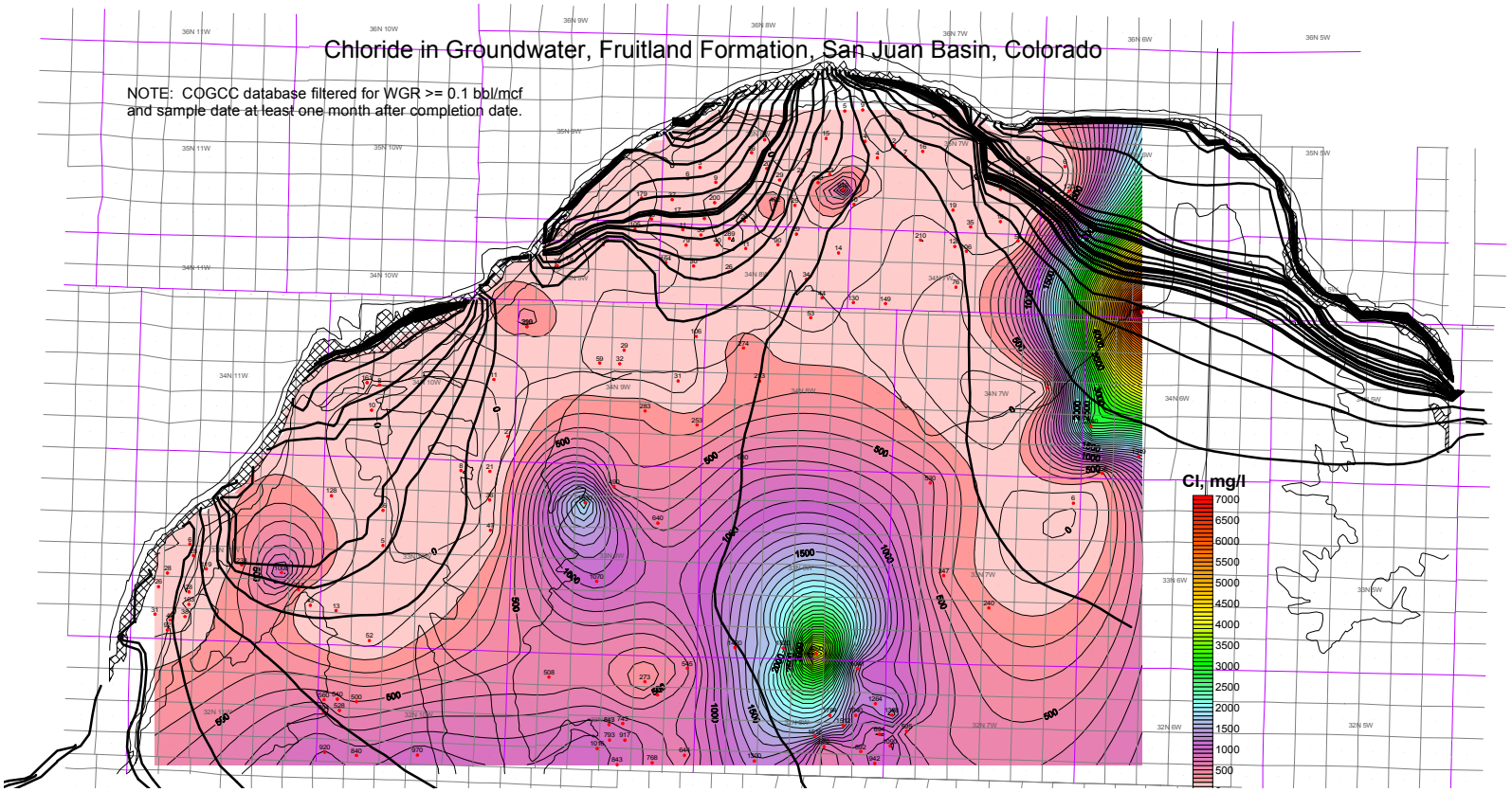

Fig. 8-5: Groundwater flows from the La Plata County outcrop, the main recharge area, to discharge points where the La Plata, Animas, Florida, Los Pinos, and Piedra Rivers intersect the outcrop. Flow paths are largely limited to the low-chloride areas, suggesting that low chloride indicates recharge water.

8.7 Stable isotope targets

Concentration ratios for stable isotopes of oxygen and hydrogen were converted to mean annual air temperature (MAAT) using the following equations (from Phillips et al, 1986):

$$\delta O18 = 0.604T - 18.2 \text{ per mil}$$
$$\delta D = 4.15T - 127 \text{ per mil}$$

As these isotope ratios are directly related to the mean annual air temperature (MAAT) when precipitation occurred, and because the MAAT varied due to the glacial climatic periods during the Pleistocene, trends in stable isotope ratios can be used to infer groundwater travel paths and distances.

Figures 8-9 and 8-10 show MAAT in degrees Fahrenheit based on ^{18}O and ^{2}H ratios for groundwater samples collected by Vastar for the 3M project. These show MAATs varying from lows of 30° F (^{2}H and ^{18}O), to highs of between 70° F (^{2}H) and 85° F (^{18}O). A MAAT of 30° F corresponds to present-day temperatures in southern Alaska, while a MAAT of 75 to 80° F corresponds to the present-day Caribbean (Owenby et al, undated). The outcrop was set at the current MAAT of 46° F. The pattern shows a temperature low centered a few miles from the outcrop, with temperatures increasing back toward the outcrop and deeper into the San Juan Basin. As glacial climates are only thought to have occurred in the post-Cretaceous San Juan Basin area during the recharge during Pleistocene glacial periods.

The modeled groundwater flow path for the Pine River area, as shown in Figures 8-9 and 8-10, matches an apparent MAAT “plume”, which like the low-Cl signature, is indicative of groundwater migrating into the San Juan Basin.

8.8 Geochemical evolution of Fruitland Formation recharge

Geochemical trends were plotted along a groundwater flow path following the Pine River low-chloride plume, as shown in Figure 8-11. Modeled 0.1 Ma flow lines are overlain on the contour maps. Flow path profiles are commonly used in hydrogeochemical studies to reveal how chemistry changes along a flow path. The combined chloride and MAAT trends indicate progressive changes with distance and time, apparently due to a combination of (1) changes in recharge chemistry, and (2) the effect of residence time in the formation on water chemistry. The following is one interpretation of how these trends may reflect the historical geology of this area.

Figure 8-9

Groundwater 0.1 Ma flow paths and Fruitland Formation ^{18}O temperature (°F) contours

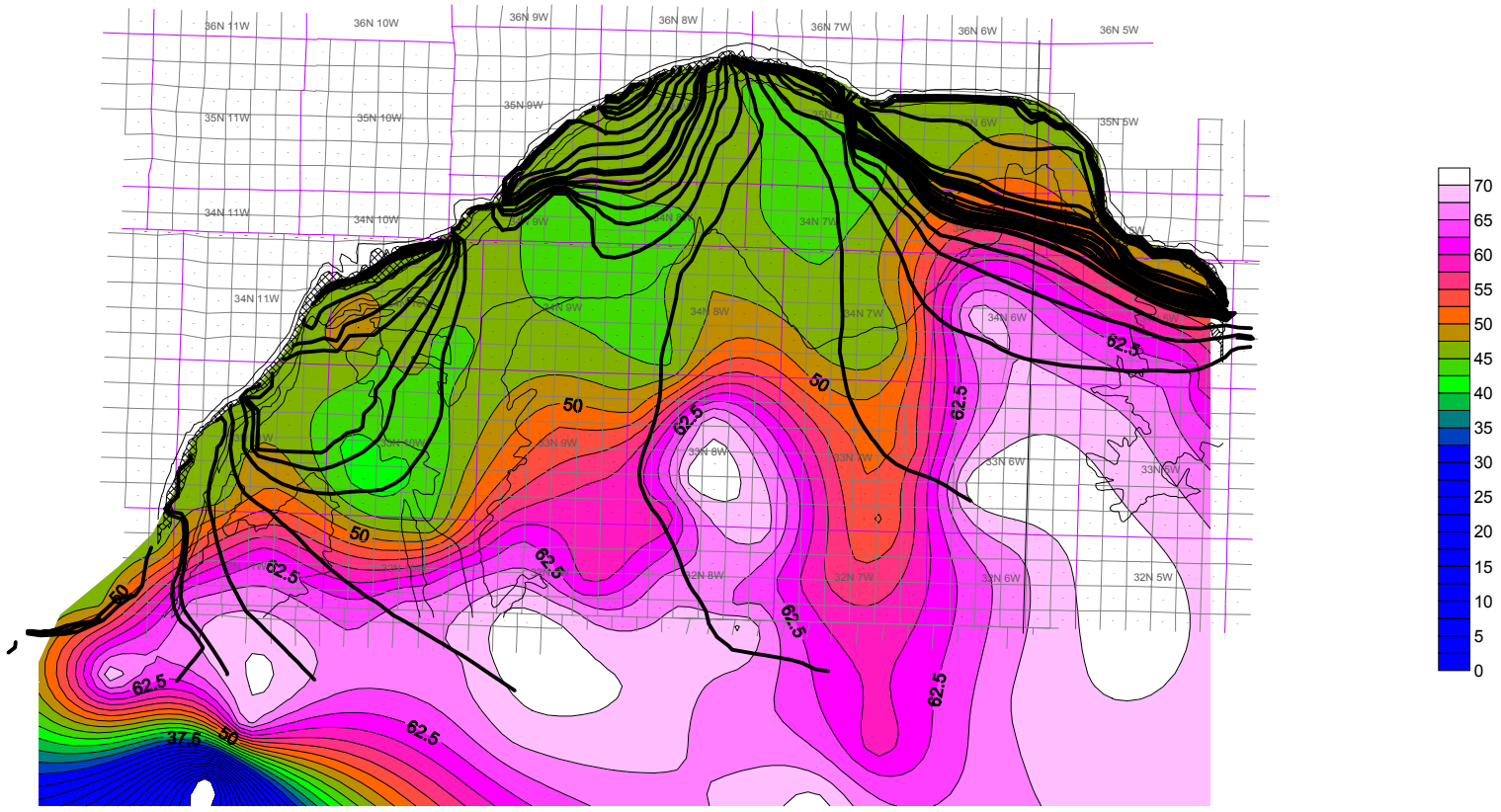

Figure 8-10

Groundwater 0.1 Ma flow paths and Fruitland Formation ^{2}H temperature (°F) contours

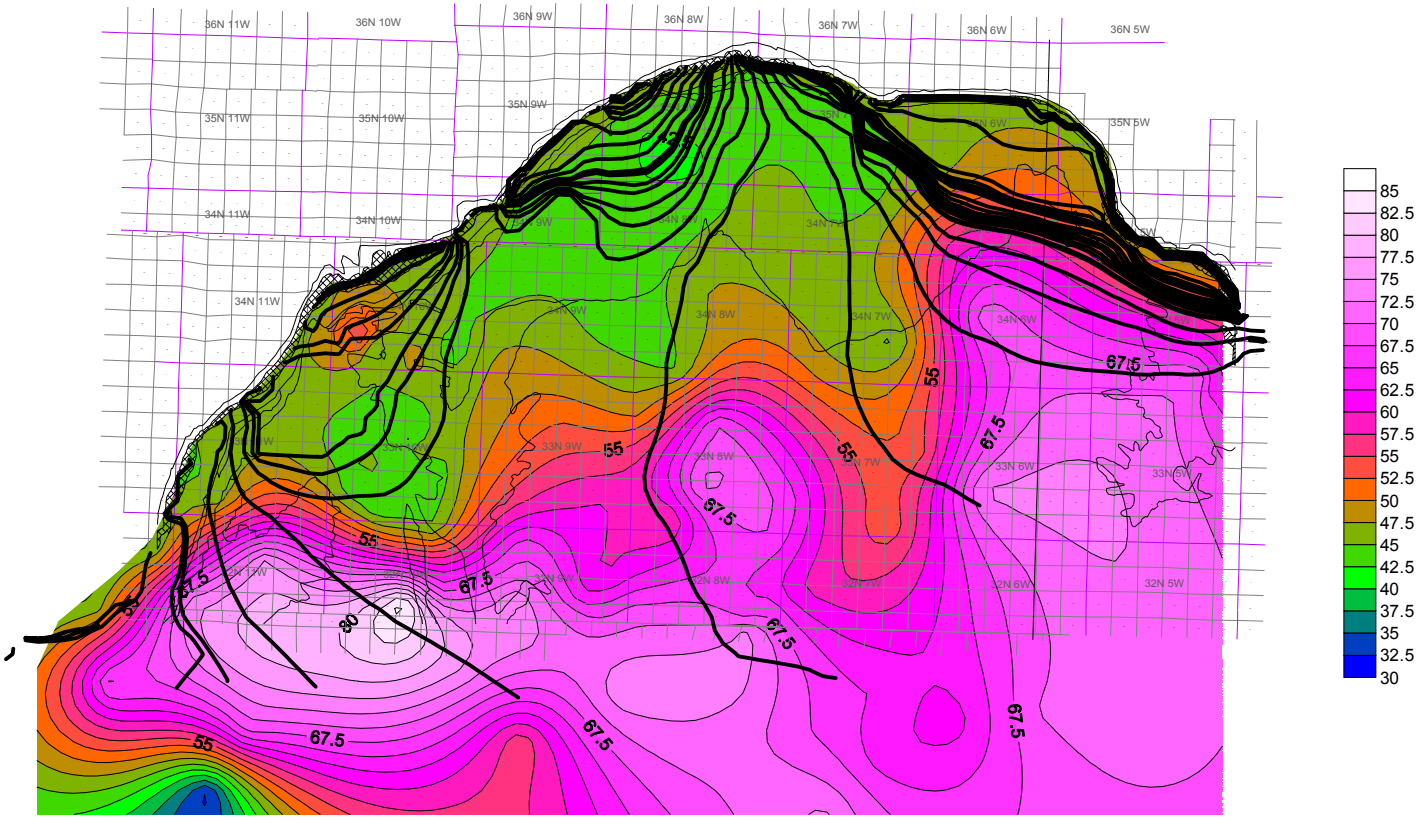

Figure 8-11

Geochemical evolution of Fruitland Formation recharge

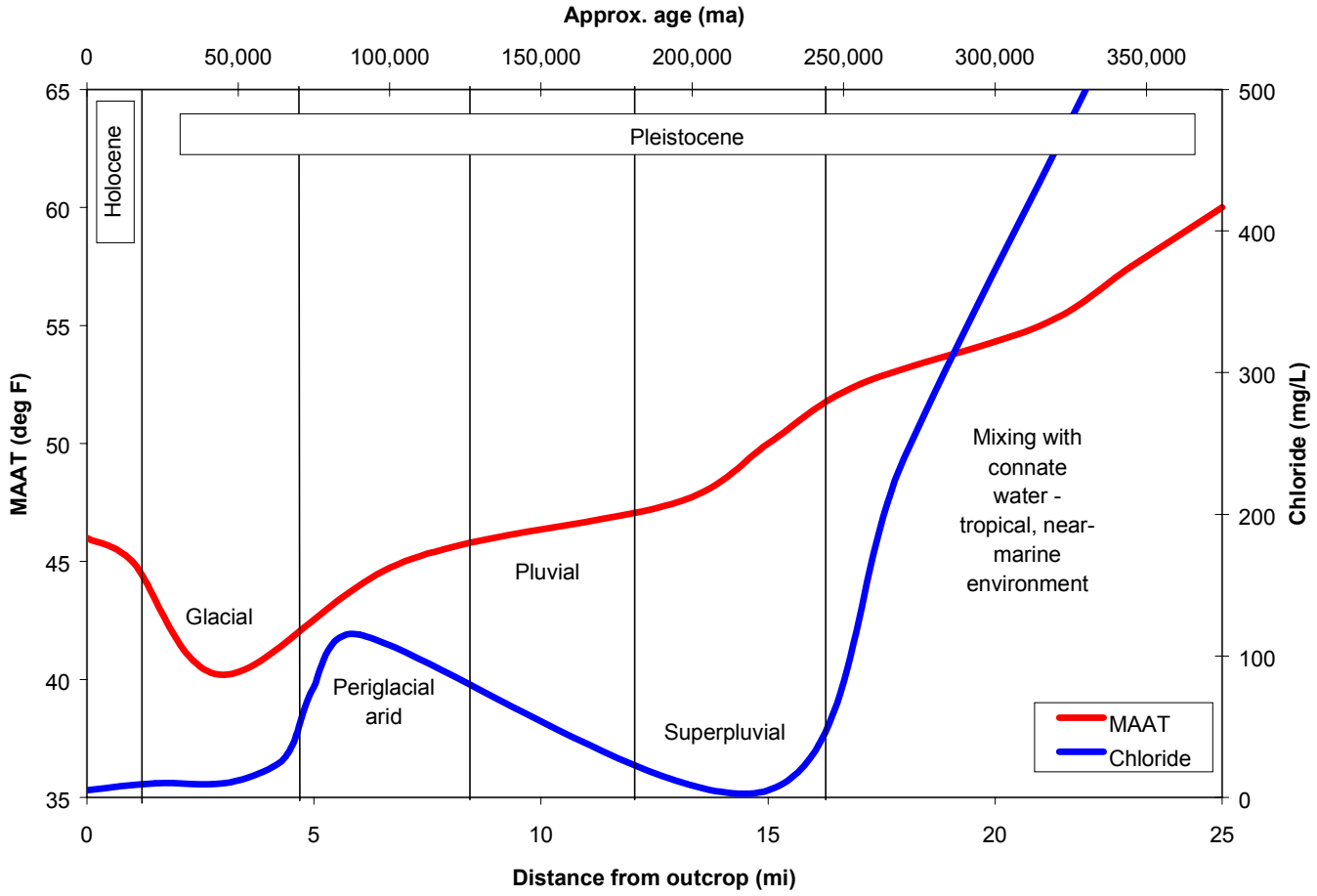

As shown in Figure 8-8, at about 15 miles from the outcrop, the very low chloride concentration may indicate recharge around 0.2 Ma during a pre-glacial climate that was extremely wet ("superpluvial"). The climate became less humid and the relatively high chloride concentration at 6 miles from the outcrop may indicate a periglacial arid climate such as exists in present-day cold deserts. At 2 to 3 miles from the outcrop, the MAAT minimum appears to indicate recharge during the last glacial epoch, which ended about 10,000 years ago.

Further than about 15 miles from the outcrop, the rapid increase in chloride indicates mixing of recharge water with more saline connate water, and the increased MAAT indicates that connate water originated as rainfall in warm, wet, tropical conditions, such are believed to have existed in this area during the Late Cretaceous. Recharge water may have migrated beyond this distance, but by this time in its evolution it would now be dominated by connate water characteristics.

8.9 Iodine-129 and chlorine-36 age dating targets

This section is based on data from the sampling and isotope analysis program performed by Vastar in 1999-2000 (Riese, 2000). This sampling and analytical program is continuing; therefore, any conclusions presented here should be considered preliminary and subject to future revision.

Sample ages for ^{129}I and ^{36}Cl were contoured and overlain with the modeled 0.1 Ma groundwater flow pathlines, as shown in Figures 8-12 and 8-13. The following features are evident from these figures:

1. ^{129}I ages generally increase from the outcrop to about 15 miles into the San Juan Basin, and then apparently decrease with additional distance. Some anthropogenic ages occur near the outcrop, others occur deep in the San Juan Basin.
2. ^{36}Cl ages generally increase from the outcrop into the San Juan Basin.
3. ^{129}I and ^{36}Cl ages do not match (see Figure 8-14): ^{36}Cl ages are between 3% and 20% of ^{129}I ages for the same sample.
4. Both ^{129}I and ^{36}Cl ages generally increase along modeled 0.1 Ma groundwater pathlines.
5. Neither ^{129}I nor ^{36}Cl ages correlate with modeled groundwater ages. Modeled groundwater ages are approximately 15% of ^{36}Cl ages.

Some discrepancy between isotope ages and modeled ages was expected, because the groundwater model does not simulate the mixing with connate water that occurs in a natural system. It appears that the effect of mixing in the San Juan Basin is complex and may include the effects of diffusion on groundwater migrating through shale units between coal beds. As a result, the isotope age dates cannot be used as a model calibration target, because the mixing effects are non-linear, and because the two age dating methods do not provide an unambiguous apparent age. Therefore, an age-dating target was not pursued for the modeling project.

Figure 8-12

Iodine-129 ages and modeled 0.1 Ma pathlines

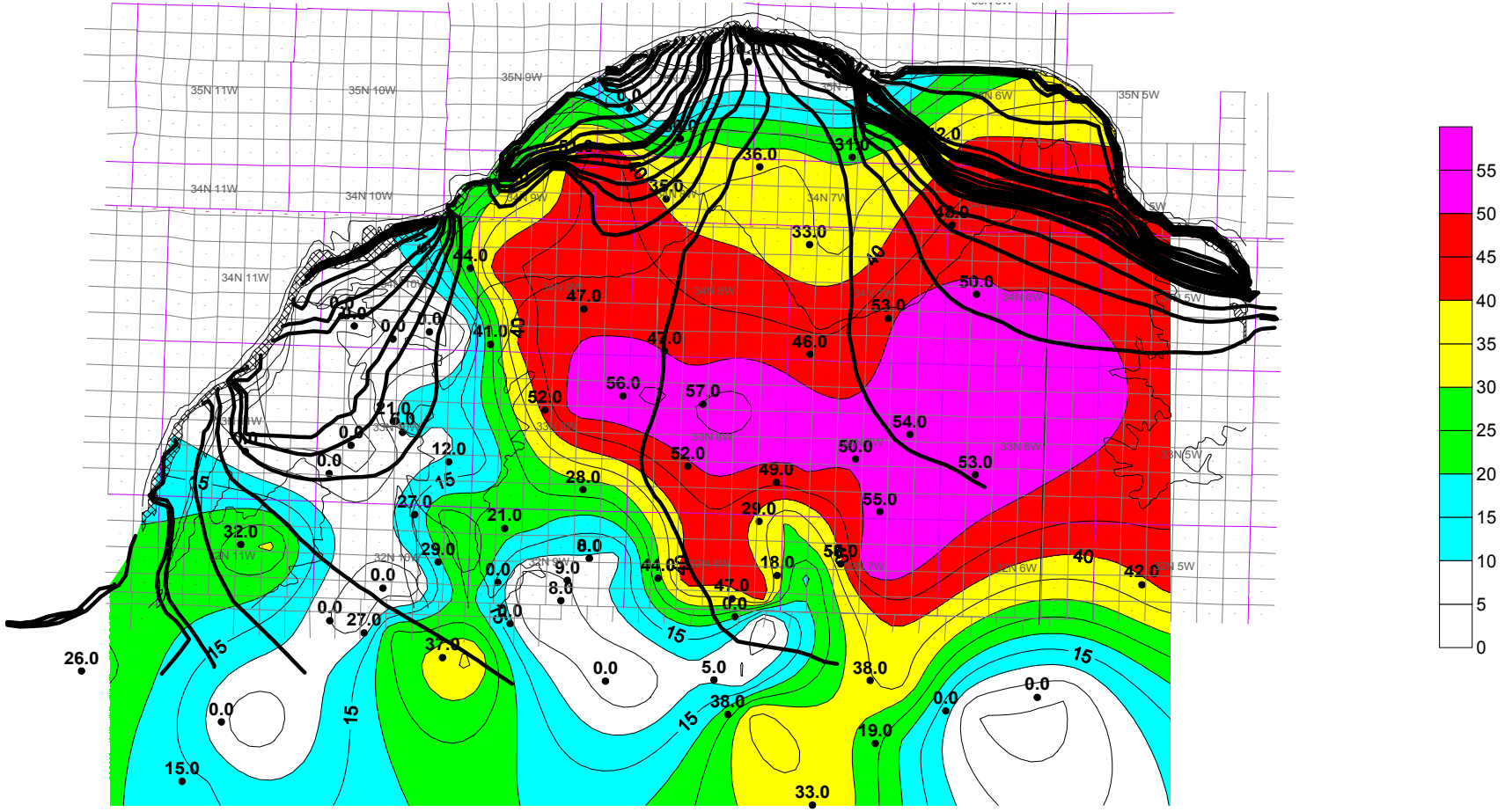

Figure 8-13

Chlorine-36 ages and modeled 0.1 Ma pathlines

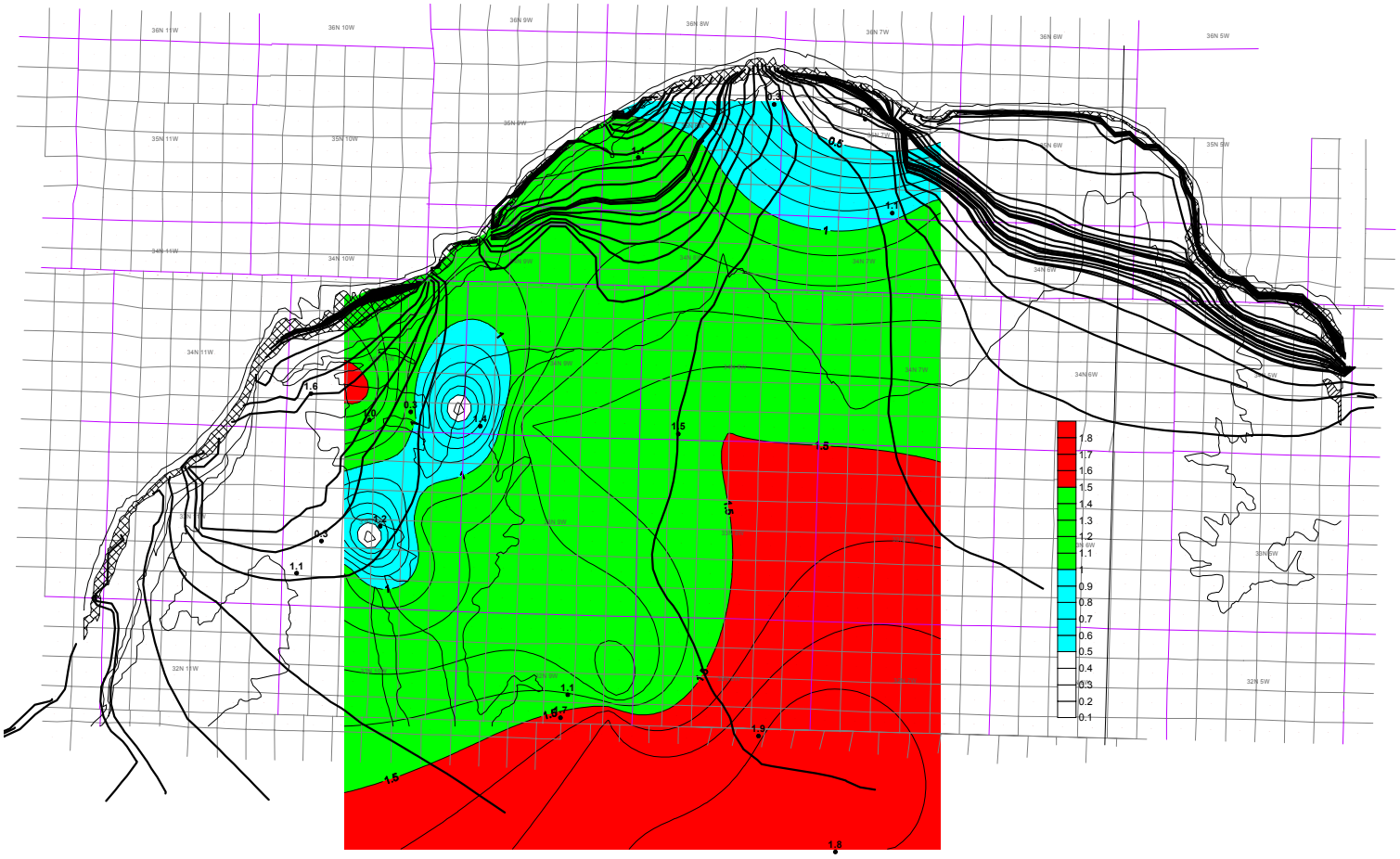

Figure 8-14

^{36}Cl versus ^{129}I apparent ages

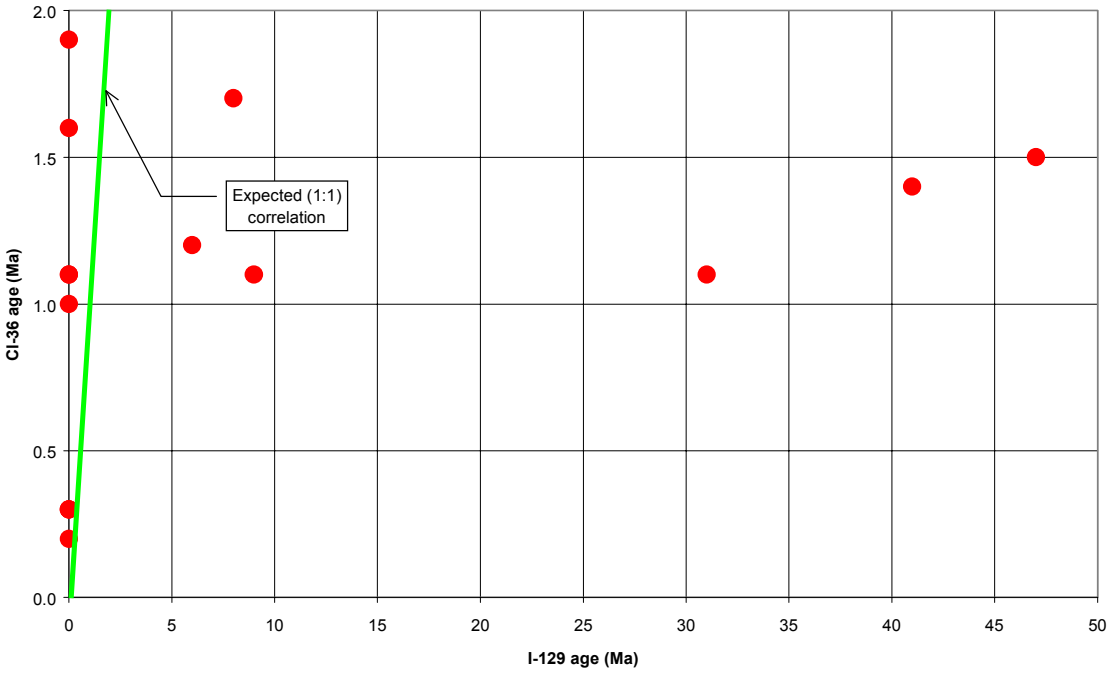

9.0 Model scenarios and results

The model was used to evaluate two conceptual models of proposed barriers or baffles, which may represent offset faulting or stratigraphic discontinuities. A number of well-documented barriers/baffles were included in the base case and both scenarios, including the Valencia Canyon and 44 Canyon faults.

The barrier scenarios simulated were:

1. The hingeline barrier
2. Internal barriers

Each scenario and its results are discussed below.

9.1 Hingeline barrier

The suggested near-outcrop “hingeline” barrier was simulated by applying a zero-permeability zone at a distance of approximately 1.5 miles from the outcrop, and running the model. The resulting potentiometric surface is shown in Figure 9-1. As can be seen, this did not provide a satisfactory model calibration. The calibration graph shown in Figure 9-2 shows “flatlining” of calculated heads at around 7,000 ft-MSL, which indicates that these calibration points (inside the barrier) have no correlation with observed heads.

This scenario was also performed in transient mode to investigate the potential for “fossil” gradients persisting after a geologically rapid hinge-line development trapping pressures inside the San Juan Basin. This was previously discussed in Section 4.1. As discussed, for “fossil” gradients to persist to the present day after a “hingeline-sealing” event, this event would have occurred within the last 2 Ma. Given the dramatic orogenic events that preceded 2 Ma, which apparently did not form a hingeline seal, it seems unlikely that such an event occurred after 2 Ma. As a result, it was concluded more probable that the outcrop and the down dip San Juan Basin are hydrologically connected.

Figure 9-1

Hingeline barrier scenario

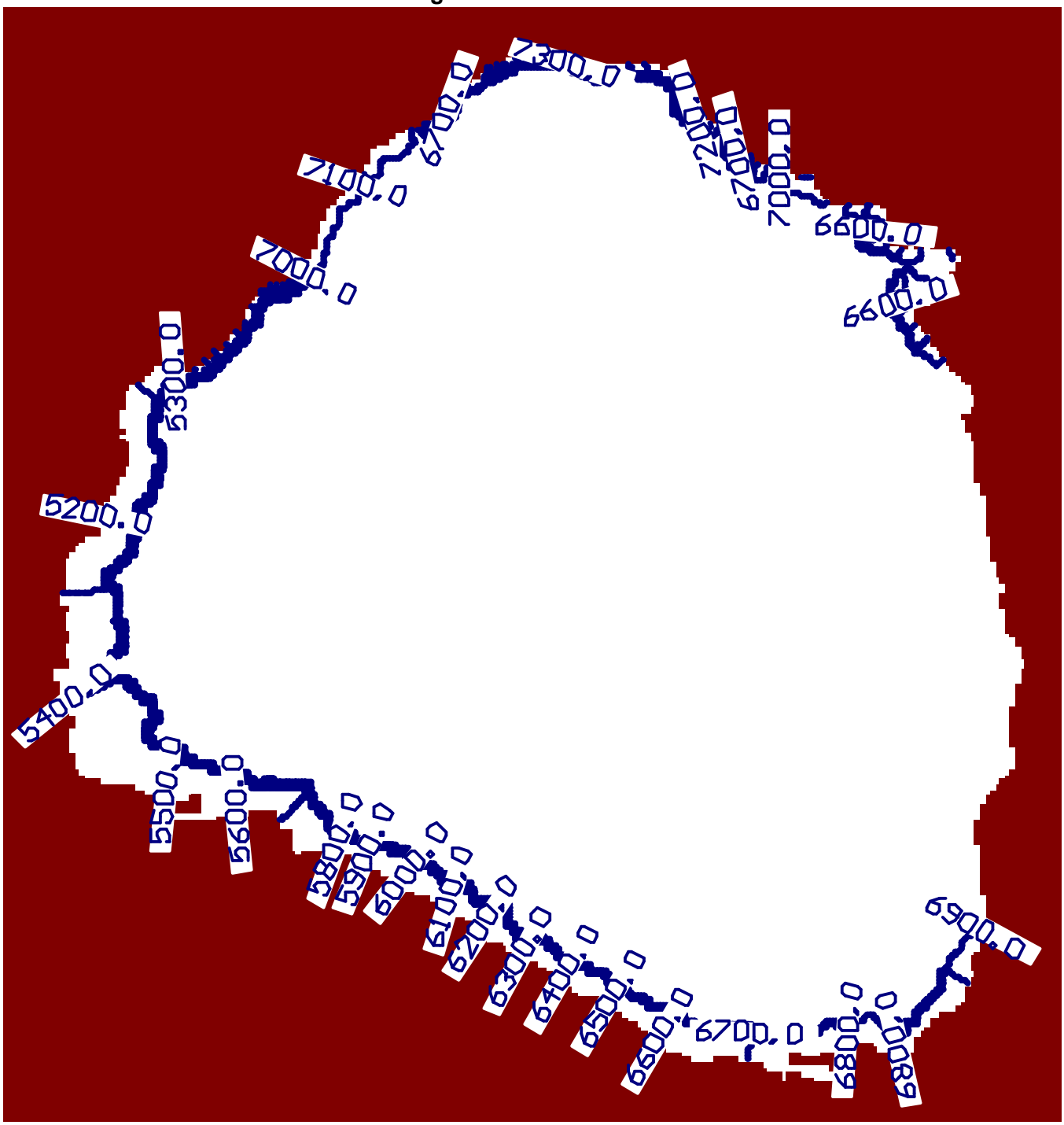

Fig. 9-1: The hingeline barrier results in a flat potentiometric field inside the barrier: recharge, discharge, and groundwater flow are restricted to the thin near-outcrop area.

Figure 9-2

Hingeline barrier calibration graph

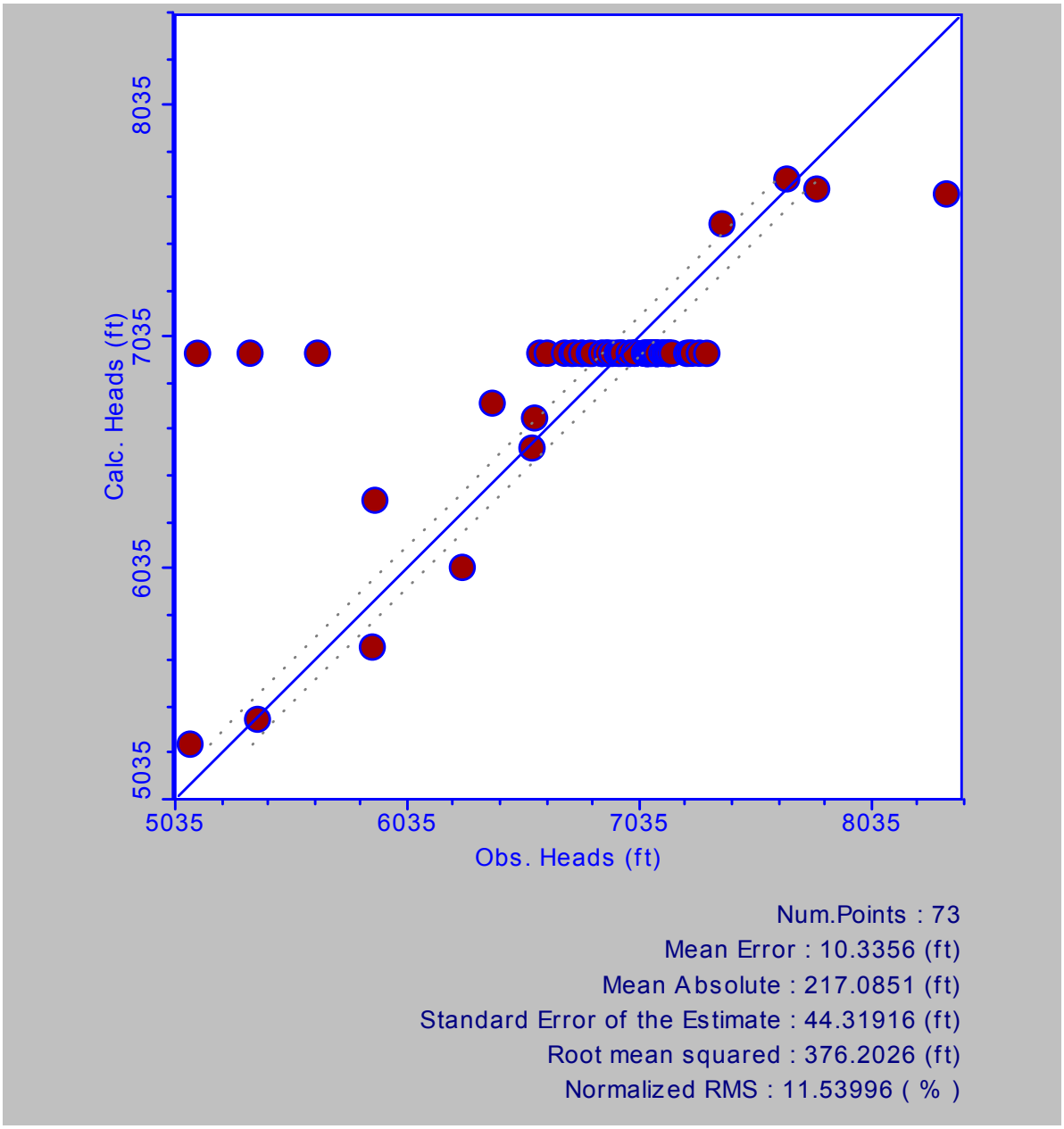

Fig. 9-2: The "flatlining" of calculated heads at around 7,000 ft-MSL indicates that these calibration points inside the barrier have no correlation with observed heads.

9.2 Internal barriers

An *en echelon* series of internal barriers suggested by the TPRT, based on magnetic and geophysical anomaly interpretation, were simulated as zero-permeability zones, as shown in Figures 9-3 and 9-4. The resulting potentiometric surface is shown in Figure 9-5. As can be seen, this did not provide as satisfactory a model calibration as the base case. As shown in the calibration graph (Figure 9-6), the constraining effect of the linear barriers results in higher calculated heads at the calibration points within the barrier area. As a result, it was concluded that, while major linear barriers may exist in the San Juan Basin, they are not necessarily indicated by regional geophysical anomalies.

Figure 9-3

Internal barriers and gravity anomalies

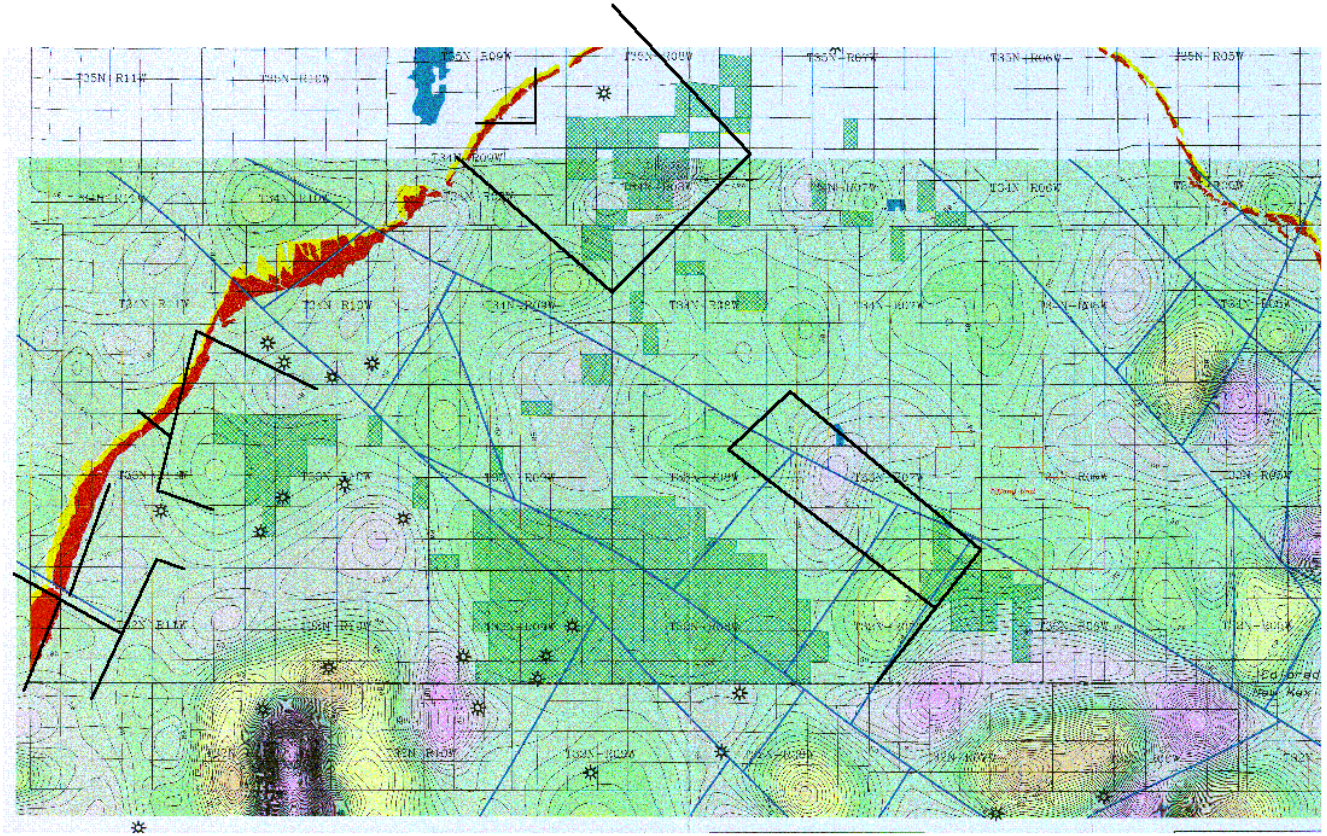

Figure 9-4

Internal barriers and magnetic anomalies

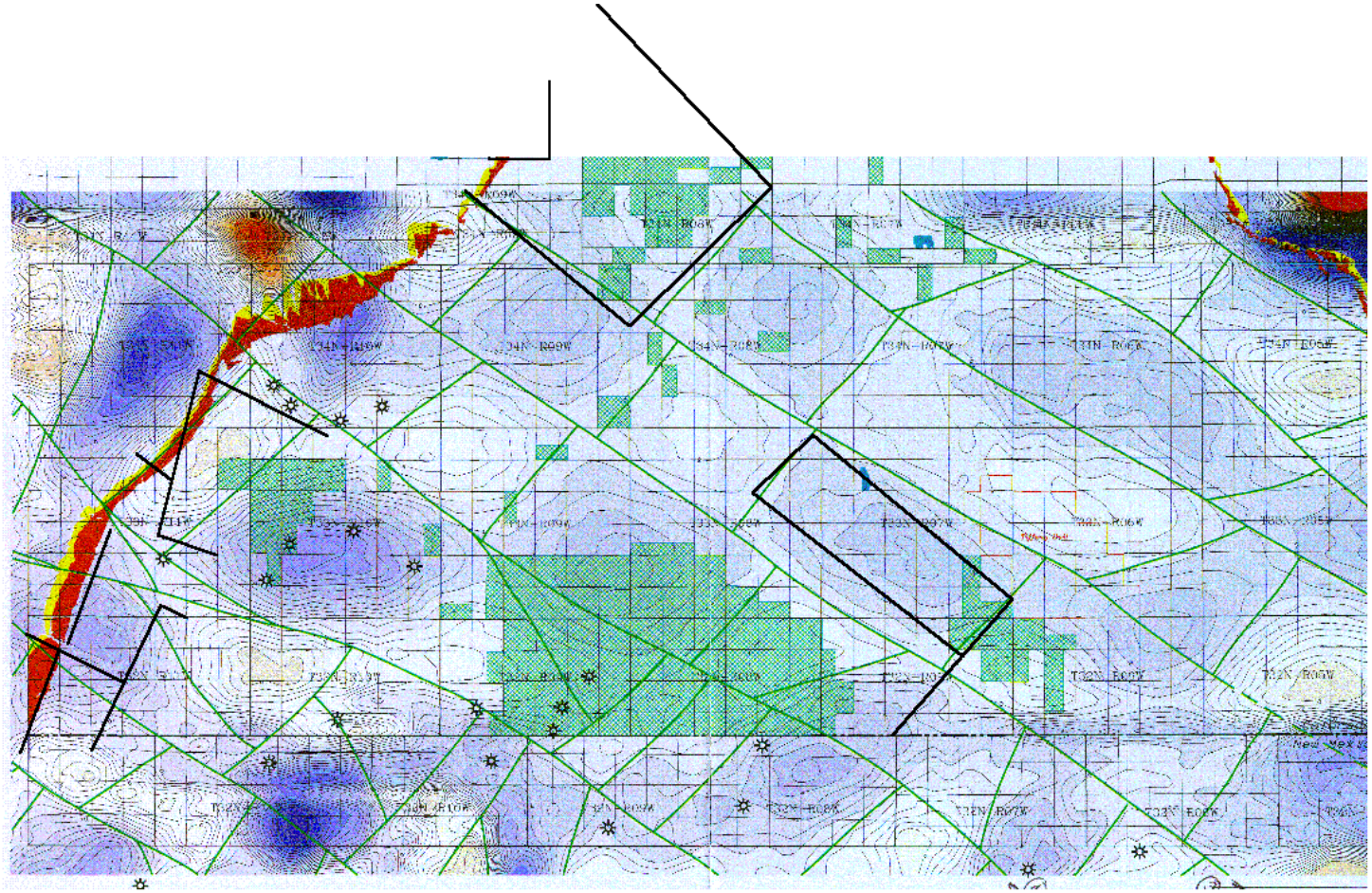

Figure 9-5

Linear barriers scenario

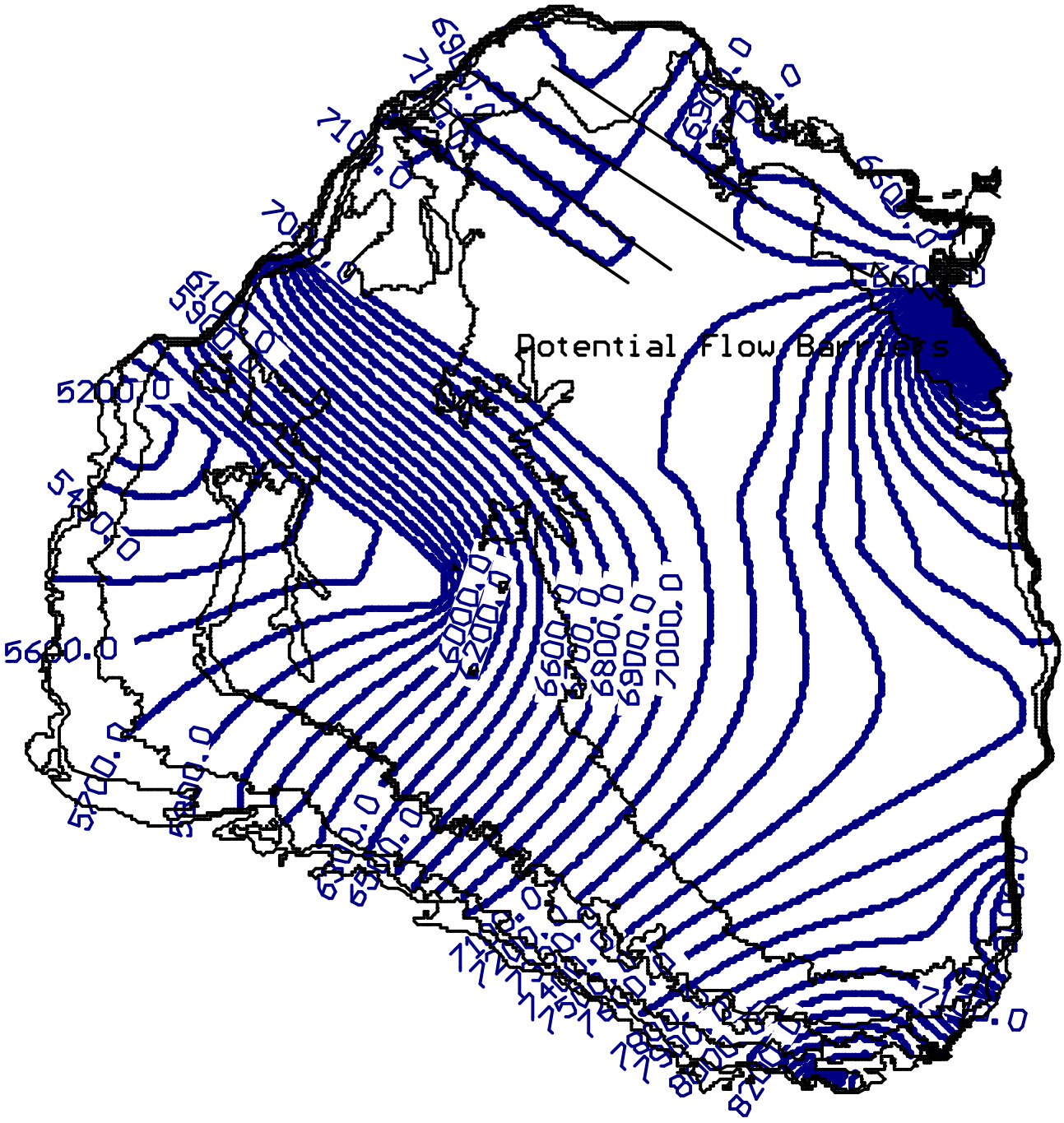

Fig. 9-5: Applying the linear barriers results in a potentiometric field generally similar to that of the base calibration, but notably distorted in the barrier area.

Figure 9-6

Linear barriers calibration graph

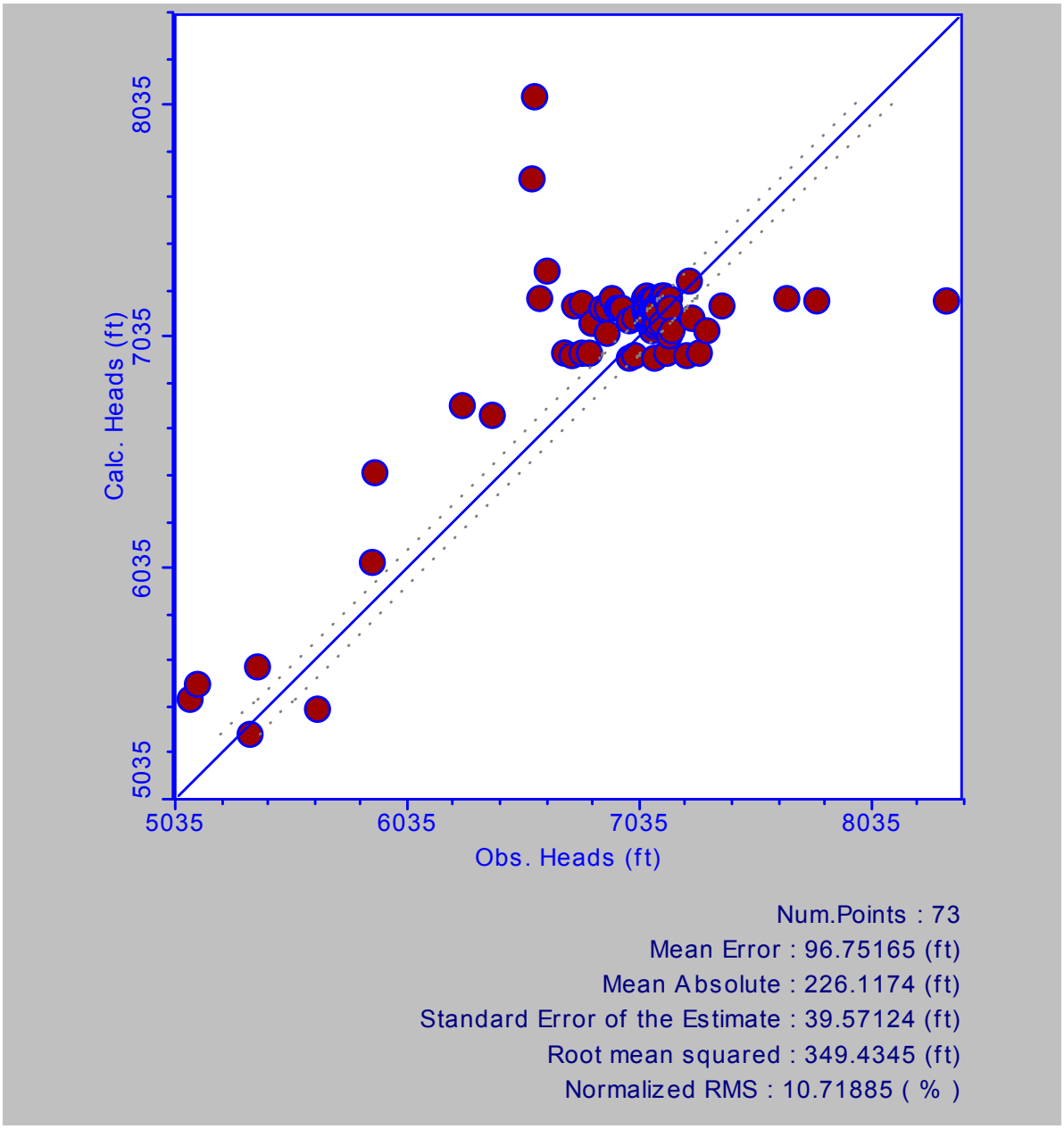

Fig. 9-6: The constraints caused by these linears result in higher calculated heads at a few calibration points within the barrier area (the vertical group at 6,700').

10.0 Conclusions and future work

10.1 Conclusions

10.1.1 Hydrologic regime

The Fruitland Formation in the San Juan Basin contains fairly low permeability rock units. The formation behaves like a classic confined aquifer system, which is regionally interconnected despite the presence of structural and stratigraphic discontinuities. The flow of groundwater through a generally-connected series of units, from an upland recharge area to a low-lying discharge area, is simple and consistent, agrees with observed patterns of chloride and stable isotopes, and requires no additional complexity to account for most observations. In nature, as in science, the simplest explanation is often the most probable.

10.1.2 Hinge line and internal barriers

The combined fossil gradient/hingeline barrier/sealed compartment theory is certainly another plausible explanation for the observed potentiometric head distribution. However, it requires a complex series of consecutive geologic coincidences to work, including a major tectonic event between 2 Ma and the present day to simultaneously seal off the entire San Juan Basin outcrop and create sealed compartments at approximately 1 to 4 mile spacing in two directions so as to trap fossil pressures.

10.1.3 Recharge and discharge

The recharge rate for the Fruitland Formation derived from model calibration is much lower than expected based on traditional estimation methods. The difference is partly a modeling artifact due to the different outcrop widths of the modeled formation and the actual coal outcrops. Resulting calculated discharge rates from the Fruitland Formation to streams are extremely low (totaling 208 ac-ft/yr).

10.2 Potential problems

Potential problems of the hydrologic model, many of which were provided as constructive input by the TPRT, are discussed below:

(1) The geology of the San Juan Basin is so complex that no model can simulate it.

The San Juan Basin is very large and has complex geologic features, which were not included in this version of the model because the necessary work to correlate coal packages and positively identify fault barriers was not yet available in a publicly available form. However, MODFLOW and other modeling codes (e.g., the finite

element code FEFLOW) can represent an almost infinite range of variations in scale, permeability, number of layers, formation thickness and elevation, discontinuities, faults, folds, etc., limited only by the computing power required to handle the level of complexity. Computing power is becoming steadily more affordable, which will allow greater modeling challenges to be attempted in future. The model does successfully simulate observed initial potentiometric heads, agrees with San Juan Basin geochemical trends, and may be consistent with isotope age information when that study is completed.

(2) *As a single-layer, lumped parameter (net coal) model, it averages individual coals and does not distinguish between flow conditions in different coal seams.*

The data against which the model is calibrated (initial potentiometric heads, and produced water sample chemistry) are necessarily average values from coal seams aggregated at a production well. In this respect, this is a limitation of the available data rather than of the model. The shingled model suggests that individual coal seams taken together do indeed act as an average net coal over long distances. Future modeling using the revised coal package correlation would distinguish between flow conditions in different coal seams.

(3) *Reported initial potentiometric heads (data against which the model is calibrated) are often extrapolated data.*

This was indeed found to be a significant data limitation, and a delaying factor in developing the models. Therefore, these data were screened to ensure that the data used represented real field measurements.

(4) *Reported produced water chemistry does not always represent Fruitland Formation water. Early production water may reflect chemistry of hydraulic fracturing fluids (too saline), and later samples may actually be condensate (too fresh).*

This was a deficiency in initial geochemical interpretation pointed out by the TPRT. Data were subsequently screened to eliminate unrepresentative samples.

(5) *Isotope age dates are much older than modeled groundwater ages.*

There is disagreement between the various types of isotope ages, and uncertainty regarding the effect of additional formation-derived iodine on the ^{129}I data set. When the isotope study is complete, future modeling should re-examine this potential discrepancy.

(6) Permeabilities derived from Fruitland Formation CBM production data reflect flow from seams connected to the wellbore, and are most likely much higher than the actual permeabilities governing regional flow in the heterogeneous coal seams.

Because production data reflect flow from seams connected to the well bore, they should already reflect the effects of formation heterogeneities, such as stratigraphic pinchouts or fault displacements.

10.3 Suggested future refinements

This study serves a first phase upon which future studies can build. The hydrologic model was necessarily simplified, but in ways that can be amended to incorporate more complex issues as they arise. For example, the model was built as a single layer, and cross-formational flow from the Pictured Cliffs or Kirtland Shale was not explicitly considered in the model. The model was simplified to use net coal thickness, so that stratigraphic changes in coal packages have been averaged. Potential flow through the Fruitland Formation shale, and shale/coal interaction, were not considered. These simplifications have not limited the applicability of the model to simulate pre-production regional baseline conditions. However, greater detail should be incorporated to apply the model to localized scale problems.

Although COGCC, SUIT, and BLM do not anticipate funding additional large scale modeling efforts at this time, further modeling studies may be undertaken. Most hydrologic models are considered to be works in progress, pending new data. For example:

1. With the final publication of the CGS's detailed stratigraphic correlations, the model could be converted to a multi-layer model using the new detailed Fruitland Formation subdivision.
2. With further publishing of evidence of outcrop or internal barriers, these factors could be incorporated with a greater degree of precision.
3. An improved calibration could likely be achieved with more and better quality initial potentiometric heads, and better production water chemistry data.
4. Potentiometric head data from the planned outcrop monitoring wells, to be installed as part of the 3M project, would also improve model calibration.
5. Further consideration of geochemical patterns, heat flow, stable isotope data, and detailed stratigraphy and structure, would improve the conceptual model of San Juan Basin hydrology.
6. In addition, new data, evaluations, and insights will likely lead to potential model improvements.

Suggestions for specific future work follow.

10.3.1 Detailed modeling

With the completion of the Colorado Geological Survey's outcrop mapping and subsurface correlation work (Wray, 2000), there now exists a more widely accepted geologic model of coal package distribution. Using this data, it is now possible to develop a model that considers coal packages separately and provides a better representation of the complex stratigraphy of the San Juan Basin. In addition, the onset of infill drilling in the San Juan Basin, which will reduce production well spacing from 320 acres to 160 acres, will provide improved stratigraphic resolution, may help to confirm (or disprove) the presence of suggested displacement faults, and can add more initial potentiometric head and geochemical information to the existing database.

10.3.2 Hydraulic testing of the Fruitland Formation shale

Possibly because of the low gas and water yields derived from shale, its permeability has been treated to date as either zero, or as so low relative to the coal units as to be ignored. The shingled stratigraphy modeling results, presented in Section 4.3, show that shale beds may contribute significantly to groundwater flow, implying that coal/shale hydraulic interaction may be a very important factor in considering overall San Juan Basin hydrogeology and hydrochemistry. Therefore, obtaining good empirical data on shale permeability is essential for future modeling activities. Testing to provide such data should be performed through open-hole pressure dissipation tests in packered intervals at depth, or falling-head "slug" tests in shallow borings, to determine lateral permeability, and laboratory tests on core samples to determine vertical permeability.

10.3.3 Effective diffusion coefficients

Quantification of effective diffusion coefficients through (1) the coal matrix and (2) adjacent shale beds would help in the interpretation of hydrochemical trends. Tests such as those described by Oakes (1977) could be performed on core samples of coal and shale.

10.3.4 Structural and historical geology

Numerous papers and reports have been prepared that describe the nature of folding, faulting, and cleat formation in the Fruitland Formation. However, there has been no synthesis of this work over the San Juan Basin, particularly with a focus on displacements relative to coal bed thickness and the resulting hydraulic effects of such structures. Such a synthesis could include, if available and non-proprietary, results of interference tests between wells, effects of gas injection, and other observations that could support or weaken evidence for hydraulic connectivity at specific locations. This study could also include a review of data that might elucidate the erosional history of the Fruitland Formation, i.e., when it first became exposed to surface water, for example, by dating alluvial or terrace sediments.

11.0 References

Allison, G. B., G. W. Gee, and others. 1994. *Vadose-zone techniques for estimating groundwater recharge in arid and semiarid regions*. Journal of Hydrology, vol. 58, pp. 6-14.

Ayers, W. B., and W. R. Kaiser. 1994. Coalbed methane in the Upper Cretaceous Fruitland Formation, San Juan Basin, New Mexico and Colorado. New Mexico Bureau of Mines and Mineral Resources Bulletin 146.

Bureau of Land Management. 2000. Technical basis for infill drilling criteria – northern San Juan Basin of Colorado. Public Lands Office, Durango, CO.

Chow, V.T., D. R. Maidment, and L. W. Mays. 1988. *Applied hydrology*. McGraw-Hill, Inc., New York p 572.

Dam, W.L., J. M. Kernodle, C. R. Thorn, G. W. Levings, and S. D. Craigg. 1990. Hydrogeology of the Pictured Cliffs Sandstone in the San Juan Structural Basin, New Mexico, Colorado, Arizona, and Utah. USGS Hydrologic Investigations Atlas HA-720-D, 1:1,000,000 and 1:2,000,000.

Fassett, J. E., and J. S. Hinds. 1971. *Geology and fuel resources of the Fruitland Formation and Kirtland Shale of the San Juan Basin, New Mexico and Colorado*. USGS Professional Paper 676.

Fassett, J. E., S. M. Condon, A. C. Huffman, and D. J. Taylor. 1997. *Geology and Structure of the Pine River, Florida River, Carbon Junction, and Basin Creek gas seeps, La Plata County, Colorado*. USGS Open-File Report 97-59.

Gee, G. W., and D. Hillel. 1988. *Groundwater recharge in arid regions: review and critique of estimation methods*. Hydrological Processes, vol. 2, pp. 255-266.

Hill, D. G., C. R. Nelson, and C. F. Brandenburg. 2000. *Coalbed methane in the rocky Mountain region: the old, the new, and the future*. In: *Coalbed methane in the Rocky Mountains*. 2000 RMAG Coalbed Methane Symposium, Denver, Colorado, June 20-21, 2000. Rocky Mountain Association of Geologists.

Hubbert, M. K. 1940. *The theory of groundwater motion*. Journal of Geology, 48, pp. 785-944.

Hunt, J. M. 1979. *Petroleum geochemistry and geology.* W. H. Freeman and Company, San Francisco. 617 pp.

Kaiser, W. R., T. E. Swartz, and G. J. Hawkins. 1994. Hydrologic framework of the Fruitland Formation, San Juan Basin. In *Coalbed methane in the Upper Cretaceous Fruitland Formation, San Juan Basin, New Mexico and Colorado*. Bulletin 146, New Mexico Bureau of Mines and Mineral Resources. p. 133-164.

Kernodle, J. K. 1996. Hydrogeology and steady-state simulation of ground-water flow in the San Juan Basin, New Mexico, Colorado, Arizona, and Utah. USGS Water-Resources Investigations Report 95-4187.

Laubach, S. E., and C. M. Tremain. 1994. Tectonic setting of the San Juan Basin. In Ayers and Kaiser, 1994, pp. 9-11.

Lerner, D. N., A. S. Issar, and I Simmers. 1990. *Groundwater recharge: a guide to understanding and estimating natural recharge*. International contributions to hydrogeology, vol. 8. International Association of Hydrogeologists.

McDonald, M. G., and A. W. Harbaugh. 1988. *A Modular three-dimensional finite-difference ground-water flow model*. Techniques of Water-Resources Investigations 06-A1. USGS, 576 p.

Molenaar, C. M. 1983. *Major depositional cycles and regional correlations of Upper Cretaceous rocks, southern Colorado plateau and adjacent areas*. In Reynolds, M. V. and E. D. Dolly. 1983. *Mesozoic paleogeography of the west central United States*. Rocky Mountain Paleogeography Symposium II, pp. 201-224. Society of Economic Paleontologists and Mineralogists, Rocky Mountain Section.

Oakes, D.B. 1977. *The movement of water and solutes through the unsaturated zone of the Chalk in the United Kingdom*. In: *Surface and subsurface hydrology*. Proceedings of the 3rd International Hydrology Symposium, Fort Collins, July 1977, pp. 447-459. Water Resources Publications.

Oldaker, P. 1999. *Monitoring data review, Pine River Ranches*. Prepared for Colorado Oil and Gas Conservation Commission and BP Amoco Production Company (USA). April 9, 1999. CD-ROM format.

Owenby, J., R. Heim Jr., M. Burgin, and D. Ezell. Undated. *Maps of annual 1961-90 normal temperature, precipitation, and degree days*. Climatography of the United States No. 81, Supplement #3. NOAA.

Phillips, F. M., L. A. Peeters, and M. K. Tansey. *Paleoclimatic inferences from an isotopic investigation of groundwater in the central San Juan Basin, New Mexico*. Quaternary Research, vol. 26, pp. 179-193.

Phillips, F. M., M. K. Tansey, and L. A. Peeters. 1989. *An isotopic investigation of groundwater in the central San Juan Basin, New Mexico: carbon 14 dating as a basis for numerical flow modeling*. Water Resources Research, vol. 25, no. 10, pp. 2259-2273.

Pine River Investigative Team (PRIT). 1995. *Pine River Investigative Team Report*. 2/21/95. 11 pp. and 9 appendices.

Prucha, R.H. 2000. *Basin-scale groundwater budget in semi-arid and arid zones: dynamic recharge analysis using a distributed parameter surface-subsurface model*. Ph.D. dissertation in progress at the University of Colorado, Boulder.

Questa Engineering Corporation. 2000. *3M CBM Final Report, Volume I: Analysis and Results*. Prepared for The Southern Ute Indian Tribe, The Colorado Oil and Gas Conservation Commission, and The U.S. Bureau of Land Management. October 2000.

Riese, R. 2000. *Interim results of produced water sampling, and hydrochemical and isotope age analyses by Vastar Resources, Inc.* Data provided to the 3M Project Technical Peer Review Team.

Robson, S. G. and E. R. Banta. 1995. *Ground water atlas of the United States. Segment 2: Arizona, Colorado, New Mexico, and Utah*. USGS Hydrologic Investigations Atlas 730-C.

Simmers, I., 1997. *Recharge of phreatic aquifers in (semi-) arid areas*. A.A. Balkema, Rotterdam, IAH, Vol. 19

Stephens, D.B. 1996. *Vadose zone hydrology*. CRC Press, Inc., Lewis Publishers, Boca Raton.

USGS. 1977. Geologic Map of the San Juan Basin, Northwestern New Mexico, and Southwestern Colorado, Professional Paper 676, Plate 1.

Wray, L. L. 2000. *Late Cretaceous Fruitland Formation Geologic Mapping, outcrop Measured Sections, and Subsurface Stratigraphic Cross Sections, Northern La Plata County, Colorado*. Colorado Geological Survey Open-File Report 00-18.

Appendices

Appendix A

Regional recharge review

Material in this Appendix is largely taken from work by Prucha (2000).

Regional recharge analysis

Groundwater recharge represents an important component in the overall hydrologic cycle described by Chow (1988). It is one of the most critical parameters in assessing groundwater flow conditions within an aquifer system, and yet it remains difficult to estimate because of its complexity. Estimating recharge to a system typically requires a detailed characterization of the system and the development of a 3-dimensional conceptual model of flow within this system. For a typical aquifer system, groundwater recharge occurs as a complex coupling of hydrologic processes that in turn depend on a number of factors. These processes and factors vary for each aquifer system and must be assessed thoroughly to determine reasonable estimates for the given system. In other words, site-specific factors such as geologic structure and aridity dramatically affect the groundwater recharge process and rates.

The general concepts of the various recharge process and factors are discussed in more detail first. Then a brief description of the types and relative accuracy of various methods currently used to estimate recharge is presented. This is followed by a brief summary of primary aquifer systems in the southwestern United States and the principal recharge processes and factors associated with each system.

A.1 Recharge processes and factors

Processes

Groundwater recharge is not only a complex process, but it is frequently poorly understood and defined. This situation has developed mainly because various groups within hydrology (i.e., groundwater hydrologists, reservoir engineers, agricultural/irrigation engineers, surface water hydrologists, meteorologists) have generally approached the concept from different viewpoints. A well-defined and unified concept of recharge has been stymied by the lack of overlap between the various groups. This situation is important to acknowledge since much of the available literature tends to reflect the different definitions amongst the different groups. As such, the general concept and importance of groundwater recharge can be and often is confusing, particularly between these different groups. Given this situation, the following discussion attempts to present an overview of recharge that incorporates all perspectives.

Relatively current and general references on groundwater recharge processes, factors, and various types of systems can be found in Simmers (1997) and Lerner (1990). Other references describe recharge, but tend to be focused on the following:

- Specific types of systems or locations
- Specific climates
- Specific methodology and techniques used to estimate recharge

References other than Simmers (1997) and Lerner (1990) will be cited in the following discussion where appropriate.

Conceptually, groundwater recharge is probably best described by showing how it fits into a simple mass-balance of flow within an aquifer segment. Figure A-1 shows an aquifer segment with lateral inflow and outflow (Q_{in} and Q_{out}), recharge, and storage. The change in storage of the aquifer segment within a given time is determined by subtracting the outflow (Q_{out}) from the inflows (Q_{in} + recharge). Based on this simple diagram, it is obvious that recharge is a critical component of even the simplest water budget for a system.

Moving on to a more sophisticated diagram, Figure A-2 shows a flow chart of the most important processes and how they interact with the groundwater flow system, herein defined as that portion of the aquifer that is fully saturated. The figure represents a generalized system. Specific aquifer systems will differ in the relative importance of each process in the overall recharge to the groundwater zone. It is apparent from the diagram that a number of processes contribute to recharging the groundwater zone. The groundwater zone in this diagram is conceptualized as a 'control volume' representing a fixed volume in space and time; however, the groundwater zone (storage) increases and decreases in response to time-varying amounts of recharge from each process. The majority of the diagram defines recharge resulting directly from precipitation, although more generally it also includes the following:

- Inflow from adjacent aquifers/formations
- Existing surface depression storage (ponds, lakes, rivers) that are not dependent on a given precipitation event
- Anthropogenic sources, like artificial recharge via injection wells, or leaking pipes which becomes a significant source in more urban settings

As shown in the diagram, recharge can be derived from precipitation as either rainfall, or snowfall and snowmelt. The specific recharge processes can differ significantly for the two different precipitation types. This is due not only to differences in their relative state (i.e., liquid or solid), but in the magnitudes of the storm events that lead to their spatial distributions and quantities.

Recharge to the groundwater zone is characterized as direct, indirect, or localized (Simmers, 1997).

Direct recharge refers to the direct infiltration of precipitation into the soils. Another term often used in the literature for this process is 'precipitation recharge', or 'diffuse areal recharge'. The majority of literature on recharge tends to be associated with this type of recharge.

Figure A-1

Simplified water balance

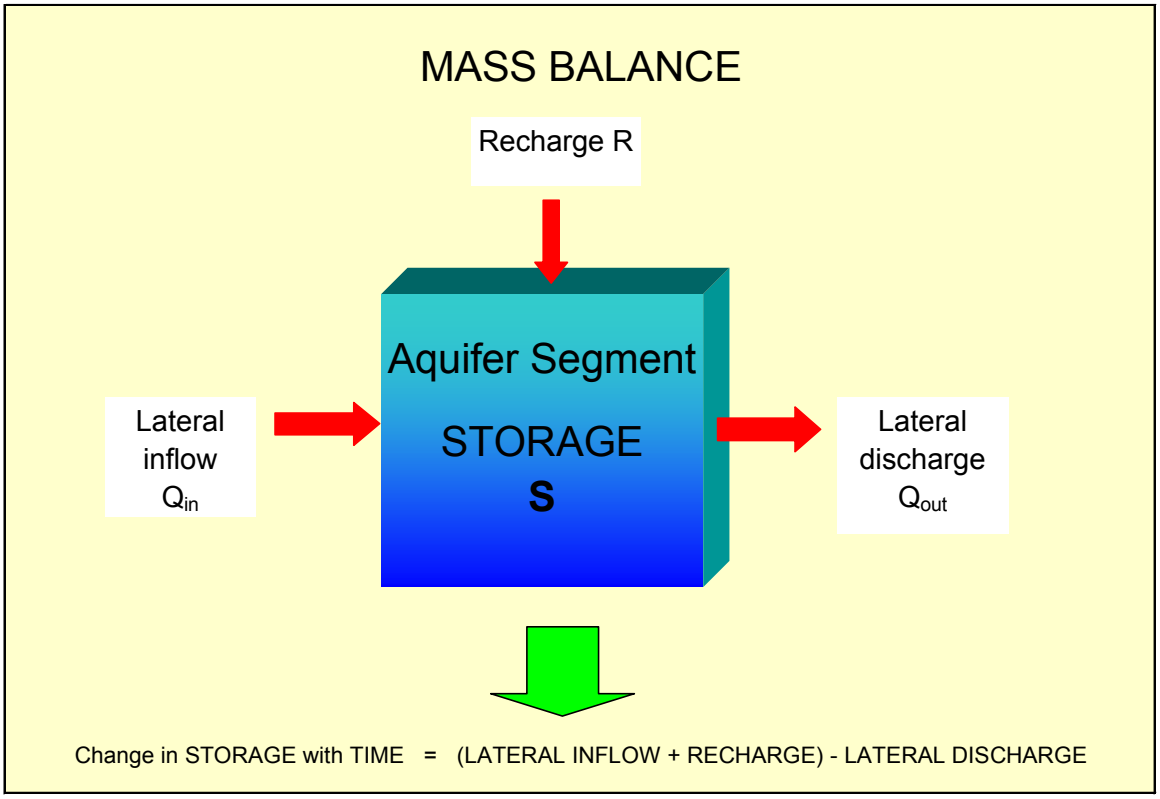

Figure A-2

Generalized Groundwater Recharge and Discharge Processes

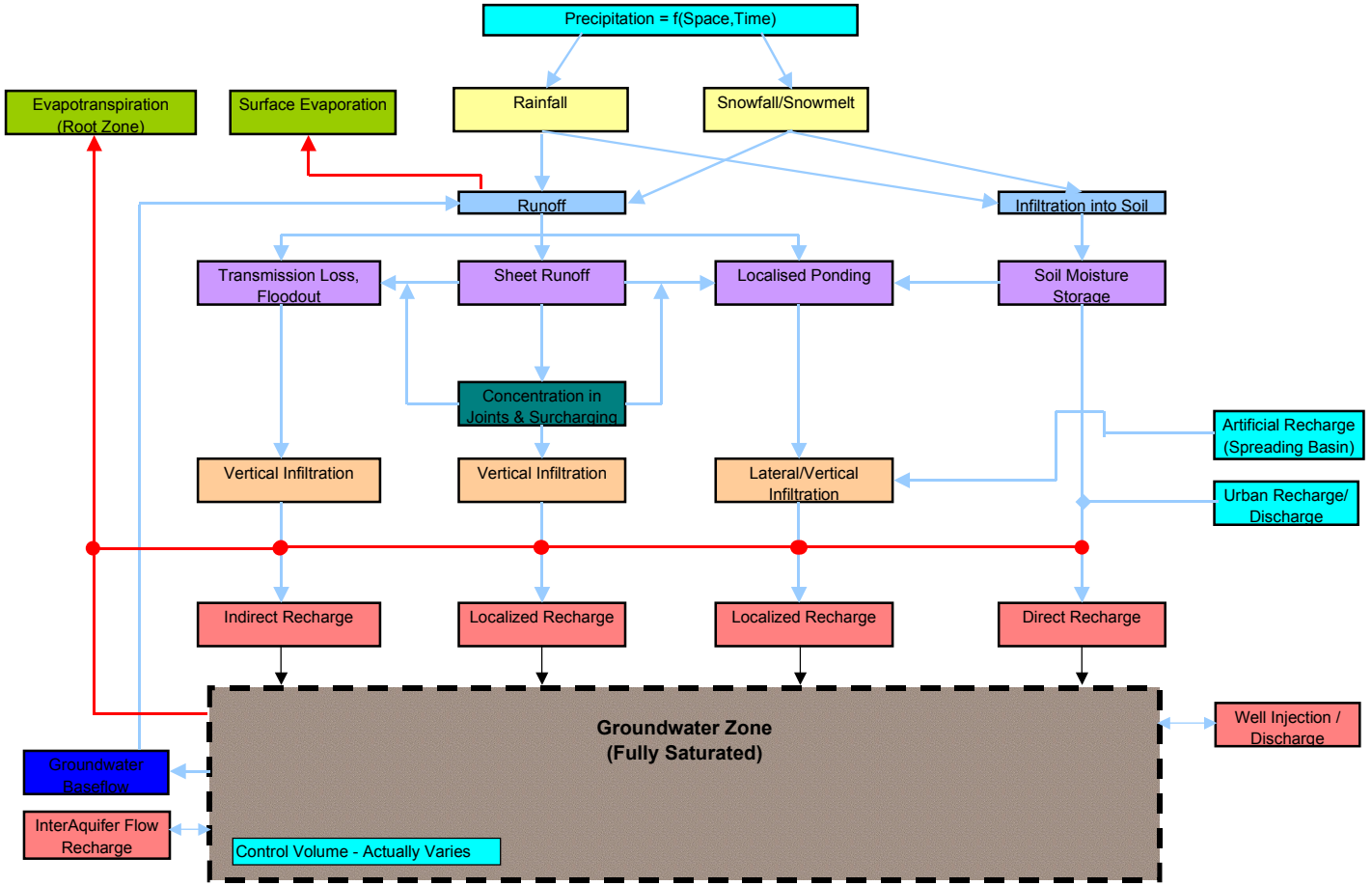

(Adapted from Lloyd, J.W., 1986, Lerner (1990), Simmers (1997))

Indirect recharge is defined as that portion of the precipitation that infiltrates below channelized runoff. This type of recharge can be very intermittent, particularly in arid or semi-arid environments where ephemeral streams occur. It is probably also the most difficult to estimate using conventional methods, because of its very transient nature.

Localized recharge results from concentrated surface water not associated with well-defined channelized runoff. This can include recharge due to preferential flow along fractures, or through macropores. Gee and Hillel (1988) indicate that 'localized recharge' can be categorized into three different scales defined as micro-scale, meso-scale, and macro-scale. These relative scales range from centimeters, to meters, and to hundreds of meters, respectively. The definition of localized recharge also includes recharge from existing, or 'permanent' surface water bodies.

System discharge occurs primarily via the following processes:

- Evapotranspiration
- Surface discharge (usually at streams as baseflow contribution)
- Inter-aquifer flows (loss or gain to adjacent aquifers/aquitards)
- Groundwater pumping

Though the discharge processes seem at first to be unrelated to recharge, a number of recharge estimation methods require a detailed knowledge of them. The process of evapotranspiration affects the entire infiltration process in addition to directly affecting the groundwater system as shown on Figure A-2. Evapotranspiration in itself also represents a complex process that is controlled by a number of factors.

Equations of Flow

Many generalized equations have been developed that show for a simple case how recharge can be estimated using estimates of other hydrologic processes. Because of the different types of recharge mentioned above, it is important to specify what the control volume is for a given equation. Figure A-3 shows two different approaches to defining a control volume for determining recharge. One approach is to specify all of the hydrologic process components for flow into or out of a respective aquifer system (i.e., includes inter-aquifer flows, evapotranspiration, groundwater withdrawals etc.). The second, more common, approach simply specifies those processes directly involved in determining the amount of precipitation that makes it from the ground surface to the groundwater table and is not concerned with other inflows/outflows into aquifer. In the latter case, typically only the following processes are considered important:

- Precipitation (P)
- Runoff (RO)
- Evapotranspiration (ET)
- Unsaturated zone infiltration, percolation, and drainage (recharge) (R)

Figure A-3

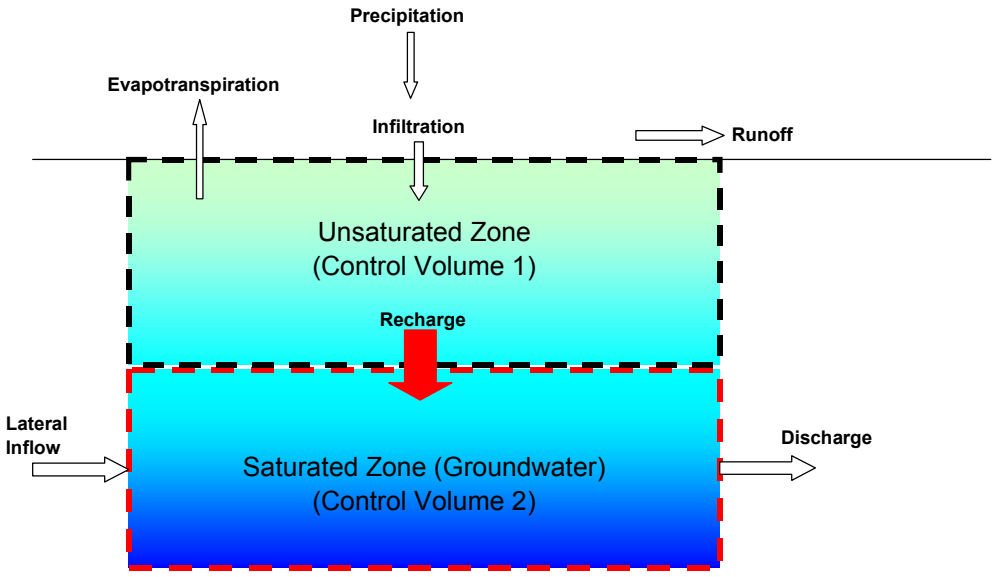

Control Volume 1: Infiltration = Recharge = Precipitation - Runoff - Evapotranspiration

Control Volume 2: Recharge = Discharge - Lateral Inflow

Generally, there are two different ways to formulate an equation to calculate recharge to a groundwater system using the above process components. These are steady state and transient equations.

Steady State:

$$\text{Recharge} = P - RO - ET$$

Transient:

$$\text{Recharge} = \Delta S/\Delta t + P - RO - ET$$

Where:

P = Precipitation
RO = Runoff
ET = Evapotranspiration
Δ = Change in property
S = Storage
t = time

The steady state equation is only useful in describing long-term, time-averaged recharge rates. Every system exhibits a transient response and should include estimates of each process as a function of time. Furthermore, the change in storage over time ($\Delta S/\Delta t$) should also be considered, since subsurface systems can store substantial quantities of water.

Despite the apparent simplicity of the above equations, recharge is probably the most complex component of the entire basin-wide water budget. This complexity is best demonstrated by expanding on the transient water-balance equation above. Each of the processes included in the transient recharge equation above are dependent on a number of factors. For example,

P = f(Temperature, elevation, wind speed and direction, season, long-term climate change, global weather patterns)[1]

ET = f(Temperature, type and distribution of vegetation, root density functions, root growth curves, moisture content and distribution in soils, wind speed and direction, season, long-term climate change, radiation, relative humidity, topographic aspect, topographic slope)

RO = f(Geomorphology, elevation, surface roughness)

Finally, some of these secondary factors depend on other factors such as:

Temperature = f(Latitude, Longitude, elevation, geomorphology, radiation)

[1] f = a function of the following factors

Wind speed/direction = f(Latitude, Longitude, geomorphology, atmospheric pressure distributions)

Vegetation = f(Latitude, Longitude, water content, groundwater depth, wind speed)

Hydrogeologic = f(Latitude, Longitude, soils cover/distribution, geologic structural surfaces, vertical heterogeneity, saturated hydraulic conductivity, specific storage, residual saturation, saturated water content, pressure-saturation parameters, unsaturated k-pressure parameters)

The point in listing these factors that influence recharge is to demonstrate that the recharge process is complex, not only because it is dependent upon a large number of factors, but also because these factors in themselves are complex and vary in both time and space. Uncertainty in these parameters can easily translate into significant errors in estimating recharge. This uncertainty is typically related to obtaining:

- Measurement accuracy of these factors
- Whether a sufficient number of samples are collected to adequately describe system heterogeneity

The parameters that are determined in the field are not collected in sufficient quantities, or accuracy to reflect the complexity of typical basin-scale flow systems. Instead, limited data are extrapolated over broad areas, which effectively lumps entire areas into a single value. This can approach can cause any analysis to mask over the true dynamics of a given area within the system. Therefore, it is very important to construct valid and reasonable conceptual models of flow systems that will adequately reflect spatial variations of parameters used in estimating recharge.

A.2 Methods used to estimate recharge

Several methods used to estimate groundwater recharge are cited in the literature. These methods can essentially be defined into two different categories, direct and indirect methods. The direct methods are considered more accurate, but only at a local scale, where they measure recharge at a point in space (i.e., borehole, lysimeter). At a basin-scale, these point estimates must be extrapolated, which can lead to significant errors if the system is not characterized adequately. The indirect methods, although not considered as accurate at a given point in space are considered more reasonable at a regional scale, because they consider basin-scale features in their estimates.

Examples of direct methods to measure recharge include the following:

- Soil lysimeters
- Tracer studies

Examples of indirect methods include the following:

- Water balance methods (simple to more complex, but takes into account basin-scale factors)
- Darcian methods (numerical solution of partial differential equations)
- Empirical methods (applicable for only specific basin - considerable uncertainty)

Water balance methods typically are simple, but include estimates of flow for all basin-wide components. These methods do not provide any means of determining transient recharge estimates and are only valid for steady state estimates.

There are many references in the literature citing the above methods. However, most focus on application of an individual method to a specific site. Lerner (1990) and Simmers (1997) discuss these methods in detail. Stephens (1996) discusses various methods mainly associated with recharge through the vadose zone. Gee and Hillel (1988) reviewed and critiqued various groundwater recharge estimation methods used in arid regions. However, these authors tend to regard point estimates as more accurate estimates of recharge, despite not being reflective of basin-wide conditions. Allison et al (1994) also describe a number of methods for estimating groundwater recharge in arid and semi-arid regions, focusing mainly on isotopic tracers. Again, these authors suggest that tracers and lysimeter methods yield more reliable estimates than water balance methods (indirect methods). However, they only discuss recharge for unconsolidated materials (not bedrock), their estimates are for points in space, and they don't consider effects of macropores, fractures, or faults.

Overall, no one good method exists to determine basin-wide recharge estimates. This is particularly true for systems that lack data. A lack of appropriate data can be more limiting than the variability in results obtained from most of the methods above.

Both Lerner (1990) and Simmers (1997) conclude that the best approach to estimating recharge to a system is to combine a rigorous numerical analysis (e.g., the Darcian method) with confirmation at specific points using more accurate point methods like lysimeters, or tracers.

Darcian methods include use of physical equations to describe infiltration, groundwater flow, and surface flow dynamics. Typical equations used to describe these processes involve the 1-dimensional Richard's equation for infiltration, the 3-dimensional Boussinesq equation for groundwater flow, and the one-dimensional St. Venant hydrodynamic equations (continuity and momentum) or the 2-dimensioal diffusive wave equation for overland and surface flows.

A.3 Southwestern United States recharge

Many aquifer systems have been studied in the arid/semi-arid southwestern United States. The USGS Groundwater Atlas (Robson and Banta, 1995) describes the three general types of aquifer systems throughout this region and include:

- Basin and Range aquifers
- Colorado Plateau aquifers
- Alluvial aquifers

To a lesser extent some limestone, or karstic, aquifer systems occur, but are not as predominant compared to the other types.

Although recharge occurs in each of these systems according to the same general processes outlined above, the specific factors controlling recharge are quite different for each aquifer system. Available literature indicates that many of the recharge estimates for each of these systems throughout the southwest have been determined by using simple empirical relationships, such as the Maxey Eakin method (Stephens, 1996).

Colorado Plateau systems with similar climate and geologic settings as the San Juan Basin include the following:

- Black Mesa system (AZ)
- Kaiparowits Plateau (UT)
- Kane and Washington counties (UT)
- Lake Powell system (UT, AZ)
- Monument Valley (UT)
- Aneth oil field (UT)

Table 1 lists water-budget estimates including recharge for different Colorado Plateau aquifer systems and also includes comparison of recharge rates to typical Basin and Range aquifer systems. It should be noted, that the estimates of recharge specified in this table represent only the recharge to more permeable aquifer units, and not to less permeable layers. All of these systems used MODFLOW models to simulate the various water-budget component estimates.

Table A-1

Comparison of hydrologic budgets for basin-wide aquifer systems in the SW U.S.

Colorado Plateau Basin - Black Mesa

Study Number	Author	Site Name/ Location	Report Date	Estimated Recharge (Units Indicated)	Estimated Discharge (Units Indicated)	Basin Precipitation (Units Indicated)	Basin Area Mile^2	Minimum Elevation in Study Area (ft)	Maximum Elevation in Study Area (ft)	Identified Recharge Mechanisms
1	Eychaner	Black Mesa	1983	13000 acre-ft/yr 4830 acre-ft/yr 4480 acre-ft/yr 3620 acre-ft/yr	N/A		5,400	4,395	8,061	
2	GeoTrans	Black Mesa	1987	12381 acre-ft/yr						
3	Brown/Eychaner	Black Mesa	1988	13380 acre-ft/yr						
4	Lopes/Hoffman	Black Mesa	1996	2600 - 3600 acre-ft/yr						
5	HSI-GeoTrans, Inc.	Black Mesa	1997	14238 - 20428 acre-ft/yr						
6	PWCC, 3D	Black Mesa	1998	N/A	N/A	2470555 acre-ft/yr	7,408	4,395	8,061	
Colorado Platuea Basins										
1	Blanchard, Paul	Kaiparowits	1986	44000 acre-ft/yr 1.5% of Precip	122000 acre-ft/yr in Runoff 2799000 acre-ft/yr in ET	2965000 acre-ft/yr 6 - 30 in/yr	4850	3116	11328	
2	Blanchard, Paul	Lake Powell Area	1986	3000 acre-ft/yr ~0.3% of Precipitation	3690 acre-ft/yr 1000 - 4000 acre-ft/yr	1100000 acre-ft/yr 6-25 in/yr	2450	3700	11522	Fractures saturated sand dunes winter precip
3	Kernodle, J.M.	San Juan Basin	1995	40,542 acft/yr .14 in/yr or 1% Precip	195 ft^3/s (141,173) ac-ft/year	8 - 40 in/yr	21600	4500	11300	
4	Heilweil, V.M., Freethey, G.W.	Navajo Aquifer, Kane County	1992	50280-68180 acre-ft/yr ~9% to 12% Precipitation 8140 ac-ft/yr Springs 2,400 ac-ft/yr ET + wells	50280-68180 acre-ft/yr Springs 8140 acre-ft/yr ET 1500 acre-ft/yr	555000 acre-ft/yr (Precip on Navajo) 10-40 in/yr 1-20% Precip. is Infiltration	2600	5000	11000	
5	Thomas, B.E.	Four Corners, Monument Valley/Mesozoic Rocks	1988	5,500-100000 acre-ft/yr from data 30390 acre-ft/yr from Model .65% of Precip 6-30 in/yr + large quan snow	1-3 ft/yr ET (roughly equal to Recharge)	2253000 acre-ft/yr	4100	4200	11360	Rainfall Snowfall Alluvial or eolian dep enhance recharge 5-15% mtns fractures
Basin and Range Aquifers										
1	Berger, David L.	Desert Valley, Humboldt and Pershing Counties, NW Nevada	1995	.04-.11 ft/yr (dunes) 7,300 acre-ft/yr basin (500-1000 dunes)	0.07 -1.1 ft/yr ET	410000	1200	4200	9000	Dunes Mtn. Blocks
2	Plume, Russel W.	Maggie, Marys, Susie Creek Basins, Elko and Eureka Counties, Nevada	1994	25000 acre-ft/yr	380000 acre-ft/yr ET 0.1 - 0.5 ft/yr .75 - 1.25 ft/yr	420000	630	5200	7690	
3	Bauer, H.H., Vaccaro, J.J.	Columbia Plateau WA, ID, OR	1988	N/A		6.5 - 45 in/yr	32800			Winter Precip Higher Elevations
4	Harrill, J.R., Hines, L.B.	Dixie Valley Area, West-Central Nevada	1995	23000 acre-ft/yr	20000-31000 acre-ft/yr	5-13 in/yr	2380	3360	9000	
5	Dinicola, R.S.	Hanford Site, Washington	1997	5425 acre-ft/yr total 868 acre-ft/yr - from runoff	81-94% ET	6.3 - 11	222	600	4000	
6	Wasiolek Maryann	Tesuque Aquifer, Santa Fe, New Mexico	1995	9600-14700 acre-ft/yr 8-13% Precp.	113000 acre-ft/yr		70	6600	12400	Winter Precip
		Rio Nambe Drainage Basin		5520 acre-ft/yr 3.03 in/yr	67% ET	24.78 in	34.24	6500	12600	
		Rio en Medio Drainage		1710 acre-ft/yr 3.73 in/yr	69% ET	24.06 in	8.66	7000	12000	
		Tesuque Creek Drainage		1530 acre-ft/yr 2.45 in/yr	69% ET	24.18 in	11.22	7440	12000	
		Little Tesuque Creek Drain		1790 acre-ft/yr 4.41 in/yr	72% ET	22.96 in	7.02	7500	11000	
		Santa Fe River Drainage					18.24			

(From Prucha, 2000)

A.4 San Juan Basin precipitation

Recharge for the San Juan Basin was determined as part of the calibration process for the 3M hydrologic model, as described in Section 8.0. To compare the modeled recharge values with actual rainfall, a rainfall map of the San Juan Basin was generated. This used data from the climate stations, which are tabulated in Table A-2 and shown in Figure A-4. Figure A-4 also shows the topographic surface, which was used as the model's upper boundary.

As can be seen from inspecting the long-term average precipitation data on Figure A-4, precipitation tends to increase with elevation and to decrease with distance south and west. These relationships were explored through a statistical analysis of climate station data, presented in Table A-2 and Figure A-5. Together, these three factors (elevation, northing, and easting) can be used to predict precipitation at any station, with a multiple R of 95.2% and a standard error of 2.23 inches. This approach provides a sophisticated way of assigning precipitation values to locations along the outcrop. Actual elevation, northing and easting were used to generate the predicted precipitation map (Figure A-6). Comparing this map with Figure A-4 illustrates the strong effect of elevation on precipitation.

Table A-2

Climatic data and predicted precipitation values

Easting (ft)	Northing (ft)	Elevation (ft-MSL)	Station	MAP (in/yr)	Predicted MAP (in/yr)
1,326,199	13,180,913	5580	Newcomb	6.0	5.6
1,337,974	13,362,773	4970	Shiprock	7.1	6.0
1,397,787	13,507,784	7110	Mesa Verde National Park	18.3	18.5
1,432,170	13,562,102	6910	Mancos	16.7	18.6
1,464,580	13,325,297	5630	Farmington Ag Science C	8.9	8.9
1,469,575	13,343,463	5540	Farmington FAA Airport	8.2	8.8
1,489,100	13,343,351	5400	Farmington 3 NE	8.0	8.3
1,524,008	13,519,095	7600	Fort Lewis	18.5	21.5
1,529,550	13,688,931	8780	Rico	26.8	29.8
1,566,526	13,082,237	6180	Chaco Canyon National Monument	9.0	7.7
1,572,558	13,537,131	6600	Durango	19.1	17.5
1,640,420	13,573,444	8090	Lemon Dam	31.9	25.2
1,645,277	13,482,454	6460	Ignacio 1 N	14.0	16.2
1,659,788	13,567,385	7650	Vallecito Dam	26.6	23.2
1,694,677	13,045,805	6640	Star Lake	9.3	9.8
1,778,762	12,997,567	6700	Torreon Navajo Mission	10.4	9.7
1,822,115	13,173,695	7360	Lindrith 2 SE	14.4	15.9
1,824,658	13,531,598	7110	Pagosa Springs	20.2	20.9
1,830,295	13,416,377	6790	Dulce	17.6	17.5
1,841,372	13,228,413	7420	Gavilan	16.8	17.2
1,842,399	13,082,851	7050	Cuba	13.3	13.0
1,846,932	13,137,471	7450	Regina	15.8	15.8
1,909,414	13,289,637	6800	El Vado Dam	14.6	15.8

Predicted = (0.0000047566*Easting)+(0.000017111*Northing)+(0.00455344*Elevation)-251.69

Figure A-4

San Juan Basin topography and climate stations

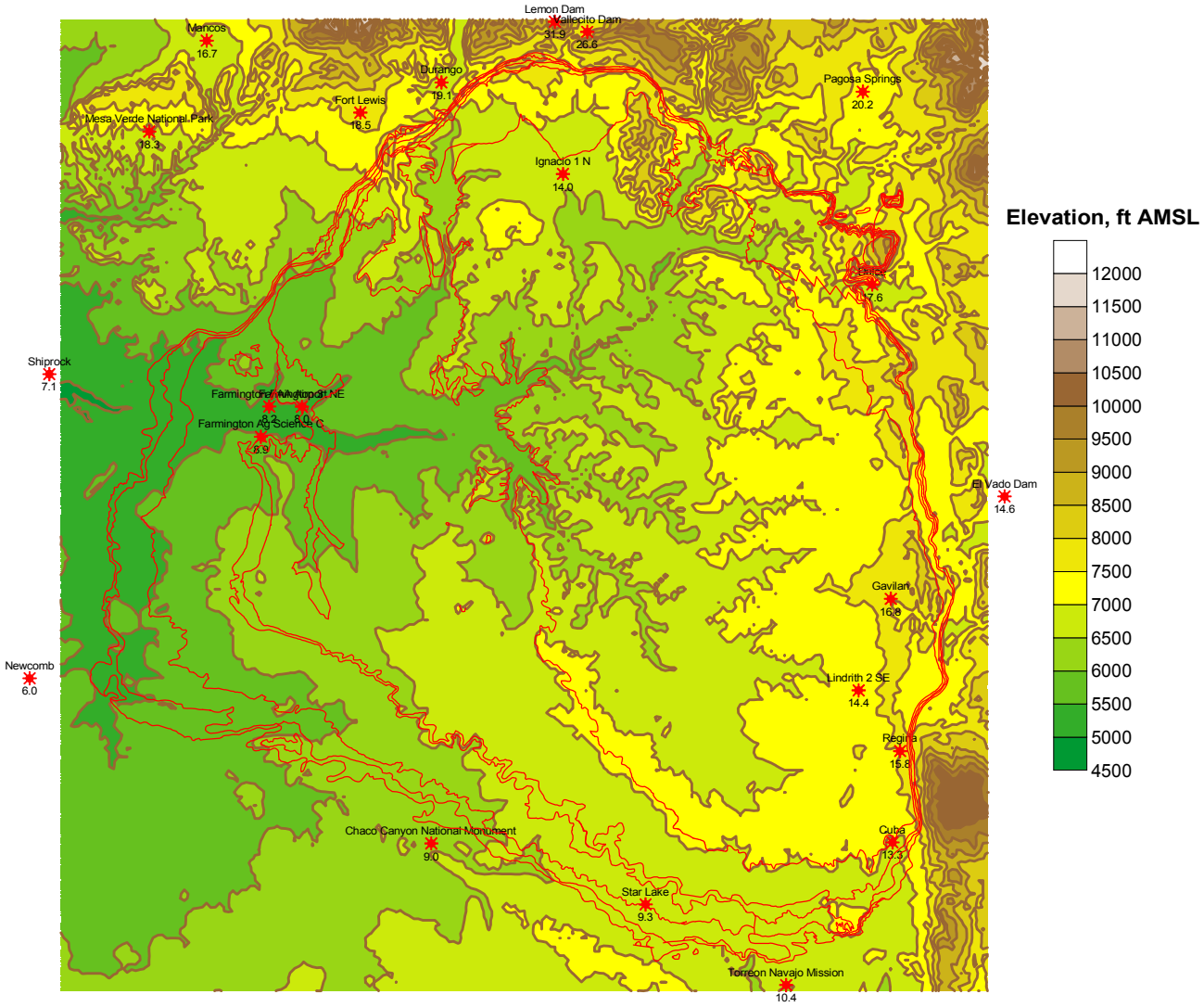

This figure was generated from USGS DEM data using SURFER®.

Figure A-5

Factors affecting precipitation

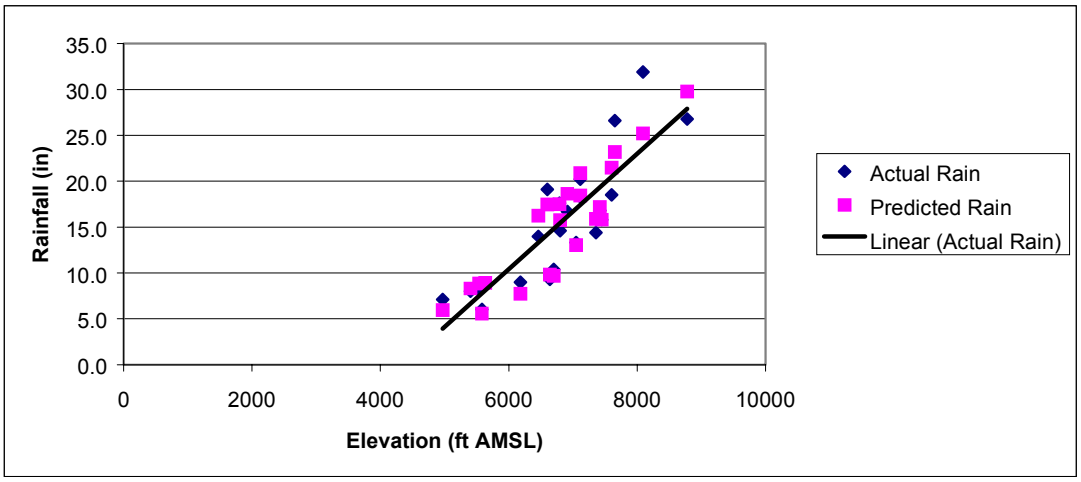

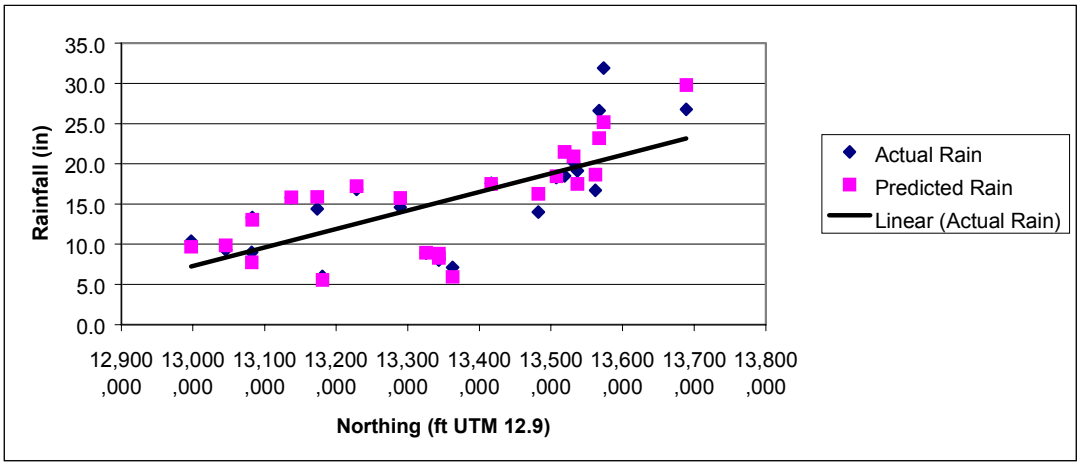

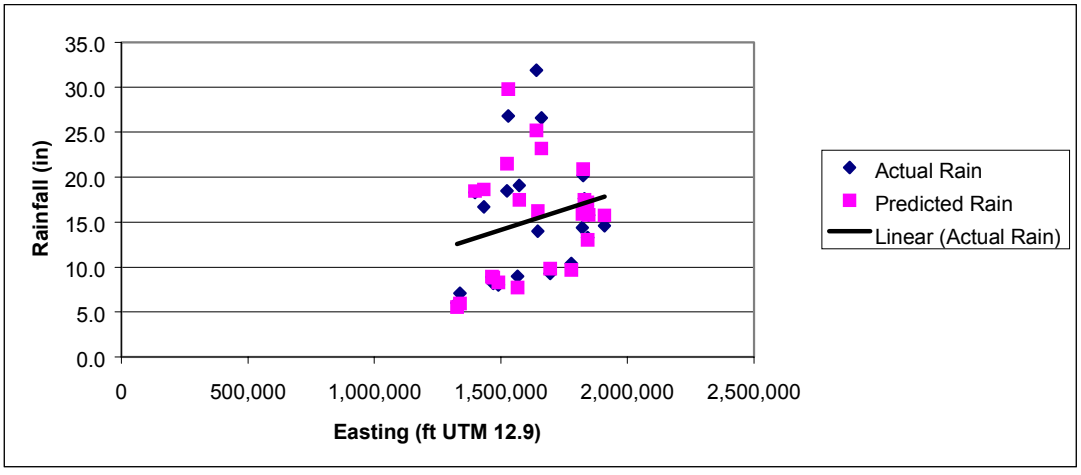

Figure A-6

Predicted precipitation

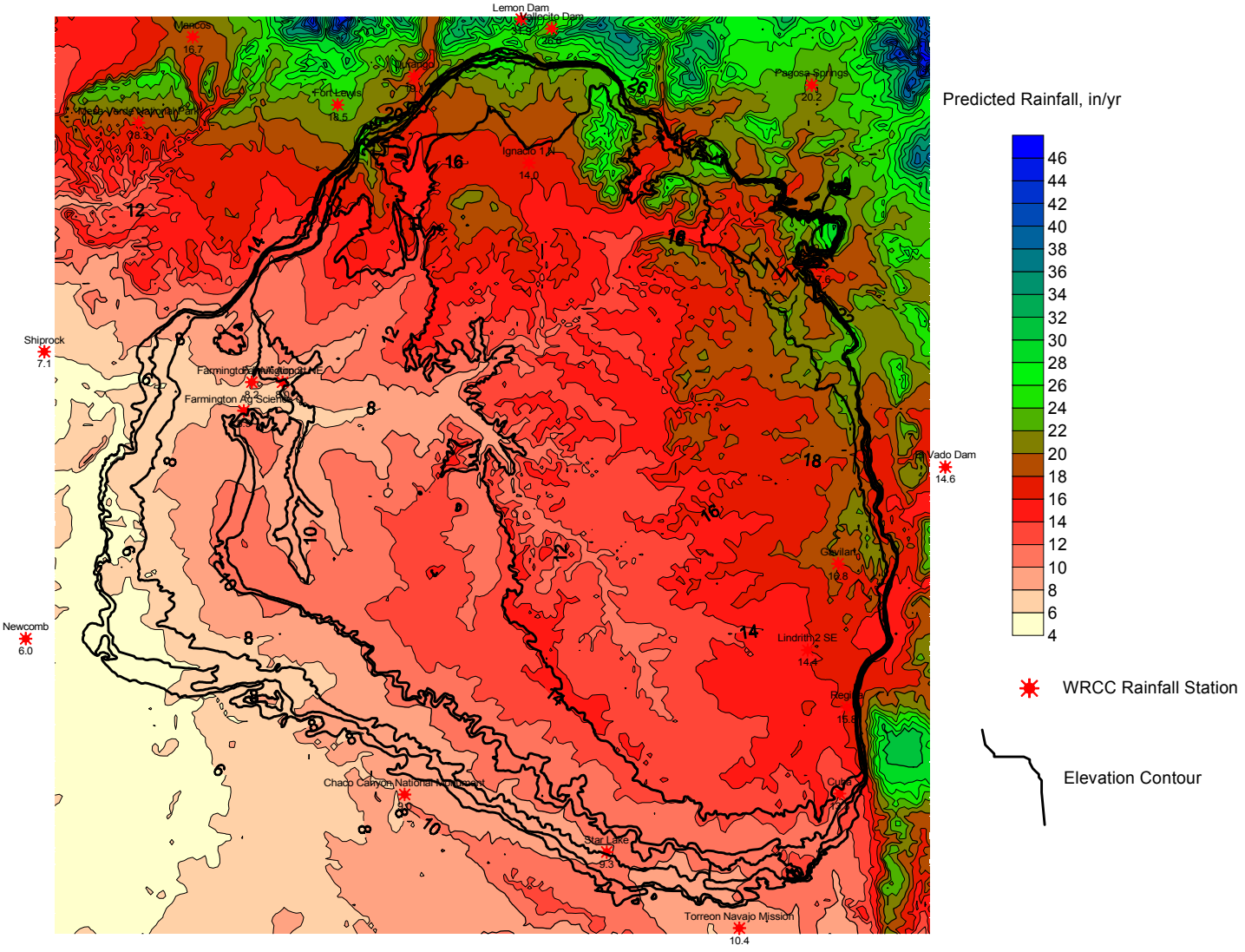

This figure was generated using USGS DEM data transformed by the equation shown in Table A-2, using SURFER®.

A. 5 Appendix A references

Allison, G. B., G. W. Gee, and others. 1994. *Vadose-zone techniques for estimating groundwater recharge in arid and semiarid regions*. Journal of Hydrology, vol. 58, pp. 6-14.

Chow, V.T., Maidment, D.R., Mays, L.W., 1988. *Applied hydrology*. McGraw-Hill, Inc., New York p 572.

Gee, G. W. and D. Hillel. 1988. *Groundwater recharge in arid regions: review and critique of estimation methods*. Hydrological Processes, vol. 2, pp. 255-266.

Lerner, D. N., A. S. Issar, and I Simmers. 1990. *Groundwater recharge: a guide to understanding and estimating natural recharge*. International contributions to hydrogeology, volume 8. International Association of Hydrogeologists.

Prucha, R.H. 2000. *Basin-scale groundwater budget in semi-arid and arid zones: dynamic recharge analysis using a distributed parameter surface-subsurface model*. Ph.D. dissertation in progress at the University of Colorado, Boulder.

Robson, S. G. and E. R. Banta. 1995. *Ground water atlas of the United States. Segment 2: Arizona, Colorado, New Mexico, and Utah*. USGS Hydrologic Investigations Atlas 730-C.

Simmers, I., 1997. *Recharge of phreatic aquifers in (semi-) arid areas*. A.A. Balkema, Rotterdam, IAH, Vol. 19

Stephens, D.B. 1996. *Vadose zone hydrology*. CRC Press, Inc., Lewis Publishers, Boca Raton.

Appendix B

Chloride mass balance analysis

Chloride mass balance analysis

AHA performed a chloride mass balance evaluation for Fruitland Formation produced water in the Colorado portion of the San Juan Basin. The evaluation comprised several tasks, including:

1. Prepare contour maps of dissolved chloride in Fruitland Formation groundwater and in shallow groundwater in La Plata County.
2. Obtain net chloride ion concentrations in precipitation from the National Atmospheric Deposition Program/National Trends Network.
3. Evaluate data.

Each of these tasks is described in the following sections.

B.1 Dissolved chloride maps

This task consisted of the following steps:

1. **Obtain existing data**. The COGCC provided their existing produced water chemistry database, containing 1,001 water analyses. Another 1,231 unentered produced water lab sheets were provided by COGCC, SUIT, BLM, BP Amoco, Enervest, Huber, and Halliburton, as follows:

Data source	Number of entries
COGCC (existing data)	1,001
Various (lab sheets)	844
SUIT/BLM (lab sheets)	250
BP Amoco (lab sheets)	112
Vastar (lab sheets)	25
Enervest (digital data)	1,263
TOTAL	3,495

Note that the number of analytical results is much greater than the number of CBM wells sampled, due to samples being collected on more than one date at the same well, particularly for the Enervest samples which include time series at several wells. A total of 619 CBM wells had at least one set of analytical results.

In addition, COGCC provided results from 150 shallow (generally <100 ft deep) water supply wells in La Plata County.

AHA also obtained data from Fruitland Formation groundwater samples collected at near-outcrop monitoring wells for surface mines in Colorado and New Mexico. Data, from Permit Application Packages, Reclamation Status Reports, and Annual Hydrologic Monitoring Reports, are available at the Office of Surface Mining (OSM) library and at the Colorado Division of Mines and Geology, both in Denver. Data were obtained for Carbon Junction mine, Navajo mine, San Juan Coal Company

surface mine and Deep Lease Extension, La Plata mine, and Cinder Buttes Extension.

2. **Enter new data**. This task took approximately one month, in June/July 1999.

3. **Check well locations.** Check well locations for incorrect coordinates or duplicate entries, and correct as required, assisted by COGCC.

4. **Filter results**. *As recommended by TPRT members:* Using COGCC's well completion and produced water and gas records, filter out samples collected less than one month after the well completion date, to avoid samples affected by frac water in young wells.

5. **Filter results**: *As recommended by TPRT members:* Similarly, filter out samples collected from wells with water-to-gas ratios less than 0.1BBL/MCF, to avoid condensate samples from old, virtually gas-only, wells. The combined filtering in steps 4 and 5 removed 465 samples from consideration, leaving 154 CBM well samples.

6. **Generate maps.** Generate maps of dissolved chloride for 154 produced water wells and 150 shallow water supply wells.

This process was followed to generate the dissolved chloride maps shown in Figure B-1 (Fruitland Formation wells) and Figure B-2 (water supply wells).

The distribution of Fruitland Formation groundwater chloride (Figure B-1) shows some distinct patterns. In general, chloride concentration is higher towards the center and east of the San Juan Basin, up to a few thousand mg/L, and lower at the outcrop, where concentrations are as low as a few mg/L. The increase with distance into the San Juan Basin is not consistent, however. A notable north-south plume of low-chloride groundwater occurs in the eastern side of the mapped area, from T35N/R7W to T33N/R7W, extending approximately 35 miles south from the outcrop. A similar but shorter plume occurs in the west, in T34N/R10W south of the Ute line and T33N/R10W, extending approximately 25 miles south from the outcrop. The simplest explanation for these patterns is that the low-chloride water represents recharge water and the higher-chloride water represents a mixture between recharge water and more saline connate water.

The pattern of water-supply well groundwater (Figure B-2), for wells in the Fruitland Formation and adjacent formations, illustrates shallow groundwater chemistry. This may be inferred to represent recharge water that may have additional dissolved constituents from mixing with connate water. Because of the low chloride concentration in precipitation in this area (see Section B-2), mixing only increases concentration; therefore, the lowest values are probably the most representative of recharge water.

Figure B-1

Fruitland Formation produced water chloride concentration

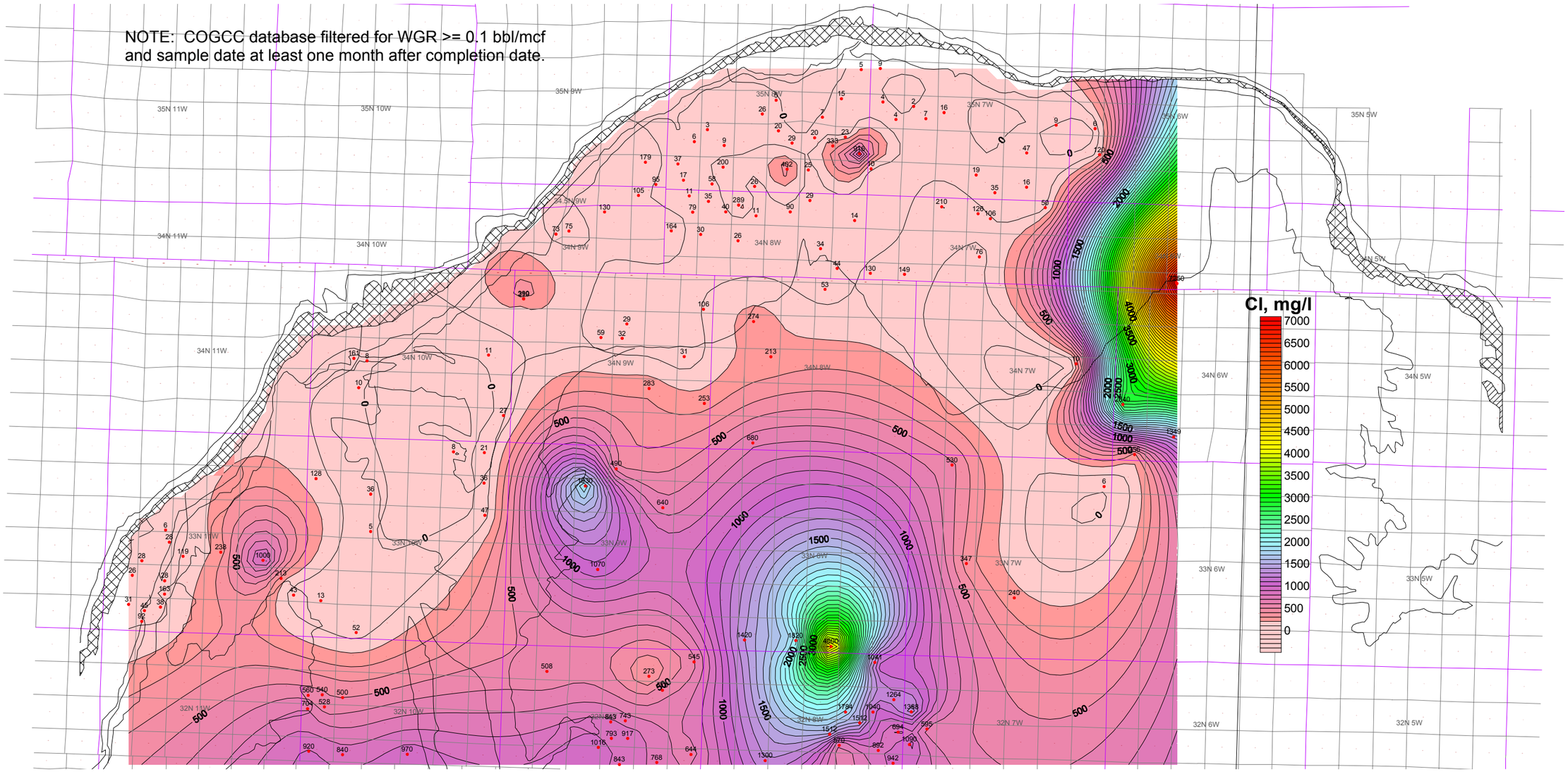

Figure B-2

Shallow groundwater chloride concentration

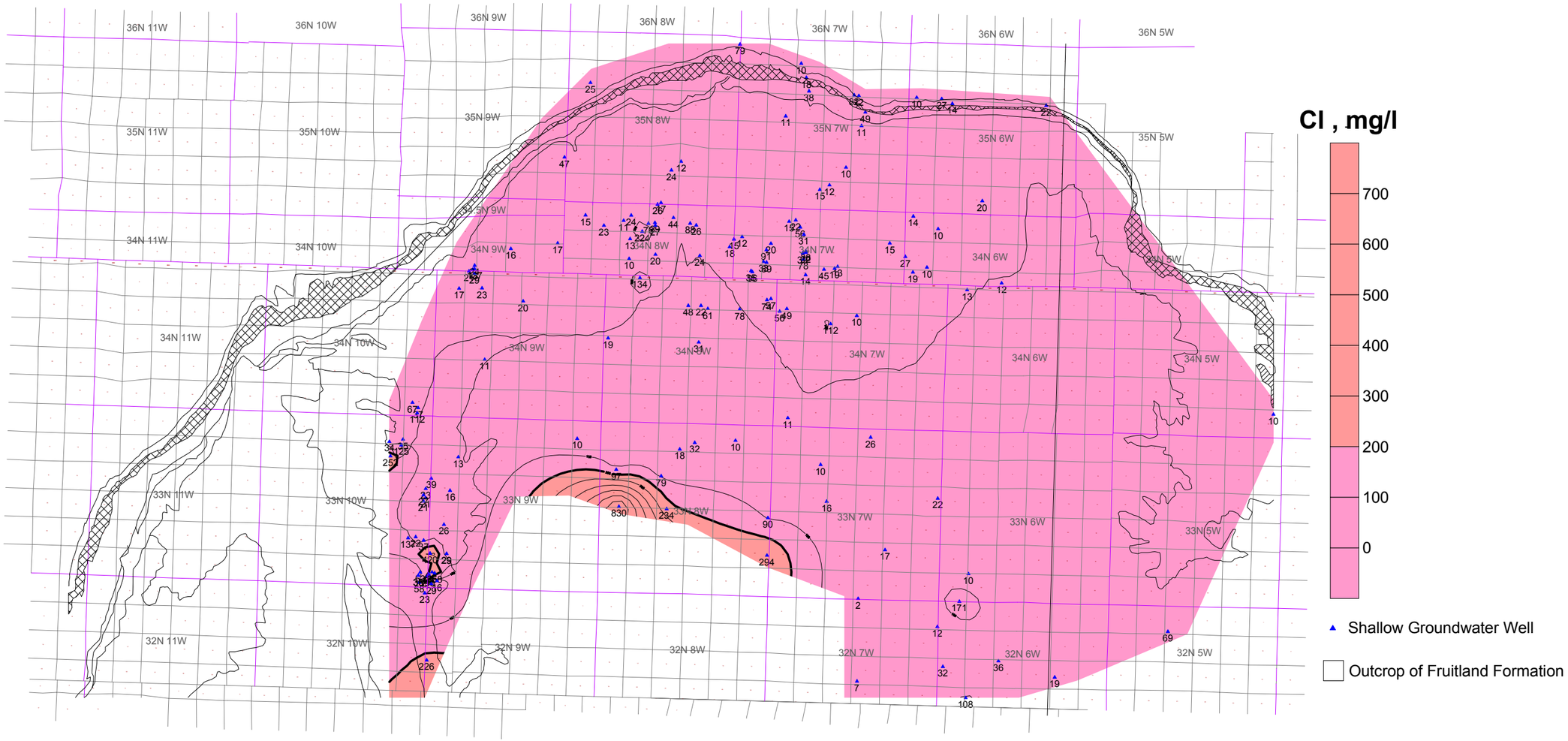

The frequency distribution of chloride values in Fruitland Formation produced water shows a positively skewed population. A histogram of these data (Figure B-3) shows that most values lie between 0 and 70 mg/L. Because of the low chloride concentration in precipitation in this area (see Section B-2), mixing only increases concentration. Therefore, the lowest values are likely the most representative of recharge water. The mean of the lower (0-70 mg/L) data is 23.3 mg/L.

The frequency distribution of chloride values in shallow water-supply wells also shows a positively skewed population. A histogram of these data (Figure B-4) shows that most values lie between 0 and 50 mg/L. This appears to show recharge water with a variable degree of mixing with connate water. The mean of the lower (0-50 mg/L) data is 22.1 mg/L; this is very similar to the mean for Fruitland produced water, and an intermediate value of 22.7 mg/L could be taken as the mean concentration of recharge.

B.2 Chloride in rainfall

The net chloride concentration in precipitation (including dry deposition or "dust") is monitored by the National Atmospheric Deposition Program (NADP) National Trends Network (NTN). This national network of precipitation monitoring stations, administered by the USGS, was originally set up in response to concerns about industrial emissions of sulfur dioxide and nitrogen oxides and their effect on the occurrence of acid rain (pH < 5). The network consists of approximately 220 sites at which precipitation samples are sampled weekly for major ion analysis under a stringent quality assurance program.

A series of maps, which show the precipitation-weighted annual mean chloride concentration in precipitation across the US from 1994 through 1999, follows this appendix.

The following stations (locations are shown in Figure B-5) were used to determine the current average annual chloride concentration in precipitation for the San Juan Basin:

NADP ID	Name	Period monitored started	Elevation (m)	Average annual chloride concentration (mg/L)
CO91	Wolf Creek Pass	5/26/92	3,292	0.060
CO96	Molas Pass	7/29/86	3,249	0.084
CO99	Mesa Verde National Park	4/28/81	2,172	0.100
NM07	Bandolier National Monument	6/22/82	1,998	0.094
NM09	Cuba	2/3/82	2,124	0.107
	Mean of stations			**0.089**

Figure B-3

Analysis of Fruitland Formation produced water chloride data

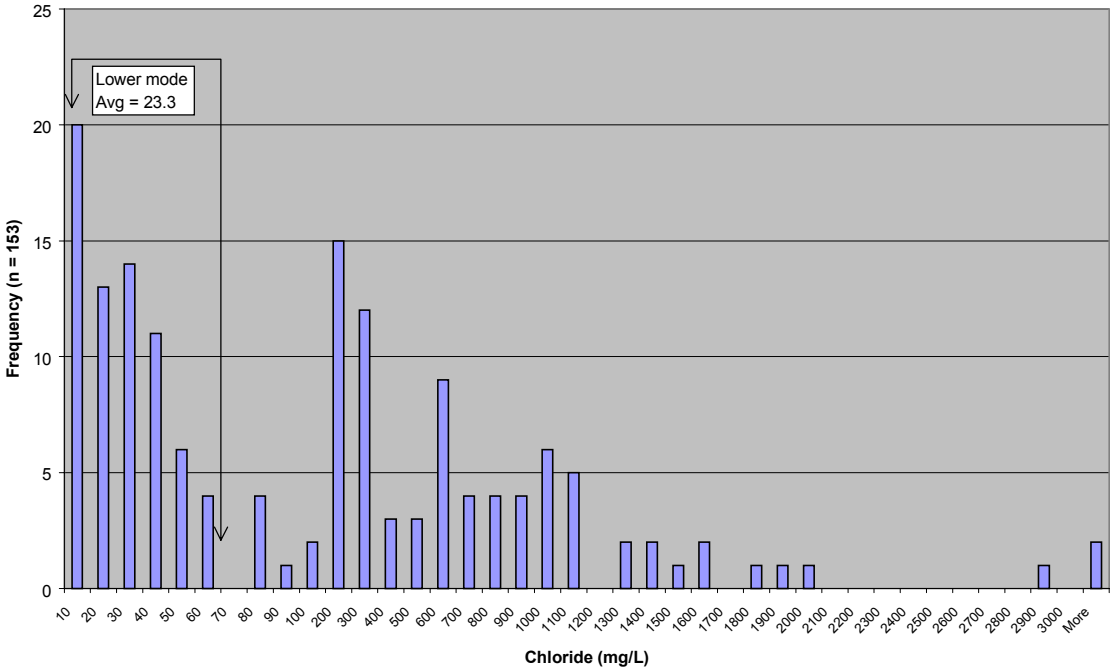

Note change in scale at 100 mg/L.

Figure B-4

Analysis of water-supply well chloride data

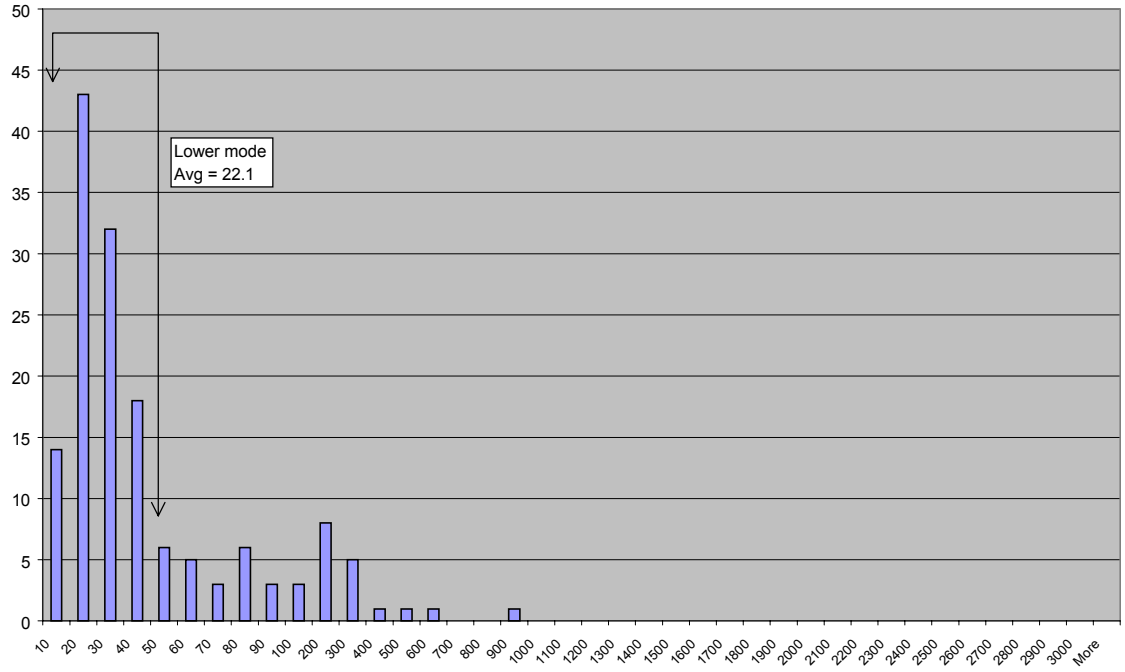

Note change in scale at 100 mg/L.

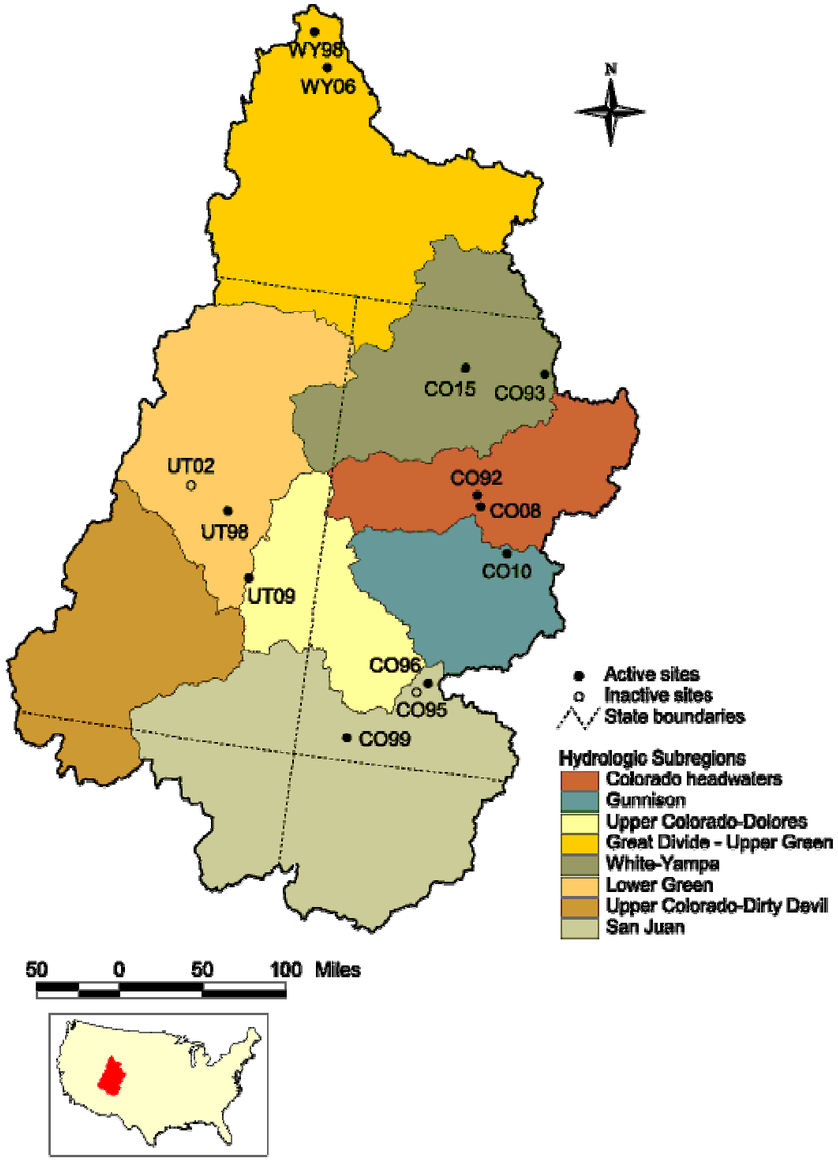

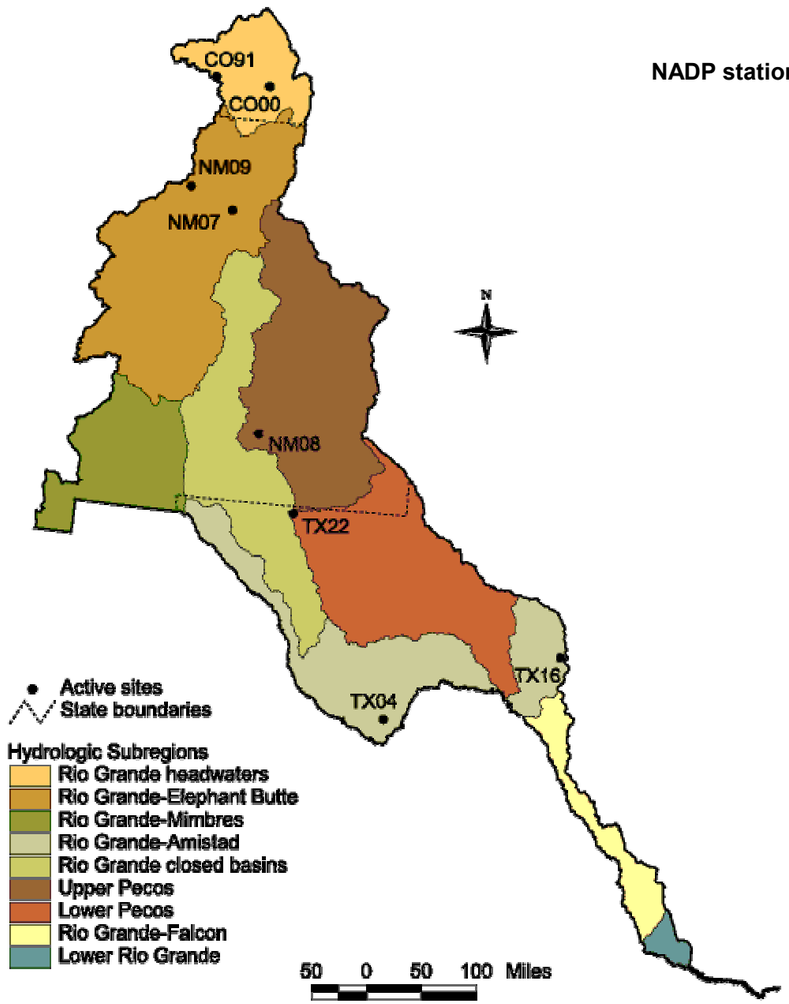

Figure B-5

NADP station locations

B.4 Data evaluation

The chloride mass balance method rests on the fact that chloride is a very soluble ion that rarely enters into chemical reactions in most groundwater systems. In the absence of a chloride contribution from the aquifer itself (i.e., dissolution of halite in evaporite beds), chloride mass can be considered to be conservative. Therefore, the relative concentrations of chloride in precipitation and groundwater will indicate the degree of concentration of precipitation due to evapotranspiration before recharge.

A simplified mass balance approach was followed, ignoring surface water inputs and outputs (run-on and runoff) and the effects of irrigation application and return flow. These elements were ignored because, for the area of the Fruitland Formation outcrop, irrigation does not occur, and surface water runoff is sufficiently fast that surface water chloride input is expected to equal chloride output.

The mass balance equation is:

Mass of chloride in precipitation = mass of chloride in recharge

$$Precip(Cl_{precip}) = Rech(Cl_{Rech})$$

Where:

Abbreviation	Value
Precip = mean annual precipitation across San Juan Basin	12 inches per year (Kernodle, 1996)
$\mathbf{Cl_{precip}}$ = mean annual chloride concentration in precipitation	0.089 mg/L
Rech = mean annual recharge	To be determined
$\mathbf{Cl_{Rech}}$ = mean annual chloride concentration in recharge	22.7 mg/L

Substituting the above values in the mass balance equation:

$$12(0.089) = Rech(22.7)$$

$$Rech = 1.068/22.7 = 0.047 \text{ in/yr}$$

Solving for **Rech**, the mean annual recharge for the Fruitland Formation is 0.047 inches per year, or 0.4% of San Juan Basin mean annual precipitation. It should be noted that this value varies linearly with the chloride value taken as representative of recharge water. The chloride value was taken as the mean of a range, so the calculated recharge rate should also be considered as the mid-point of a range of expected values.

The mean annual recharge value of 0.047 inches per year is an estimate for the San Juan Basin as a whole, whereas recharge would be expected to be higher in the higher-precipitation northern outcrop and lower in the more arid south and west of the San Juan Basin. Therefore, the percentage of annual precipitation (0.4%) was applied to the

outcrop precipitation values, calculated as described in Section A.3 and shown in Figure A-6, to obtain location-specific recharge values for use at the start of the calibration process. Location-specific recharge values are shown in Figure A-7. These values were used as the starting point for model calibration.

Figure A-7

Predicted recharge values

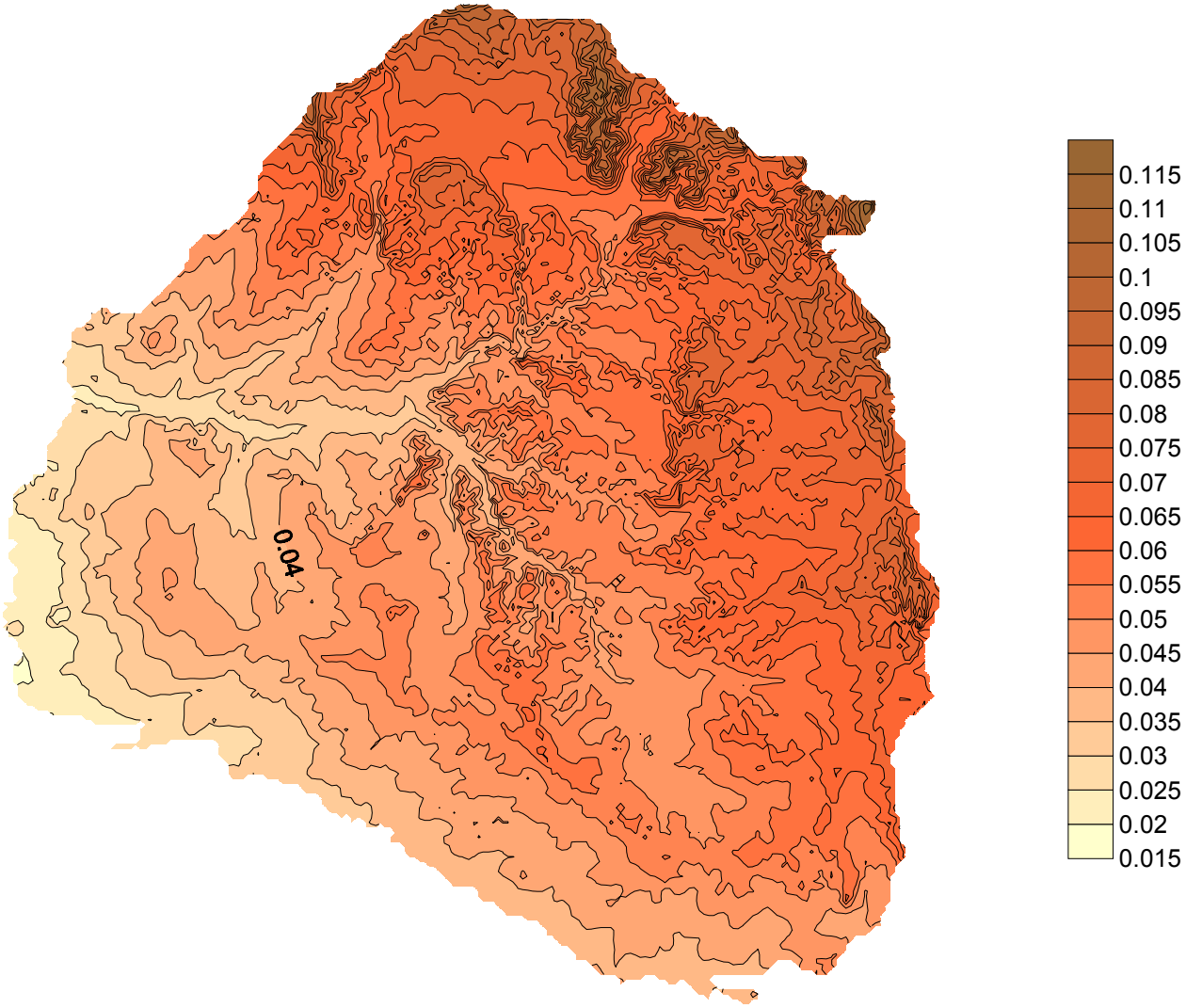

ATTACHMENT B-1

NADP/NTN Chloride concentration maps, 1994-1999

Chloride ion concentration, 1994

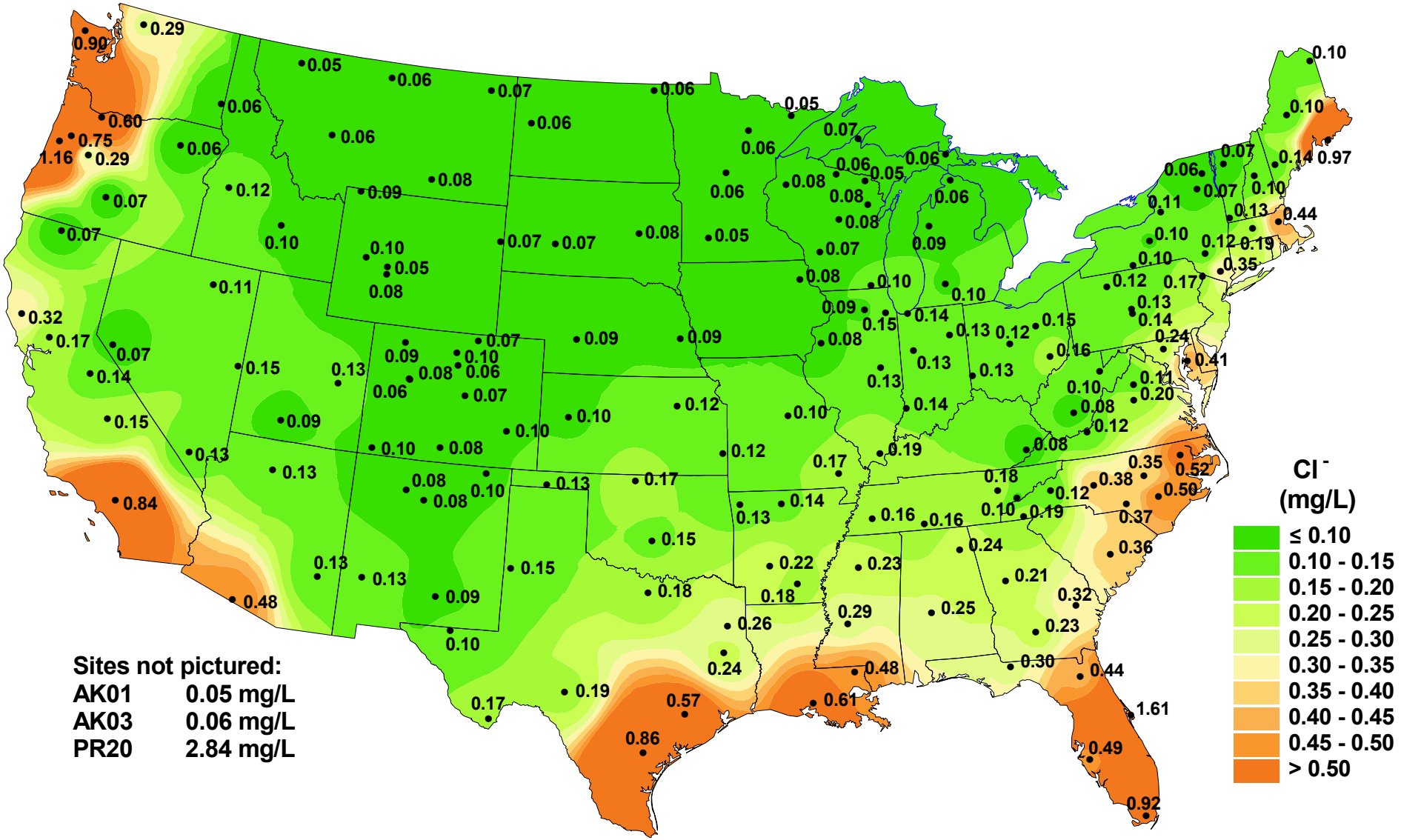

National Atmospheric Deposition Program/National Trends Network
http://nadp.sws.uiuc.edu

Chloride ion concentration, 1995

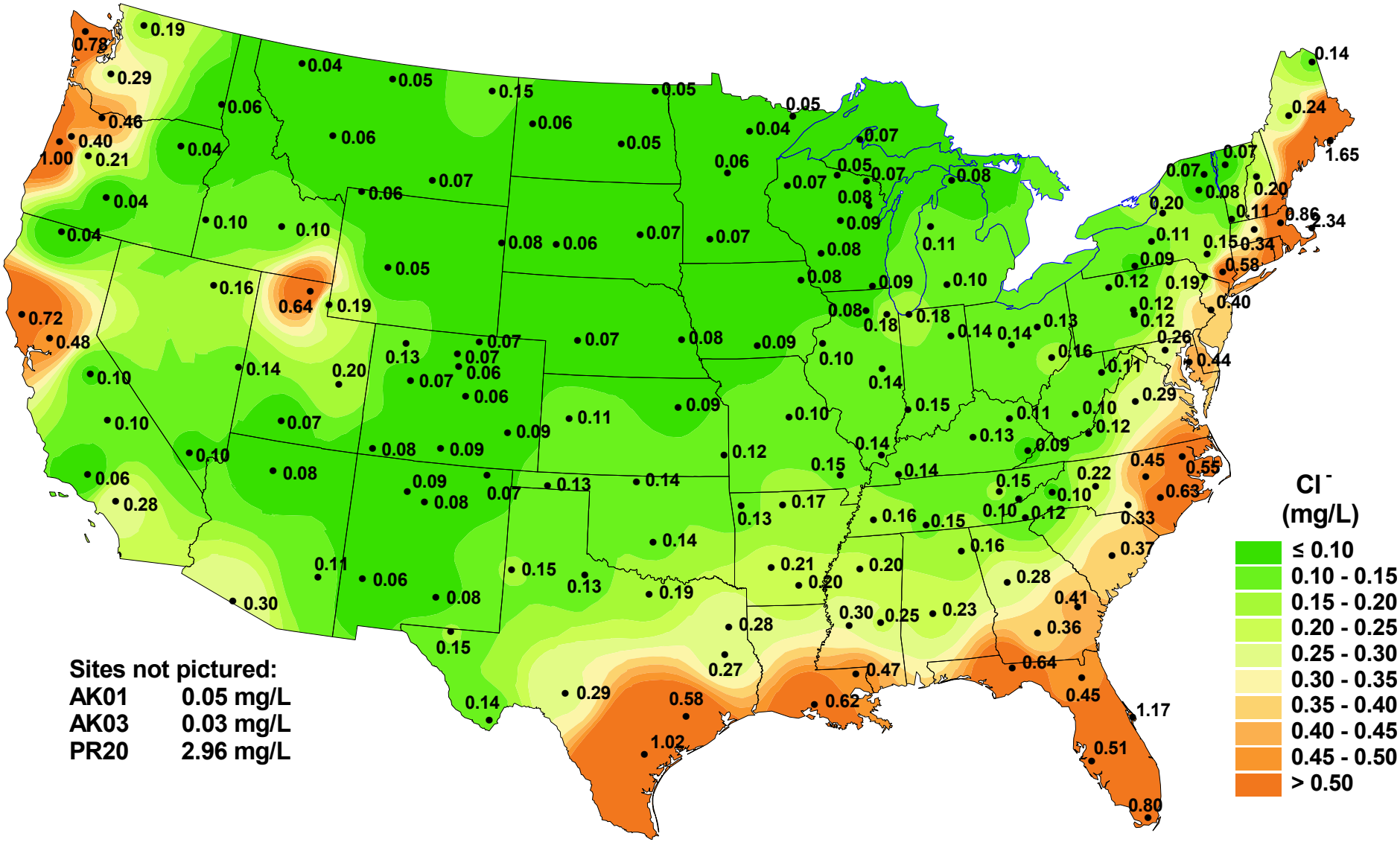

National Atmospheric Deposition Program/National Trends Network
http://nadp.sws.uiuc.edu

Chloride ion concentration, 1996

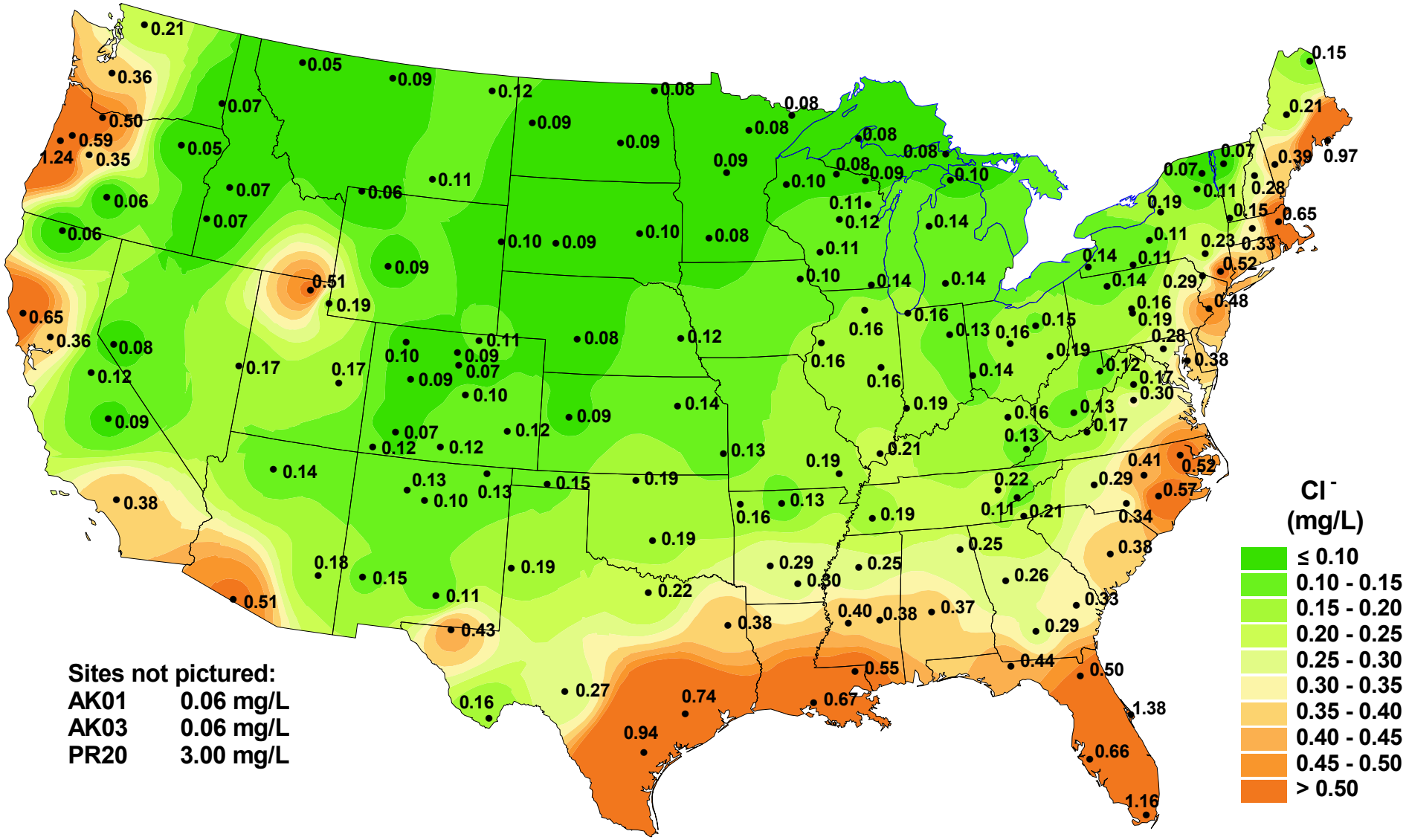

National Atmospheric Deposition Program/National Trends Network
http://nadp.sws.uiuc.edu

Chloride ion concentration, 1997

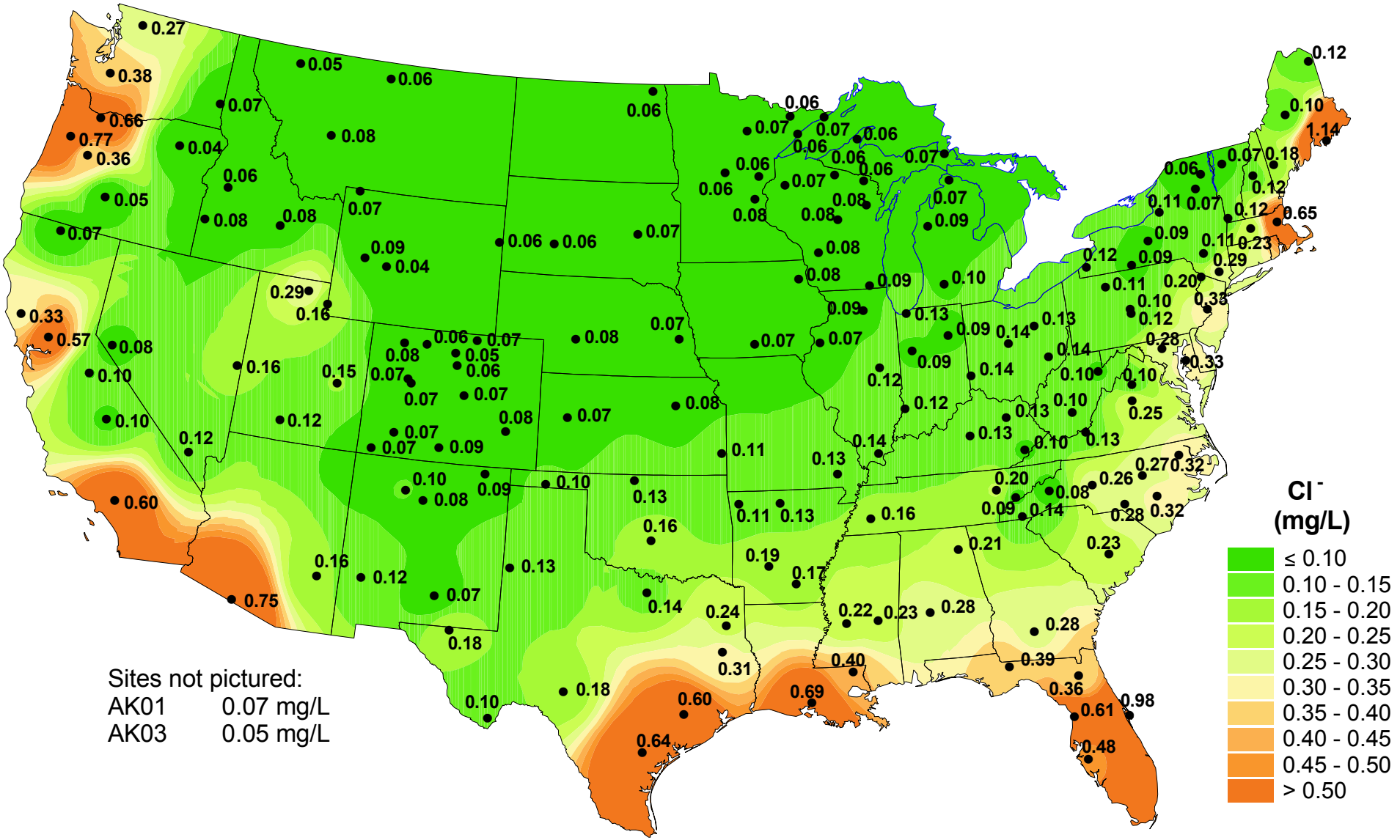

National Atmospheric Deposition Program/National Trends Network
http://nadp.sws.uiuc.edu

Chloride ion concentration, 1998

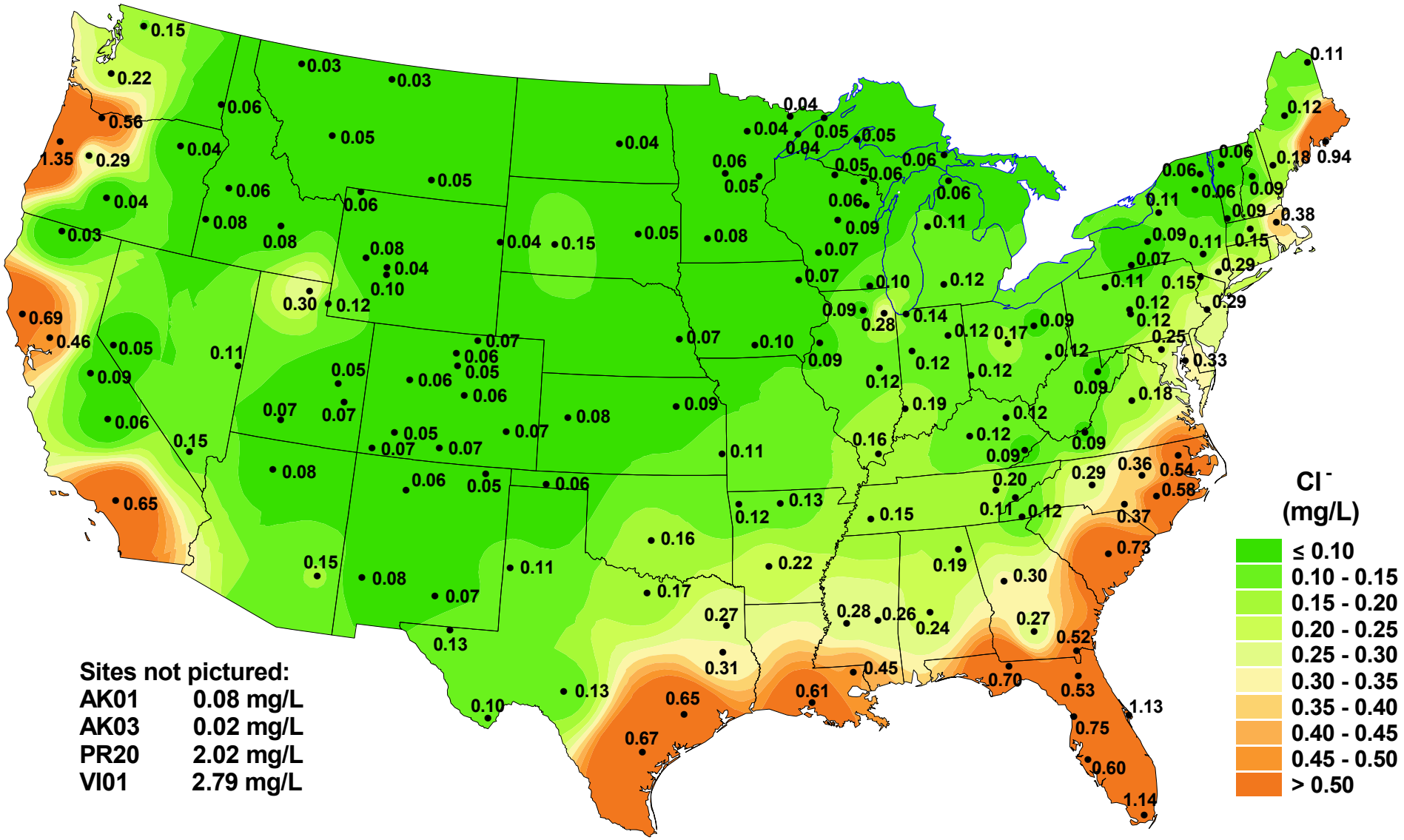

National Atmospheric Deposition Program/National Trends Network
http://nadp.sws.uiuc.edu

Chloride ion concentration, 1999

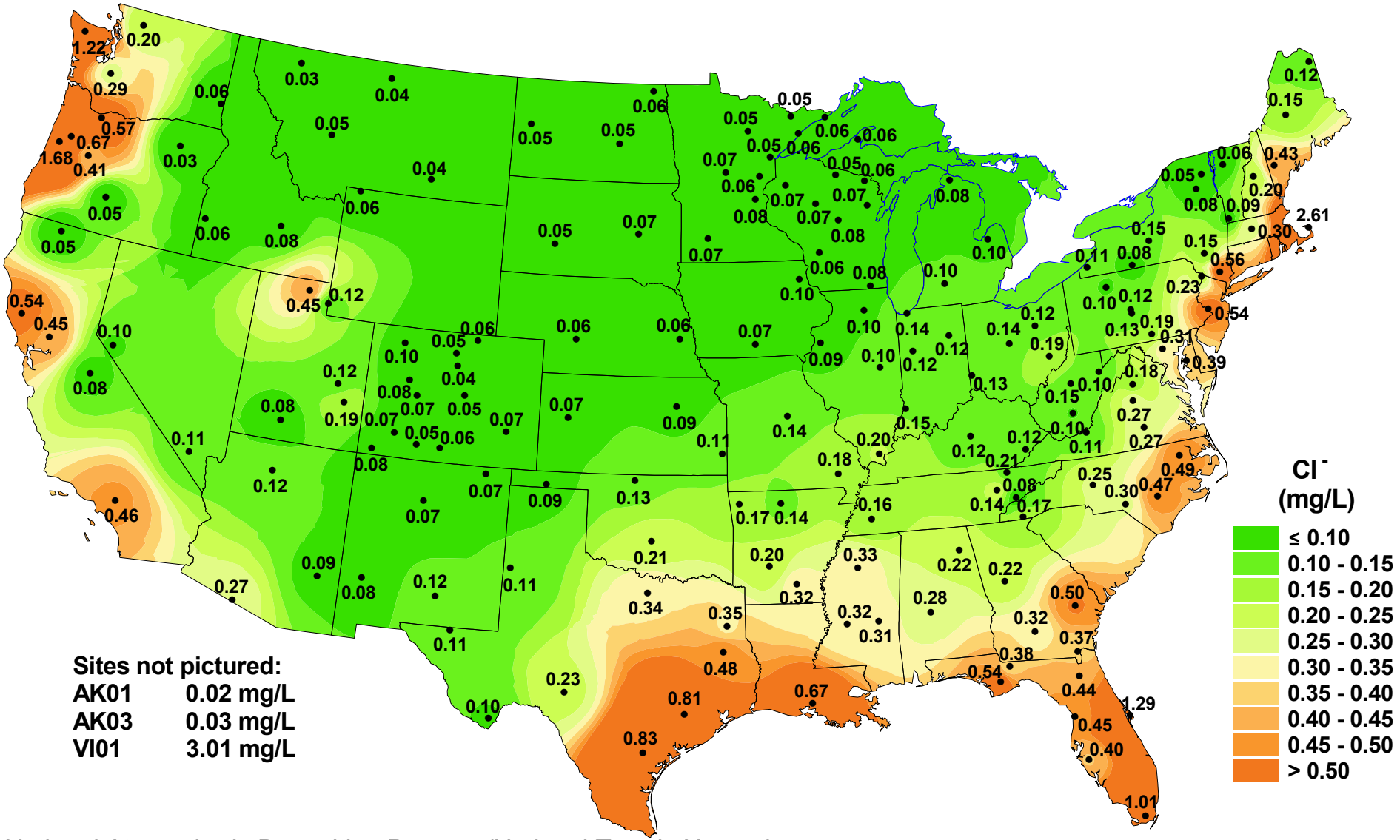

National Atmospheric Deposition Program/National Trends Network
http://nadp.sws.uiuc.edu